

Accepted Manuscript

Journal of the Geological Society

Age, depositional history and tectonics of the Indo-Myanmar Ranges, Myanmar

Tin Tin Naing, S. A. Robinson, M. P. Searle, C. K. Morley, I. Millar, O. R. Green, P. R. Bown, T. Danelian, M. R. Petrizzo & G. M. Henderson

DOI: <https://doi.org/10.1144/jgs2022-091>

To access the most recent version of this article, please click the DOI URL in the line above. When citing this article please include the above DOI.

Received 24 June 2022

Revised 10 March 2023

Accepted 26 March 2023

© 2023 The Author(s). This is an Open Access article distributed under the terms of the Creative Commons Attribution 4.0 License (<http://creativecommons.org/licenses/by/4.0/>). Published by The Geological Society of London. Publishing disclaimer: www.geolsoc.org.uk/pub_ethics

Supplementary material at <https://doi.org/10.6084/m9.figshare.c.6487105>

Manuscript version: Accepted Manuscript

This is a PDF of an unedited manuscript that has been accepted for publication. The manuscript will undergo copyediting, typesetting and correction before it is published in its final form. Please note that during the production process errors may be discovered which could affect the content, and all legal disclaimers that apply to the journal pertain.

Although reasonable efforts have been made to obtain all necessary permissions from third parties to include their copyrighted content within this article, their full citation and copyright line may not be present in this Accepted Manuscript version. Before using any content from this article, please refer to the Version of Record once published for full citation and copyright details, as permissions may be required.

Age, depositional history and tectonics of the Indo-Myanmar Ranges,

Myanmar

Tin Tin Naing¹, S. A. Robinson^{1*}, M. P. Searle¹, C. K. Morley², I. Millar³, O. R. Green¹, P. R. Bown⁴, T. Danelian⁵, M. R. Petrizzo⁶, G. M. Henderson¹

¹*Department of Earth Sciences, Oxford University, South Parks Road, Oxford OX1 3AN, UK*

²*Department of Geological Sciences, Chiang Mai University, 239 Huaykaew Road, Chiang Mai, 50200, Thailand*

³*BGS Keyworth, Nottingham, NG12 5GG, UK*

⁴*Department of Earth Sciences, University College London, Gower Street, London WC1E 6BT, UK*

⁵*Univ. Lille, CNRS, UMR 8198 – Evo-Eco-Paleo, F-59000 Lille, France*

⁶*Dipartimento di Scienze della Terra “A.Desio”, Università degli Studi di Milano, via Mangiagalli 34, 20133 Milano, Italy*

*Corresponding author; stuart.robinson@earth.ox.ac.uk

Abstract

The Indo-Myanmar Ranges (IMR) are an enigmatic mountain belt that occupy a complex tectonic zone in western Myanmar extending from the northern continuation of the active Sunda-Andaman arc into the eastern Himalayan syntaxis. The IMR are part of an accretionary fore-arc basin-arc complex that includes the Central Myanmar Basin and the Wuntho-Popa Arc to the east. New biostratigraphic, petrologic, and detrital zircon U-Pb age data are presented that are used to test and refine the divergent tectonic models that have been proposed for western Myanmar. These data suggest: 1) that the Upper Triassic Pane Chaung Formation was originally deposited adjacent to the NE Indian continental margin within northern Gondwana during the

Late Triassic, and 2) that the Upper Cretaceous – Paleogene rocks of the IBR were mainly derived from the Wuntho-Popa Arc and Inner Belt, with a subordinate input from a crustal source, potentially from the Naga metamorphic-type Paleozoic basement. The Kalemio ophiolite has an Early Cretaceous age similar to ages of ophiolites in the Indus Yarlung-Tsangpo suture zone, south Tibet and Nagaland, reinforcing the hypothesis that they were once part of the same Neo-Tethyan ocean floor.

Keywords: Indo-Myanmar Ranges, Tethyan closure, ophiolites, flysch

The Indo-Myanmar Ranges (IMR; but also known in the literature as the “Indo-Burma Ranges”) form an enigmatic mountain belt running the length of western Myanmar, extending into India and Bangladesh. To the SW lies the Indian Ocean, and to the east lies the Central Myanmar Basin and Wuntho-Popa Arc (CMB, WPA Fig. 1). The IMR connect the Himalayan orogen to the north with the Sunda-Andaman trench to the south (Fig. 1). Rangin et al. (2013) interpreted the existence of a so called “Burma (Myanmar) micro-plate” that includes the IMR, the complex core of the IMR and the Central Myanmar Basin. A major belt of ophiolites and deep marine sediments, including the Nagaland and Kalemio ophiolites, separates the IMR to the west from the CMB to the east, splitting the micro-plate. The tectonics of the Myanmar micro-plate are dominated by the oblique, north northeastwards subduction of Tethyan Oceanic crust beneath Asia, and subsequent clockwise rotation due to the indenting Indian plate to the west. The Myanmar micro-plate obliquely accreted with NE India as it moved northwards and underwent considerable strike-slip translation (Rangin et al., 2013; Rangin, 2017, 2018). However, the details of how deformation evolved within the IMR, how much dextral strike-slip translation has

affected the region, and the tectonic context and timing of emplacement of the fragments of oceanic crust all remain controversial. The IMR has been interpreted in the context of originally N to NE-directed subduction during the Mesozoic-Cenozoic (Mitchell, 1993; Westerweel et al., 2019). Like the Indus Yarlung Tsangpo Suture Zone (e.g. Hébert et al., 2012; Kapp and DeCelles, 2019), the IMR contains a very important record of the Neo-Tethys subduction history that can be used to test and refine Mesozoic-Cenozoic plate reconstructions.

The origin and tectonic affinity of the IMR remain open to multiple interpretations. Some earlier workers considered that the west-verging IMR sediments were an accretionary prism formed during subduction of various stages of the Tethys Ocean beneath the Eurasian plate and postulated that sediment was sourced from the emerging Himalaya to the north (Curry et al., 1979; Bender, 1983; Hutchison, 1989; Curry, 2005). More recent studies of the IMR dispute this view and infer a much more complex tectonic setting for the IMR (see review in Morley et al., 2020). Some have interpreted the IMR as the main India-Asia suture zone, marked by a discontinuous belt of ophiolites including the Naga Hills ophiolite (NHO) in the northern part of the IMR, NE India (Acharyya, 2007; Singh, 2013; Ghose et al., 2014) and the Kalemio ophiolite in the Chin Hills in the eastern IMR (Liu et al., 2016).

Several palaeogeographic reconstructions have been proposed for western Myanmar that can be summarized in two groups. According to the first group of models, the West Myanmar Terrane (WMT, including the CMB and the WPA; also known in the literature as the “West Burma Terrane”) was part of SE Asia by the Early Mesozoic and the IMR developed on this margin. These models support suggestions that the IMR were part of Gondwanan Sibumasu or the

Cathaysian West Sumatra terrane (e.g. Mitchell, 1992; Barber and Crow, 2005, 2009; Hall, 2009; Metcalfe, 2011; Hall, 2012; Morley, 2012, 2018; Metcalfe, 2013; Hall, 2014). In the second group of models, a west Myanmar “microplate” (Mount Victoria Land) separated from Western Australia in the Jurassic and was added to the WMT, and thus, SE Asia in the Cretaceous (e.g. Mitchell, 1986, 1989; Sengör, 1987; Veevers, 1988; Metcalfe, 1990; Audley-Charles, 1991). Recently, the palaeo-position of West Myanmar has been tested using provenance data (particularly detrital zircon U-Pb ages and geochemistry) applied to Triassic deep water sediments (Pane Chaung Formation) in the IMR. Sevastjanova et al. (2016) suggested West Myanmar was part of SE Asia before the Triassic-Early Cretaceous Indosinian orogeny and that it is of neither Cathaysian nor Indian Plate affinity. Another model argues that detrital zircon ages of the Pane Chaung Formation are comparable to NW Australia and Greater India and that they were all deposited during the Late Triassic on a submarine fan that developed along the northern and NW margin of Australia (Cai et al., 2016; Yao et al., 2017).

An additional constraint on tectonic reconstructions is a recent palaeomagnetic study on Upper Cretaceous igneous and Eocene sedimentary rocks from the northern part of the terrane, which indicates a position around 5° S in the Late Cretaceous, and ~4° N in the Late Eocene (Westerweel et al., 2019). Palaeomagnetic data from additional Cenozoic sites in the CMB that constrain the location of strata of different ages are consistent with the 2019 data (Westerweel, 2020). A key problem with the WMT is that much of it is covered by Cenozoic deposits, and outcrops of Mesozoic and Palaeozoic units are geographically restricted. It possibly developed through multiple collisions of tectonic blocks and is a composite terrane (see Morley et al., 2021 for a discussion). For example, palaeomagnetic data constraints can be accommodated in the

Late Triassic submarine fan model for northern Gondwana (Cai et al., 2016; Yao et al., 2017) if a continental fragment (Mt Victoria Land, Mitchell, 1993) collided with a volcanic arc (WMT) during the Early Cretaceous (see discussion in Licht et al., 2020; Morley et al., 2020, 2021). Fundamental challenges to understanding the IMR include: historically highly limited access along rudimentary roads and trails; limited exposures in high relief terrain covered by forest and restriction of outcrops to river courses; highly complex structure; very extensive, highly monotonous marine facies known as flysch units with a broad age-range (Triassic-Paleogene) and limited biostratigraphic age control (e.g. Brunnschweiler, 1966; Bannert et al., 2011). At the time of fieldwork (2016), access to some parts of the Rakhine coastal area was prohibited or restricted. Road building has created some new outcrops, and some excellent exposures exist along river sections. U-Pb dating of zircons and other dating methods have been applied to understanding the timing of tectonic, igneous, and metamorphic events and stratigraphy (see review in Sevastjanova et al., 2016; Liu et al., 2016a; Yao et al., 2017; Zhang et al., 2017, 2018; Bandopadhyay et al., 2022; Najman et al., 2022).

Understanding the tectonic evolution of the IMR requires knowledge of its prior location, when and where it separated from Gondwana, and when and how it collided with SE Asia.

Disagreement still remains regarding the presence and extent of continental basement in the IMR (see discussions in Morley et al., 2020, 2021). Furthermore, many existing lithologic correlations are solely based on comparable lithologies and remain untested using geochronologic techniques. In this paper, the results of biostratigraphic, petrographic, detrital zircon U-Pb age and Hf isotope investigations of the Triassic-Paleogene flysch sandstones in the IMR of western Myanmar are presented. Additionally, existing U-Pb age data along the IMR are also reviewed. The aim is to

constrain stratigraphic ages, interpret the palaeoenvironmental significance, structural and tectonic history of the rocks from the IMR and to aid palaeogeographic reconstruction of western Myanmar. Three major points of interest are discussed: (1) The palaeogeographic location of the Pane Chaung Formation during its deposition, (2) the ages of ophiolites, and associated radiolarian chert and mélangé, (3) the timing of suturing between India and the WMT (closure of Neo-Tethys).

Geological Background

Regional geology of Myanmar

Myanmar is located on the eastern edge of the indenting India plate and form a southeast continuation of the Himalayan orogenic belt, south of the eastern Himalayan Syntaxis. Myanmar is a transition between the continental collision along the Himalaya in the north to the active Indian ocean subduction beneath the Sunda Arc (Sumatra-Andaman Trench) in the south (e.g. Mitchell, 1993; Curray, 2005; Morley, 2009; Morley and Searle, 2017) . Geologically, Myanmar can be subdivided into three N-S trending tectonic belts (Fig. 1). The Shan Plateau is part of the Sibumasu Terrane, whereas the CMB is associated with the so-called West Myanmar Terrane, west of the Sagaing Fault. The IMR are juxtaposed along the western margin of the CMB. This investigation concentrates on the western two belts.

The CMB lies between the Sagaing Fault and the IMR and extends southward to the Andaman Sea. It is composed of a thick succession of Upper Cretaceous-Pleistocene marine and fluvial sediments that are locally overlain by Pliocene-Quaternary calc-alkaline volcanoes (e.g. Pivnik et al., 1998; Mitchell et al., 2010; Licht et al., 2016). The CMB has traditionally been subdivided

into Upper Cretaceous-Cenozoic western forearc and eastern backarc basins (Pivnik et al., 1998), separated by the Wuntho-Popa Arc (Mitchell et al., 2012; Gardiner et al., 2015). The basin is bounded by two major faults, the long, linear dextral strike-slip Sagaing Fault, whose trace is clearly expressed in satellite images, and is located along the eastern margin of the CMB (e.g. Soe Thura Tun and Watkinson, 2017), and the dextral Kabaw Fault along the western margin, whose trace is possibly discontinuous, and is less clearly expressed in satellite images (e.g. Morley et al., 2020).

The IMR lie west of the CMB, and are composed of a thick imbricated thrust succession of Mesozoic and Cenozoic flysch deposits associated with several large and numerous smaller ophiolite fragments. The ophiolites in the IMR (in particular the Kalemio area) and India (Nagaland) are interpreted as Penrose-type obducted ophiolite (e.g. United Nations, 1979a; Mitchell, 1993; Socquet et al., 2002; Acharyya, 2007; Rangin, 2018) or accretionary-type ophiolites (e.g. Harlow et al., 2014; Fareeduddin and Dilek, 2015; Hla Htay et al., 2017; Barber et al., 2017). The ophiolites comprise small, highly dismembered bodies of ultramafic rocks up to about 10 km long (N-S), together with smaller bodies of pillow lavas, and gabbros (Mitchell, 1993; Mitchell et al., 2010; Zhang et al., 2017, 2018; Morley et al., 2020). The largest serpentinised peridotite body (Webula, Fig. 5d) has a low-angle thrust at its base (Brunnschweiler, 1966), and a small patch of metamorphic sole rocks outcrops at its southern end (Zhang et al., 2017). The basal thrusts of three of the peridotite bodies in the Kalemio area were estimated to dip east between 10° and 34° and underwent top to the west displacement (Morley et al., 2020). Sheared mélanges, with matrices of mudrock, or serpentinite, are sometimes juxtaposed with the ultramafic rocks (United Nations, 1979a; Mitchell et al., 2010;

Zhang et al., 2018; Morley et al., 2020), and these dismembered and thrust ophiolite-association rocks are present within the belt of Kanpetlet Schists and Pane Chaung Formation. The earlier thrusting and folding is overprinted by swarms of closely-spaced, later (Cenozoic?), approximately N-S trending dextral strike-slip faults (Morley et al., 2020). The ophiolite fragments define a north-south suture zone that separates the IBR to the west from the CMB to the east. The IMR is an active fold and thrust belt above an east-dipping active subduction zone, along which numerous earthquakes occur (e.g. Steckler et al., 2016a; Searle et al., 2017; Sloan et al., 2017). As the main focus of this paper, the IMR is described in more detail below.

The Indo-Myanmar Ranges (IMR)

The IMR constitute a north-south trending, approximately 1300 km long, arcuate fold-thrust belt (Fig. 1). They lie on the eastern margin of the highly oblique convergent zone that extends from the collisional Himalayan region in the north to the subduction-related Sunda-Andaman trench on the south (Acharyya, 2015). Published accounts indicate the IMR initially formed in an accretionary prism setting during the Jurassic- Early Eocene, then during the Late Eocene began to evolve into a sub-aerial fold-and-thrust belt after collision between Sundaland and the Indian plate (e.g. Theobald, 1871; Chhibber, 1927, 1934; Brunnschweiler, 1966, 1974; Mitchell, 1993; Maurin and Rangin, 2009; Mitchell et al., 2010; Bannert et al., 2011; Rangin et al., 2013; Rangin, 2017).

The IMR belt comprises a thick sequence of westward-younging Mesozoic-Cenozoic flysch deposits associated with several large and numerous small ophiolite fragments. Low-grade greenschist facies metamorphic rocks to the east reflect minor amount of crustal thickening

(Brunnschweiler, 1966; Socquet et al., 2002; Bannert et al., 2011; Morley et al., 2020). The thick Mesozoic-Cenozoic flysch deposits of the IMR are typically poorly fossiliferous, and difficult to differentiate due to their monotonous nature, particularly in the Inner Belt (Brunnschweiler, 1966; Bannert et al., 2011). Reworking of older fossils into younger deposits is common (Brunnschweiler, 1966; United Nations, 1979a), making biostratigraphic resolution complicated. The ranges are flanked to the east by the CMB and to the west by basins in eastern Bangladesh and NE India (e.g. Ghose et al., 2014; Steckler et al., 2016a). The eastward extent of the oldest part of the IMR is obscured by the Upper Cretaceous-Recent sedimentary cover of the CMB (forearc basin). Traditionally, the IMR have been divided into Inner and Outer belts (e.g. United Nations, 1979a; Mitchell et al., 2010). Maurin and Rangin (2009) refer to the Eastern Belt as the core of the IMR and subdivide the Western Belt into an Inner Belt, and a westernmost Outer Belt. The central and the Inner Belt are separated by the Lelon Fault (Maurin and Rangin, 2009) and by the transpressional Kheng Fault (Mitchell et al., 2010; Mitchell, 2017). The Inner and Outer belts are divided by strike-slip Kaladan Fault (Maurin and Rangin, 2009). The Outer Belt is composed of Neogene sediments, while the Inner Belt consists of predominantly Upper Cretaceous-Palaeogene sediments. The central part of the IMR is a tectonically complex zone, marking a broad suture zone containing units derived from the Tethys Ocean and related back-arc basins comprising oceanic crust-related materials (including large and small bodies of ultramafic rocks and serpentinite, pillow lavas, radiolarian chert, *mélange*), Upper Triassic flysch (Pane Chaung Formation), and metamorphic units that include fragments of a metamorphic sole to the ultramafic bodies. A larger region of low-grade to greenschist facies metamorphic rocks, named the Kanpetlet Schists (Fig. 5b) crops out in the southern Chin Hills area (United Nations, 1979a; Socquet et al., 2002).

Ophiolites

Ophiolitic rocks are best preserved along the eastern margin of the IMR from the Naga Hills in the north to Andaman Islands in the south, and are referred to as the Western Ophiolite Belt (Mitchell et al., 2010; Acharyya, 2015; Hla Htay et al., 2017; Morley and Searle, 2017). These ophiolites are generally interpreted to represent the eastern suture of the Indian plate (Mitchell, 1981; Acharyya, 1986; Searle et al., 2017). The ophiolite belt contains blocks of peridotite, gabbro, pillow basalt, radiolarian chert, and some metamorphic rocks within a matrix of serpentinite (Mitchell, 1993; Acharyya, 2007; Bannert et al., 2011; Ghose et al., 2014; Acharyya, 2015; Liu et al., 2016; Hla Htay et al., 2017; Zhang et al., 2017). Three major peridotite massifs occur in the Chin Hills: Mwe Taung, Bophi Vum and Webula. Mantle peridotites mainly consist of harzburgites with minor lherzolites and dunites. There are some associated massive chromite-bearing bodies, particularly around Mwe Taung. The gabbros are limited in extent, and several exposures (small size blocks <10 m²) in the Mindat and Yazagyo area occur in a serpentinite matrix (Zhang et al., 2017, 2018; Morley et al., 2020). The best exposed ophiolitic mélangé is found in the spillway area of the Yazagyo Dam, where an ultramafic klippe overlies Triassic flysch (Zhang et al., 2018). The spillway outcrops reveal a mélangé, whose blocks include bedded red cherts, limestones and serpentinite, sheared together with basalts which likely represent the downgoing plate (Zhang et al., 2018; Morley et al., 2020). In Khwekha, a low-grade metamorphic mélangé unit, overlain by a greenschist to amphibolite grade metamorphic sole, occurs below the southern outcrops of the Webula ophiolite (Hla Htay et al., 2017).

U-Pb dates of magmatic zircons in gabbros and rodingites from the ophiolitic *mélange* in Kalemryo yield Early Cretaceous ages, ranging between 126 ± 2 Ma and 133 ± 2 Ma (Liu et al., 2016; Zhang et al., 2018). These Early Cretaceous ages are inferred to represent the age of oceanic crust formation (Searle et al., 2017) with the ophiolite forming above an intra-oceanic subduction zone (Liu et al., 2016). For the Nagaland ophiolite, Singh et al. (2017) obtained zircon U-Pb ages from plagiogranites of 116 ± 2 Ma to 118 ± 1 Ma and similar ages are reported for ophiolitic gabbros in Manipur (Aitchison et al., 2019). Late Jurassic (Kimmerigian-Late Tithonian) radiolarians occur in a chert block in the *mélange* in Nagaland (Baxter et al., 2011) with both Jurassic and Early Cretaceous radiolarians occurring in red and green cherts, respectively in Manipur. Notably, the cherts occur in association with basalts of MORB affinity and are considered to present fragments off-scraped from the lithospheric slab subducting beneath the ophiolite.

U-Pb zircon ages of 115 ± 1 Ma to 119 ± 3 Ma from amphibolites at Kalemryo are interpreted as part of a metamorphic sole to the ophiolite and thus indicate the timing of its emplacement within an accretionary prism (Liu et al., 2016; Zhang et al., 2017; Morley et al., 2020). Some authors suggest ophiolite fragments were emplaced prior to the deposition of Aptian-Cenomanian limestones (United Nations, 1979a; Mitchell, 1993; Mitchell et al., 2010). Geochemical studies indicate that mafic volcanic rocks included within the *mélange* have a range of mid-ocean ridge and supra-subduction zone affinities (Liu et al., 2016; Singh et al., 2016; Niu et al., 2017). Searle et al. (2017) considered the IMR to contain at least two different ophiolites: (1) a more westerly zone that involves ophiolite fragments embedded into the Cenozoic section and emplaced during the Paleogene in the Naga-Manipur region (Ghose et al., 2014; Aitchison et

al., 2019); and (2) a more easterly zone of ophiolites emplaced prior to the mid-Cretaceous, closely associated with overthrust Triassic sediments (Pane Chaung Formation) and metamorphic rocks (Kanpetlet Schists, Nimi Formation) that are unconformably overlain by the Upper Cretaceous Paung Chaung and Kabaw formations. In the northern half of the IMR the Naga Ophiolites are overthrust by various Palaeozoic units attributed to the Naga Metamorphic Complex (Brunnschweiler, 1966; Aitchison et al., 2019), where the metamorphic rocks occur above and below folded and thrust fragments of ophiolites on both the western and eastern margins of the Chindwin Basin, including the Jade Belt region (Brunnschweiler, 1966; Hla Htay et al., 2017).

Sedimentary and meta-sedimentary units of the IMR

The primary stratigraphic units in the core of the IMR are thick sequences of turbidites (flysch) assigned to the Triassic Pane Chaung Formation, the Kanpetlet Schists, and related metabasites, together with fragments of ophiolites including gabbros, ultramafics, radiolarian cherts and pillow lavas (e.g. United Nations, 1979a; Mitchell, 1993, 2017). Despite strong thrusting, strike-slip deformation and folding, along some river sections the Pane Chaung Formation is seen to grade into greenschist-grade Kanpetlet Schists (United Nations, 1979a; Maurin and Rangin, 2009; Bannert et al., 2011). The age of the Kanpetlet Schists was originally considered pre-Mesozoic (Brunnschweiler, 1966) or Triassic (Socquet et al., 2002). Recently obtained detrital zircon age data indicates a Triassic or younger age (Zhang et al., 2017; Najman et al., 2019).

The Pane Chaung Formation is widely exposed along the eastern flank of the Chin Hills outwards to the Rakhine area and is composed of indurated turbiditic sandstones and shales (Fig.

5a). The Triassic depositional age of the Pane Chaung Formation is based on the rare occurrence of *Halobia* fossils (Gramann, 1974; United Nations, 1979a; Bannert et al., 2011; Yao et al., 2017; Zhang et al., 2017). However, identification of the Pane Chaung Formation is commonly based on lithological characteristics across large tracts of the IMR, without any supporting fossil evidence. The discontinuous nature of outcrops in the IMR, and lithologically similar overlying Cretaceous units, generates considerable uncertainty with mapping of the Pane Chaung Formation (Brunnschweiler, 1966; Bannert et al., 2011). Limited fossil occurrences prevent resolution of the full age range of the formation. Recent detrital zircon analysis (Sevastjanova et al., 2016; Yao et al., 2017) indicates maximum depositional ages are predominantly Late Triassic, with some Early Jurassic ages, and help to address correlation difficulties.

IMR Inner Belt

The thick Mesozoic-Cenozoic flysch deposits of the IMR are typically poorly fossiliferous and difficult to differentiate (Brunnschweiler, 1966; Bannert et al. 2011). In the central area of the IMR, along the Kalemyo-Falam and Webula-Falam road sections, the Triassic Pane Chaung Formation is apparently unconformably overlain by the Upper Cretaceous Falam Formation (Mitchell et al., 2010) (Fig. 5c). The latter is remarkably monotonous, composed of mudstones with minor fine-grained turbidite sandstones and exotic *Globotruncana* limestone blocks (United Nations, 1979a, Brunnschweiler, 1966). The Falam Formation is stratigraphically overlain by the Chunsung Formation (United Nation, 1979a). Biostratigraphic data of the Chunsung Formation indicate that it is Paleocene to Lower Eocene, and is probably equivalent to part of the Disang Group of Assam (Mitchell et al., 2010; Mitchell, 2017). Lokho et al. (2020) recorded Planktonic Foraminiferal Zones E14-16 correlative to upper middle Eocene to upper Eocene in the Upper

Disang Formation. The Chunsung Formation passes stratigraphically up into the Kennedy Sandstone (Fig. 5e, f), of probable Eocene age (Mitchell et al., 2010; Mitchell, 2017). In the more southerly Rakhine area of the IMR, the geological team of the United Nations (1979a) maps the Padaung-Taungup road section as Upper Cretaceous-Palaeogene flysch, which may be laterally equivalent to (part of?) the Falam Formation, Chunsung Formation and Kennedy Sandstone further north. However, this area in Rakhine consists almost entirely of a thick, monotonous, succession of sandstones and mudstones flysch units with no stratigraphic divisions obvious either in the field or on aerial photographs. Limestones with *Globotruncana* are very common as exotic blocks.

IMR Outer Belt

The Outer Belt crops out in the furthest western parts of the IBR as well as on offshore islands of the Rakhine coastal, and continues along strike into Bangladesh (Fig. 1). It is predominantly composed of Neogene flysch-type sediments with minor deformed Campanian-Maastrichtian pelagic limestones and mudstones, assumed to be olistoliths (Bender, 1983; Mitchell, 1993; Allen et al., 2008). Sediments in the Outer Belt range from Miocene, and furthest west, are Miocene to Pleistocene (Maurin and Rangin, 2009; Kyi Khin et al., 2017). Maurin and Rangin (2009) noted the Outer Belt is affected by the detached fold and thrust system.

Materials and methods

Three sampling campaigns were undertaken in the Rakhine, Mt. Victoria and Kalemyo areas in the IMR in 2016, 2017 and 2018 (Fig. 2a, b, 3a, 4a). Fieldwork was conducted to sample many of the Triassic-Eocene exposures in the IMR for biostratigraphic, petrographic and geochemical

analysis. Biostratigraphy is used to ascertain the depositional ages of sediments. Petrographic and geochemical data presented herein provide insight into the origins of the sediment and better inform palaeogeographic reconstructions. Structural orientation and fault kinematic data were collected in the field (Fig. 2b, Fig. 3a, Fig. 4a), and local and regional cross-section were made (Fig. 3b, 4b), field relationships between different units were investigated (Fig. 5), these data are also provided in Morley et al. (2020).

Samples

In the Rakhine area, samples were collected along the Padaung-Taungup and Gwa road sections and Rakhine coastal area (Fig. 2b). In the Mt. Victoria area, sample collection was carried out along the Saw to Mt. Victoria road, main Mindat-Kyaukhtu road, Mindat-Kanpetlet road, and Saw River (Fig. 3a). In the Kalemyo area, samples were collected along the Kalemyo-Falam-Kennedy Peak road, Wabula Taung-Falam road, and Kalemyo-Kalewa road (Fig. 4a). Sample location details are presented in the Supplementary data file 1.

Techniques

Analytical methods are summarized below and provided in full together with all data tables in the supplementary material.

Biostratigraphy

Shale samples were prepared for foraminiferal analysis by using a freeze-thaw technique. Four chert samples (KM37, KM37b, KM39a, KM39b) were collected from ophiolitic mélangé at the Yazagyo Dam in the core of the IMR. They were prepared at Oxford University using standard

radiolarian extraction techniques for cherts with the use of dilute hydrofluoric acid (Pessagno and Newport, 1972; De Wever et al., 2001). Planktonic foraminiferal taxonomy follows the pforams@mikrotax database at <http://www.mikrotax.org/pforams> (Huber et al., 2016) and Huber et al. (2022).

Petrography

Thin-section petrographic analyses were performed on 20 sandstones following the Garzanti classification (Garzanti, 2016) and Gazzi-Dickinson methods (Dickinson, 1985). A minimum of 500 grains (including matrix and cement) were counted per thin section and mineralogical compositions were recalculated on a matrix-free basis prior to plotting essential components.

Detrital zircon U-Pb and Hf isotope analysis

U-Pb age determinations were undertaken out at the Geochronology and Tracers Facility of the British Geological Survey, Keyworth, UK. U-Pb analyses were carried out on 24 samples using a multi-collector Nu Plasma HR mass spectrometer coupled to a New Wave 193SS solid state laser. Six sandstone samples from the Upper Cretaceous – Eocene flysch unit were then selected for Hf-isotope analysis using a Thermo Scientific Neptune mass spectrometer coupled to a New Wave Research UP193UC Excimer laser ablation system. Details of reference materials and analytical methods are given in Supplementary file 2.

Results

Biostratigraphy

Cretaceous-Paleogene flysch units of the Inner Belt are highly monotonous, and it is difficult to differentiate between Cretaceous and Eocene strata. We attempted to establish new, more robust biostratigraphic control for this region, based on foraminifers and nannofossils extracted from eleven shale samples. However, only samples IBR06, IBR12, IBR98, IBR103 and IBR108 yielded rare foraminifers and nannofossils. Three samples mapped as Cretaceous (IBR98, IBR103, IBR108; Fig. 2b), contain *Planoheterohelix globulosa* (Ehrenberg), *Planohedbergella ultramicra* (Subbotina) and *Muricohedbergella planispira* (Tappan) (Plate 1a-d). Nannofossils adhered to planktonic foraminifers in sample IBR98 were identified by co-author, Paul Bown in SEM images as *Prediscosphaera columnata* (Stover) and *Watznaueria* sp., (Plate 1g, h). Planktonic foraminifers indicate an Albian-Maastrichtian range, while nannofossils indicate correlation with the Albian-Turonian. Two samples mapped as Paleogene (IBR06, IBR12; Fig. 2b), include of *Chiloguembelina wilcoxensis* (Cushman & Ponton), and *Chiloguembelina ototara* (Finlay) (Plate 1e, f), but did not yield any nannofossils. The planktonic foraminiferal assemblage is assigned to the Paleocene-Eocene. Despite these rare identifications, there are simply too few occurrences of fossils from shales in the Inner Belt to be sure of the full stratigraphic range of these sediments.

In the Yazagyo Dam section, abundant and well-preserved radiolarians were obtained from sample KM37b with the most significant taxa being illustrated in Plate 2. The occurrence of *Zhamoidellum ovum* (Dumitrica), and *Fultacapsa sphaerica* (Ozoldova) indicates correlation with the Unitary Association Zones (U.A.Z.) 9 – 11 of the biozonation of Baumgartner et al. (1995) and with the mid-late Oxfordian to late Kimmeridgian/early Tithonian interval. In addition, the co-occurrence of the above two species (*Z. ovum* and *F. sphaerica*) with

Cinguloturris carpatica (Dumitrica) indicates the studied radiolarian assemblage also correlates with U.A. Zones B – D of Beccaro (2004), which corresponds to a mid (?)–late Oxfordian to early Kimmeridgian interval.

Petrography

Six sandstone samples mapped as Triassic from the core of the IMR (KM04, KM23, KM25, KM38, KM76a, TT19), eight samples from the Inner Belt (IBR10, IBR45a, IBR101, KM15, KM34, KM34a, KM54b, KM60), and six samples from the CMB (TT04, TT09, TT11, TT15, KM40a,b) were analysed to understand better the general petrography and provenance of the IMR and CMB.

All sandstones in this study were plotted on ternary diagrams of Dickinson (1985), Garzanti (2016), and Garzanti (2019) (Fig. 7). All analysed samples from the core of the IMR are litho-quartzose and feldspatho-litho-quartzose (fLQ) (Fig. 7a) composed predominantly of angular to subrounded monocrystalline quartz with subordinate polycrystalline quartz, plagioclase and lithic fragments, which include phyllite, mudstone, chert, and intermediate to basic volcanic rocks (Table 1) (Fig. 6a). Monocrystalline quartz grains constitute 37–56% of total framework grains. Lithic fragments constitute 9–41% of framework grains. Some plagioclases have been partly altered to clays and clay cement formed around the detrital grains. Muscovite, biotite, chlorite and heavy minerals are present in all samples (Table 1). The locally pore-filling matrix in all sandstones is dominated by clay minerals, authigenic cement (siderite, calcite and pyrite) and organic matter. Texturally, the sandstones are immature and poorly to moderately sorted. On

quartz, feldspar, lithics (QFL) ternary diagrams, Upper Triassic sandstones lie within the recycled orogenic province (Garzanti, 2019) (Fig. 7b).

Petrographic examination of sandstone samples from the Inner Belt reveals they are feldspatho-quartzo-lithic (fQL) and quartzo-lithic (Fig. 7a) composed predominantly of monocrystalline quartz with subordinate polycrystalline quartz and lithic fragments. The lithic fragments include volcanic detritus (felsic) with subordinate sedimentary (argillaceous) and metamorphic (phyllitic) fragments (Fig. 6b). Lithic fragments constitute 46-67% (IBR10, IBR45a, IBR101, KM15, KM60) of the total framework grains (Fig. 6c, d). On a QFL plot, Eocene sandstones lie within the magmatic arc province (Table 1, Fig. 7b). Angular to subrounded poorly sorted monocrystalline quartz grains constitute 23-46% (KM34, 34a, 54b) of total framework grains and on a QFL diagram the sandstones lie within the recycled orogenic province (Table 1, Fig. 7b). On the LmLvLs plot, sandstones from the IMR are distributed in the magmatic arc field (Fig. 7c) (Garzanti, 2019). Feldspar is dominated by plagioclase that exhibits euhedral crystal outlines and well-developed twinning. The matrix content is high in these mineralogically and texturally immature sandstones.

Detrital zircon U-Pb ages

Six sandstone samples (KM23, KM25, KM32, KM76a, TT05, TT19) from the Pane Chaung Formation in the core of IMR, yielded over 100 concordant zircon U-Pb ages (Fig. 8). Detrital zircon U-Pb ages range from 3474 ± 37 Ma to 211 ± 9 Ma. Age distributions are consistent with three main clusters in the Mesoproterozoic (1.25-1.0 Ga, 17% of total analysed grains), Neoproterozoic-Cambrian (750-490 Ma, 31%), and Late Paleozoic-Early Mesozoic (350-210

Ma, 29%), and scattered Paleoproterozoic-Archean (3.4-1.6 Ga) and Ordovician-Devonian (480-370 Ma) ages. The youngest zircon is 211 ± 9 Ma and weighted average ages range from 221 ± 2 Ma – 235 ± 2 Ma (Fig. 8).

Twelve samples from the thick Mesozoic-Cenozoic flysch unit in the Inner Belt of IMR were analysed. Of these, six samples (KM34, KM34a, KM54b, KM58, IBR102, IBR110A) are from outcrops mapped previously as Cretaceous and six (IBR01, IBR11, IBR48A, IBR71B, KM15, KM60) as Paleogene, based on fossil evidence (Bender, 1983) and geological maps (United Nations, 1979a, Myanmar Geosciences Society, 2014). A total of 445 zircons were analysed from the Falam Formation near Kalemyo (KM34, KM34a, KM54b, KM58), yielding 354 concordant zircon ages. The zircon-age spectra from all samples display a prominent age peak at 120-80 Ma, and scattered Proterozoic, Paleozoic and Mesozoic ages (Fig. 9). The youngest ages are 82-67 Ma with a weighted average age of 74 ± 1 Ma (MSWD = 0.23, n = 3) (Fig. 9). A total of 221 zircon grains were analysed from the samples previously mapped as Cretaceous along the Padaung-Taungup road section in the more southerly IMR in Rakhine (IBR102, IBR110A). These analyses yielded 214 concordant zircon ages that range from 1734 ± 17 Ma to 43 ± 1 Ma. The samples exhibit a prominent Cretaceous cluster at 110-80 Ma, with a subordinate cluster at ~50 Ma, as well as scattered Triassic and Precambrian ages (Fig. 9).

A total of 396 zircon grains were analysed from samples mapped previously as Paleogene along the Padaung-Taungup road section (IBR01, IBR11, IBR48A, IBR71B, KM60) and one sample (KM15) from the Eocene Kennedy Sandstone, west of Kalemyo. Padaung-Taungup road samples yielded 327 concordant zircon ages with 118 concordant ages from KM15. Detrital

zircon U-Pb ages from the Paleogene samples range 2759 ± 20 Ma to 43 ± 2 Ma. They contain abundant Cretaceous (65-71%), Eocene (7-18%), Paleocene (3-6.5%), as well as some Jurassic, Triassic, Permian and Precambrian ages (Fig. 10). IBR48A contains an abundant Paleocene (21%) population but yielded no Eocene grains. The zircon-age spectra from all samples display a prominent age peak at 120-80 Ma. Cretaceous zircons are predominantly euhedral and subhedral. They exhibit a simple oscillatory growth pattern on CL images, suggesting a contemporaneous igneous provenance.

Detrital zircon Hf isotopes

Six samples (KM15, KM34, KM34a, KM54b, IBR71B, IBR102) from the Inner Belt of the IMR were selected for Hf isotope analysis using the same zircon grains measured for U-Pb. ϵ_{Hf} values are predominantly positive for both Cretaceous and Eocene samples ranging from +0.5 to +17 (Fig. 11a, b). A few grains have negative values ranging from 31 to -1. The majority of the ϵ_{Hf} values are located between the depleted mantle and chondritic lines, with a few grains below the chondritic line.

Discussion

Depositional environments and refinements of IMR regional stratigraphy

Triassic flysch

The United Nations (1979a) mapping project identified Triassic flysch exposed in the IMR. The Triassic age of the Pane Chaung Formation is based on the rare occurrence of *Halobia* fossils (Gramann, 1974; United Nations, 1979a; Bannert et al., 2011; Yao et al., 2017; Zhang et al., 2017), and detrital zircon U-Pb dating (Sevastjanova et al., 2016; Yao et al., 2017; this study). In

the southern IBR along the Gwa road section, ultramafic rocks are thrust over sediments (Zhang et al., 2018, their Fig. 13), that are of either Triassic (Pane Chaung Formation; p. 32 in United Nations, 1979a, and their Fig. 20) or Eocene (Zhang et al., 2018; their Fig. 11c) age. Detrital zircons from a flysch sample (KM76a) collected in close proximity to the eastern margin of the ultramafic rocks at this locality have an age profile similar to other Pane Chaung Formation samples, and are considered to be Triassic, supporting the interpretations of the United Nations (1979a). We also consider it likely that the western margin of the ultramafic rocks is thrust over Triassic sediments (on the basis of Figure 20 in United Nations 1979a), although a few kilometers further west, Zhang et al., (2018) have reported Eocene plant fossils and detrital zircons, so it is possible that Eocene sediments are also present in some areas along this boundary. The discontinuous nature of ultramafic rocks and Triassic sediments in the IMR, leads to considerable uncertainty in mapping the extent of the Pane Chuang Formation but detrital zircon analysis provides a clear path forward to reconstructing the occurrence and extent of the Triassic flysch.

Jurassic-Early Cretaceous deposition

The abundant and well-preserved Upper Jurassic radiolarians from chert associated with the Kalemio Ophiolite provide age constraints on the timing of deep-marine sedimentation in this portion of the Naga-Andaman suture zone (Plate 2). Based on the radiolaria, chert sample KM37b was probably deposited during the mid-late Oxfordian to late Kimmeridgian/early Tithonian interval. The age of this chert sample from the Kalemio Ophiolite is broadly consistent with previous biostratigraphic results from the same area, that yielded a Jurassic–Cretaceous radiolarian fauna with a likely Middle Jurassic age (Zhang et al., 2018). Reworked

chert pebbles of Callovian–Kimmeridgian age in the Pondaung Formation in the Central Myanmar Basin have been inferred to have been derived from the Kalemio Ophiolite (Suzuki et al., 2004) and are consistent with the biostratigraphic ages reported here and in Zhang et al. (2018). A Middle–Late Jurassic age for the cherts is also consistent with radiometric dating (U–Pb ages and K–Ar ages) of the Kalemio Ophiolite that suggests an Early Cretaceous age for the ophiolite itself (Mitchell, 1981; Liu et al., 2016; Zhang et al., 2018). Importantly, these biostratigraphic and radiometric results from the Kalemio Ophiolite are comparable to temporal constraints of deep-marine sedimentation from the Nagaland ophiolite (e.g. Baxter et al., 2011; Sarkar et al., 1996; Aitchison et al., 2019) and ophiolites in Tibet (e.g. Xialu, Zedong, Zhongba) (Matsuoka et al., 2002; Aitchison et al., 2007a,b; Li et al., 2013), and, thus, consistent with an hypothesis that Kalemio, Nagaland and Indus Yarlung Tsangpo Suture Zone (IYTSZ) ophiolites were once part of the same Neo-Tethyan ocean floor (Fig. 12a, b).

Jurassic to Lower Cretaceous sediments are only demonstrably known from the radiolarian cherts associated with the Nagaland-Manipur and Kalemio ophiolites (Baxter et al., 2011; Zhang et al., 2018; Aitchison et al., 2019). Other than these occurrences, there appears to be an almost total absence of Jurassic–Lower Cretaceous sedimentary rocks in the IMR (Bannert et al. 2011), although this might be due to a lack of fossiliferous sediments. Recently published detrital zircon analyses from the Pane Chaung Formation indicate maximum depositional ages are predominantly Late Triassic, together with some Early Jurassic ages for a small number of grains (Sevastjanova et al., 2016; Yao et al., 2017). Hence, upper portions of the Pane Chaung Formation extend into the Lower Jurassic. Kyi Khin et al. (2022) interpreted the presence of Jurassic greywackes in the IMR, but their extrapolation does not seem to be supported by detrital

zircon or biostratigraphic ages, for which further work is required. Although Early Cretaceous-age zircons are present in the Upper Cretaceous Falam Formation, it has not been possible to identify any Lower Cretaceous clastic sediments in the IMR.

Paleogene deposition

The rarity of Cretaceous-Paleogene planktonic foraminifers suggests microfossils are generally diluted by the clastic input in the IMR 'flysch' facies. Also, presumably some degree of post-depositional removal took place by diagenesis/dissolution. Three mudstone samples mapped as Cretaceous (IBR98, IBR103, IBR108) contain Cretaceous planktonic foraminifers, however detrital zircon U-Pb dating of sandstone samples (IBR102, IBR110A) in the same unit, yields Paleogene detrital zircons, with the youngest population indicating assignment of a Lutetian, (or younger), depositional age. This suggests that either the Cretaceous planktonic foraminifera were reworked into younger sediments or that some unrecognized structural complexity exists that juxtaposes Cretaceous fossil-bearing strata with Eocene units. We favour the first hypothesis, given that previous authors have also noted the allochthonous nature of some of the Cretaceous outcrops and the reworking of some Cretaceous fossils into Cenozoic units (Gramann, 1974; Bender, 1983). Brunnschweiler (1966) suggested that the bulk of the flysch is not older than Eocene based upon the youngest fossils known at that point. In contrast to the samples mapped as Cretaceous, Paleogene sandstones yield youngest zircon age populations that are consistent with their mapped age.

Flysch source terranes

Upper Triassic provenance

Sandstone compositions in the Pane Chaung Formation indicate a recycled orogenic provenance. This is further supported by a broad spread of zircon U-Pb age distribution in sandstones, indicating contributions from multiple sources, which is also diagnostic of mixed provenance and reworking. The Upper Paleozoic-Lower Mesozoic Pane Chaung zircon grains have euhedral to subhedral morphologies and well-developed oscillatory compositional zoning, suggesting a contemporaneous volcanic provenance. Upper Paleozoic-Lower Mesozoic zircons have a wide range of ages from ~300 Ma to 200 Ma, and ϵ_{Hf} values from -6 to +11 (Yao et al., 2017), suggesting magma contribution from a juvenile source. The youngest zircon grains approximate the depositional age of samples, which confirms the existence of contemporaneous volcanic activity, corroborated by abundant mafic to intermediate volcanic lithic fragments and plagioclase. The combination of evidence from Upper Triassic sandstones indicates a long-lived magmatic-arc source.

Four models have been proposed to explain the source terrane for the Pane Chaung Formation. Model A: during the Triassic West Myanmar was part of the Sibumasu terrane or part of a neighbouring terrane (Sevastjanova et al., 2016; Zhang et al., 2018), Model B: West Myanmar lay adjacent to the future NE part of India in northern Gondwana received sedimentary detritus from sources to the south (Wang et al., 2016); Model C: West Myanmar lay adjacent to the future NE part of India in northern Gondwana received sediment derived from the future eastern Australia Plate, to the east (Cai et al., 2016; Yao et al., 2017; Fang et al., 2018), Model D: West Myanmar received sediment sourced from the eastern future Australian Plate and rifted from the northern Australian margin at a location attributed to Argoland (Zhang et al., 2021). These models imply three significantly different scenarios for the tectonic position of the WMT and its subsequent

evolution and will be discussed individually. In order to assess these models, published U-Pb and Hf isotopic analyses for detrital zircons in the age-equivalent sandstones in the Sibumasu terrane, Lhasa terrane, northwest Australia, and the Langjiexue Formation of southern Tibet are reviewed and compared to the new and published data from the Upper Triassic Pane Chaung Formation (Fig. 13).

In model A (Sevastjanova et al., 2016), the Upper Triassic Pane Chaung Formation was part of SE Asia prior to the Indosinian orogeny, with perhaps a close affinity to Sibumasu sandstones. In this view, the Pane Chaung Formation cannot be associated with the Indian Plate. However, the age spectra of detrital zircons from Upper Triassic-Lower Jurassic sandstones exposed in the Loi-an Group (or Shweminbon Group) of the Sibumasu terrane (Cai et al., 2017) are significantly different from those from the Pane Chaung Formation (Fig. 13). Both units contain Triassic zircons, but as discussed in Morley et al. (2020) key peaks in the Pane Chaung Formation occur at around 500-700 Ma, and 1000-1200 Ma correlating with troughs in the Loi-an Group. Similarly, while peaks for the Loi-an Group occur at around 400-500 Ma, 700-900 Ma, and 1800-1900 Ma, these time intervals are represented by troughs in the Pane Chaung Formation (Sevastjanova et al., 2016; Yao et al., 2017; Cai et al., 2017; this study). This suggests the Pane Chaung and Sibumasu terranes were not derived from the same source area. However, to be more certain of this conclusion, a broader spectrum of samples from the Loi-an Group needs to be analysed. A further issue is that an early position in SE Asia fails to explain how the Lower Cretaceous amber deposits, in the northern WMT preserve an extensive flora and fauna of Gondwana origin, which implies rifting of the WMT from Gondwana in the Early Cretaceous (Poinar, 2019).

In model B (Wang et al., 2016), Upper Triassic turbidites of the Langjiexue Group, exposed south of the IYTSZ in southern Tibet, have similar petrographic composition, biostratigraphy and yield broadly similar U-Pb age spectra for detrital zircons (Fig. 13) and ϵ_{Hf} values (Yao et al., 2017) as to the Pane Chaung Formation. Coupled U-Pb age and Hf isotopic signatures of detrital zircons in the Pane Chaung differ from those of Upper Triassic sandstones of the Sibumasu and Lhasa terranes, but instead are similar to the Langjiexue Group in the northern Tethys Himalaya. Paleocurrent directions from the Langjiexue Group indicate WNW-directed sediment transport (Wang et al., 2016). Unfortunately no reliable paleocurrent data exist, nor could they be measured in the field, for the Pane Chaung Formation for comparison. The Langjiexue Group was originally deposited along or adjacent to the northern passive continental margin of the future Indian continent region of northern Gondwana in a deepwater fan system (Wang et al., 2016), where the Pane Chaung Formation was derived from the eastern part of the system. A plausible sediment source was a distant Gondwanide Orogeny to the south generated by Pan-Pacific subduction beneath the southeastern margin of Gondwana with the sediment-routing system from the east (Wang et al., 2016). This model implies the Pane Chaung Formation was either part of the future NE Indian continental margin within northern Gondwana or adjacent to NE India.

In model C (Cai et al., 2016; Yao et al., 2017), the Pane Chaung was deposited on a huge submarine fan extending from NW Australia to the NE India continental margin on the northern margin of Gondwana. This scenario shows a location for the Pane Chaung Formation, adjacent to NE India, similar to that proposed by Wang et al. (2016), but the sediment source area is

different. In the model of Cai et al. (2016) and Yao et al. (2017) the extent of the sedimentary system incorporating the Langjiexue Group is a vast region north of the future Australian Plate on northern Gondwana, with the sediment sourced primarily from the ESE (including the Birds Head region). Fang et al. (2018) propose a similar source area, but the submarine fan is of much smaller extent (similar to Wang et al., 2016). The Langjiexue Group in this scenario lies at the SW limit of a fan on the future northern Greater India, while the Pane Chaung Formation lies just to the south. This scenario is based mainly on similar Permian-Triassic detrital zircon populations in the Pane Chaung Formation and age-equivalent rocks from the Bird's Head in western Papua and Mungaroo Formation in the Carnarvon Basin on the NW Shelf of Australia. However, in detail there are several differences in the zircon-age spectra (Wang et al., 2016). The Bird's Head samples yielded ages dominantly between 280 and 200 Ma, with less than 15% Early Paleozoic-Precambrian ages (Gunawan et al., 2012). A striking feature of the Pane Chaung sandstones is a large Permian-Triassic zircon population, but the Carnarvon Basin data shows these ages are only from a very small population of the total number of zircons (Lewis and Sircombe, 2013). Zircons in the Carnarvon Basin display notable age clusters at 1000-1250 Ma and 1500-1850 Ma that are rare in the Pane Chaung Formation. Cr-spinel is present in the Pane Chaung, whereas in Western Australia Cr-spinel is rare (Sevastjanova et al., 2016).

In Model D, West Myanmar is located on the northern Australian margin, and is considered to represent a continental block that fits into the area from which Argoland is proposed to have rifted (Zhang et al., 2021). The sediment source area for the Pane Chaung Formation is similar to model C. The link with the Langjiexue Group is minimized, which is a potential weakness with the model.

The close affinity of the Pane Chaung Formation with the Langjiexue Group (models B and C), and paleomagnetic data (Westerweel et al., 2019) support post-Triassic rifting of a continental (and oceanic?) terrane upon which the Pane Chaung Formation was deposited (Fig. 14).

Furthermore, this fragment was probably bearing Gondwana flora and fauna, suggesting that rifting occurred in the Early Cretaceous (Poinar, 2019). This terrane could be the Indian Plate, the WMT, or a small continental fragment (the Mount Victoria Block) that is postulated to have collided with the WMT in the mid-Cretaceous (Mitchell, 1993; see discussions in Morley et al., 2020; Licht et al., 2021). These different tectonic models are further discussed in the subsequent sections.

Upper Cretaceous – Paleogene provenance

A broad similarity in the U-Pb zircon ages distribution and Hf isotope compositions for Upper Cretaceous – Paleogene samples in the IMR and CMB (Fig. 15) appears, at first, to suggest that sediments were derived from the same source as those in the CMB, i.e., from the Wuntho-Popa Arc (e.g. Allen et al., 2008; Wang et al., 2014; Tin Tin Naing et al., 2014; Licht et al., 2019; Zhang et al., 2019; Najman et al., 2019). However, the Kalemmyo-Nagaland suture zone, which we correlate with the Himalayan Indus-Yarlung Tsangpo suture, containing Jurassic and Cretaceous ophiolites, deep ocean sediments and volcanics, points to the IMR being separated from the CMB. This suture finally closed at c.50 Ma (Green et al., 2008) or even 60 Ma (Kapp and DeCelles, 2019), suggesting that prior to closure the IMR were separated from the CMB by the closing Neo-Tethys ocean. However, there is significant provenance and stratigraphic evidence to suggest that the closure was complex and there is conflicting evidence for regarding how closure occurred.

The provenance of sediments in the CMB has largely been assessed through petrography, zircon, titanite and apatite U-Pb dating and geochemistry, rutile geochemistry, and Sr-Nd bulk analysis to identify arc-derived sediment input from continental crust-derived input (Wang et al., 2014; Licht et al., 2013, 2014, 2018; Cai et al., 2020; Arboit et al., 2021; Zhang et al., 2021; Najman et al., 2022). Commonly in these studies the arc component is thought to be derived from the Wuntho-Popa arc, while the crustal component is considered to be derived from the Himalayas or the Mogok Metamorphics, along with the Kanpetlet Schists and Pang Chaung Formation. While there is widespread agreement in these studies that the Paleocene-middle Eocene sediments contain a significant component of material derived from the Wuntho-Popa Arc, there is more divergence of interpretation for provenance of the post-middle Eocene section, which shows more crustally-derived sediment. In particular whether the Mogok Metamorphic rocks were a key early source for sediment or not, is disputed. A late Middle Eocene to Late Eocene arrival of Mogok Metamorphic Belt-sourced sediments in the CMB has been proposed by Licht et al. (2019) Zhang et al., (2021), Arboit et al. (2021), while Westerweel et al. (2020), Morley et al. (2021) and Najman et al. (2022) considered that the early metamorphic component was derived from within the WMT (for example, the Naga Metamorphic complex). One major issue for the Mogok Metamorphic rocks being an Eocene-Oligocene sediment source is that at this time these rocks were experiencing amphibolite to granulite grade regional metamorphism (e.g. Searle et al., 2007, 2020; Lamont et al., 2021). Exhumation and retrograde metamorphism only occurred after c. 30 Ma (Searle et al., 2017) and in places after 20 Ma (Lamont et al., 2021). Even during the Early Miocene micas were forming in basement rocks of the Shan Scarp during deformation at temperatures between 250 and 300°C (Bertrand et al., 2001). In contrast, derivation of zircons from the Naga Metamorphics to the south of Mt Saramati (i.e. within the

WMT) seems more plausible than the Mogok as these schists and gneisses containing Early Ordovician-age zircons were uplifted and eroded by the Eocene (Aitchison et al., 2019). The Katha Metamorphic rocks, to the north of Mogok, have been suggested as a possible additional source of sediment to the CMB but this seems unlikely given that they were exhumed relatively late, between 40 and 15 Ma (Myo Min et al., 2022).

Detailed comparison of the IMR and CMB data shows petrographic, zircon-age spectra and Hf isotope data exhibit several subtle differences between the Upper Cretaceous samples from the two regions. Samples from the Upper Cretaceous Kabaw Formation in the CMB fall in the undissected arc and indicate the Wuntho-Popa Arc (WPA) was the proximal magmatic arc source (Cai et al., 2019; Wang et al., 2014; this study). Upper Cretaceous Falam Formation sandstones from the IMR contain less abundant volcanic lithics compared to the CMB (Fig. 6e, f) and indicate a recycled orogenic provenance falling in the transitional and undissected arc fields (Fig. 7). However, the more distal position of the Falam Formation can explain the difference as loss of the more unstable volcanic lithic component during transport. When considering details of the zircon-age spectra, the Kabaw and Falam formations display prominent peaks at 110-90 Ma (Fig. 16a, b). Cretaceous CMB zircons have entirely positive ϵ_{Hf} values, Cretaceous zircons from the IMR are also characterized by positive ϵ_{Hf} values, indicating a juvenile mantle source. However, a few grains with negative ϵ_{Hf} values, indicative of re-melting of older crust are also present in the IMR samples (Fig. 16e, f). Therefore, detrital zircon characteristics of the Upper Cretaceous Falam Formation are slightly different from those of the Kabaw Formation. The new provenance data from the Falam Formation indicate detritus from contemporaneous volcanic rocks mixed with sediment recycled from older siliciclastic units. The

maximum depositional age (84 ± 1 Ma) determined from zircon geochronology is close to the actual depositional age of the sediments, and indicates contemporaneous magmatism played an important role in the morphological evolution of the source region. Recently published U-Pb zircon and whole rock Ar-Ar ages for the Mawgyi volcanics from the Wuntho Ranges include ages between 110 - 90 Ma and 46 - 32 Ma (Li et al., 2019; Westerweel et al., 2019; Licht et al., 2020, Fig. 10) but Upper Cretaceous zircons younger than 85-90 Ma are unknown (Licht et al., 2020).

Mitchell (1992, 1993) interpreted the Mawgyi Nappe as an intra-oceanic arc that was emplaced onto the western margin of SE Asia along with the Woyla Arc of Sumatra during the mid-Cretaceous. In this model the CMB/Myanmar Terrane (“Burma Terrane” in Mitchell, 1992, 1993) did not exist as a separate entity during the Cretaceous. However, palaeomagnetic data indicate the Myanmar Terrane was a separate entity during the Cretaceous, and was too far south in the Cretaceous to be part of the SE Asian margin (Westerweel et al., 2019). This model is incompatible with the Mawgyi Nappe model. The peak of WPA volcanism (including Mawgyi volcanics) around 100 Ma indicate active subduction in the vicinity of the IMR/CMB. Therefore, the Mawgyi volcanics are most likely part of the WPA and can probably be correlated with the intra-oceanic mid-Cretaceous Woyla Arc. The onset of the Woyla Arc collision with Sumatra at 113 Ma (Advokaat et al., 2018), occurred close to the time at which the Aptian-Cenomanian Limestone unconformity developed, and formation of the metamorphic sole in the Inner Belt of IMR (Zhang et al., 2017) indicating a possible link between the unconformity, ophiolite emplacement and the Woyla Arc collision. In their 2020 interpretation Morley et al. proposed that the Mt Victoria Terrane collided with the western side of the WMT, and that the ophiolites

are unconformably overlain by Aptian-Cenomanian limestones (Mitchell, 1993). Deposition of the Falam and Kabaw formations initiated around 84 Ma and both unconformably overlie Mesozoic IMR units (Kanpetlet Schists, Pane Chaung Formation). This unconformable relationship indicates that by the Late Cretaceous the Inner Belt of the IMR and the CMB were part of the same plate (Morley et al., 2021). Therefore, the Falam Formation was derived mainly from the Wuntho Ranges, with subordinate input from a more crustal source, potentially Ordovician Nagaland metamorphic rocks (Aitchison et al., 2019).

Allen et al. (2008), Tin Tin Naing et al. (2014) and Najman et al. (2019) suggested that Paleogene sandstones of the IMR were derived predominantly from the WPA to the east, rather than off-scraped Himalayan-derived Bengal Fan material as earlier work proposed (Curry, 2005). This conclusion is based on the more arc-like provenance signatures as evidenced by petrography and proportions of arc-derived Mesozoic-Paleogene zircons. Comparison of the IMR data with that of the CMB (Wang et al., 2014; Tin Tin Naing et al., 2014; Licht et al., 2019; Zhang et al., 2019; Cai et al., 2019; Arboit et al., 2021; Najman et al., 2020, 2022; this study) shows that in the Paleogene, age spectra for the IMR and CMB are similar. However, a detailed comparison indicates differences in zircon-age spectra. Detrital zircons from Paleogene sandstones in the IMR display a notable age peak at 90 Ma whilst the CMB has a major age peak at 90 Ma and a lesser peak at ca. 60 Ma (Fig. 16c, d). Zircon U-Pb age clusters for the IMR match well with the WPA magmatism (Mitchell et al., 2012; Gardiner et al., 2015, 2016; Zhang et al., 2017). New and published (Tin Tin Naing et al., 2014) Hf-isotope data from Cretaceous-Eocene zircons from the IMR show ϵ_{Hf} values are predominantly positive, with a few grains with negative ϵ_{Hf} values (Fig. 16e, f). This IMR signature contrasts somewhat with data from

the CMB (Wang et al., 2014; Zhang et al., 2019). On QFL and LmLvLs plots, Paleogene sandstones from the IMR lie within the magmatic arc field (Fig. 7b, c). New data and previously published work (Allen et al., 2008; Tin Tin Naing et al., 2014; Najman et al., 2019) clearly show additional older crustal material identified in petrography as low-grade metamorphic and siltstone lithic fragments, by negative ϵ_{Hf} values, and the presence of Palaeozoic and older zircons and older fission track ages. These data all indicate that the Paleogene IMR contains a significant component of arc-derived material from the WPA, with a subordinate component of crustal-derived material from the Kanpetlet Schists and Naga metamorphic basement. If the palaeomagnetic model of Westerweel et al. (2019) is viable, then the Palaeozoic and older 'Myanmar basement' that provided the old zircons could not have been the Shan Plateau region as the separation from the IMR involved several hundred kilometers width of oceanic crust between the two regions.

The peak of c. 100 Ma age for zircons of arc-affinity strongly indicates the Wuntho-Popa Arc as a source for the Falam Formation. The absence of older zircons is also significant in eliminating the possibility of any Indian source. These observations are important because it is commonly considered that the deepwater, shale-prone Falam and Chunsang formations are lateral equivalents of the Disang Formation in India. However, as discussed here, they are predominantly sourced from the WMT (i.e. they occupied an upper plate position) while the Disang Formation appears to be predominantly sourced from India (Aitchison et al., 2019; Lin et al., 2022) (Fig. 15), (i.e. a lower plate position). These conclusions are based on relatively few studies of a limited number of samples from geographically restricted areas and a lateral

transition between these India and WMT-sourced deepwater deposits involving mixed sources likely exists, perhaps in the Manipur area.

The difference in source area for Falam and Disang formations is critical in respect of origins of the Pane Chaung Formation. The Indian provenance of the Disang Formation makes it possible to argue that the Pane Chaung Formation is part of the Indian margin that collided with the WMT in the Cenozoic. The presence of the WMT-derived Falam Formation overlying, and to the west of the Pane Chaung Formation implies this Triassic formation was present on the WMT margin prior to the Late Cretaceous, and therefore unlikely to have been part of the leading edge of India.

Relationship to the Indus-Yarlung Tsangpo Suture Zone

It is debated whether two ophiolite belts (Kalemyo ophiolite/Western Ophiolite Belt, and Myitkyina ophiolite/Eastern Ophiolite Belt) within Myanmar belong to a single suture, and furthermore, their relationship with the Indus-Yarlung Tsangpo Suture Zone (IYTSZ) in the Tibetan Plateau is not clear (Mitchell, 1993; Yang et al., 2012; Morley et al., 2021). Recent radiometric dating and geochemical studies on ophiolites in Myanmar and Tibet are summarized in Table. 2.

The Nagaland – Kalemyo zone of ophiolites of the IMR (the Western Ophiolite Belt) contains fragments of Cretaceous oceanic lithosphere, Mesozoic radiolarian cherts, alkali volcanic rocks and mélanges very similar to the IYTSZ in Tibet. Mineralogical and geochemical characteristics of the Nagaland – Kalemyo zone of ophiolites indicate both mid-ocean ridge and

suprasubduction zone affinity types are present (Ghose et al., 2014; Liu et al., 2016; Zhang et al., 2018), similar to ophiolites along the IYTSZ (Table 2). Moreover, the discovery of well-preserved Middle Jurassic–Late Jurassic radiolarian assemblages from the Kalemio ophiolite (Zhang et al., 2018; this study), and Naga ophiolite (Baxter et al., 2011; Aitchison et al., 2019), and Early Cretaceous assemblages from the Manipur Ophiolite (Aitchison et al., 2019) provides age constraints on deep-marine sedimentation that are consistent with those reported from ophiolites in Tibet (Fig. 12a, b) and reinforces the hypothesis that these ophiolites were once part of the same Neo-Tethyan ocean floor. Comparison of the timing of events in the IYTSZ (e.g. reviews in Hébert et al., 2012 and Kapp and DeCelles, 2019) with those in the IMR is instructive. Kapp and DeCelles (2019) proposed the following key events associated with the IYTSZ. 1) Jurassic ophiolites formed in a forearc or an intra-oceanic arc setting (e.g. McDermid et al., 2002; Aitchison et al., 2007b). 2) Lower Cretaceous ophiolites formed in a proximal position to the Lhasa Terrane, in a forearc extensional or an intra-oceanic arc setting (e.g. Hébert et al., 2012), including local developments within Jurassic oceanic crust, possibly related to subduction re-initiation, or due to slab rollback. 3) A 120–105 Ma high intensity magmatic belt developed, coeval with widespread marine limestone deposition over the Lhasa Terrane. This magmatic event is not seen in the Gangdese Arc. 4) A 90–80 Ma tectono-thermal event involving metamorphism and magmatism was followed by a quiescent period in the Gangdese arc between 78 and 72 Ma of uncertain origin, but possibly related to slab rollback, or subduction of a slab window. 5) Intra-arc or retro-arc shortening of the Gangdese magmatic arc, accompanied by metamorphism, and a high intensity magmatic event from 70–45 Ma, and shortening within the northern Lhasa and Qiangtang terranes. Initially this event was related to Cordillera style deformation that around 60 Ma probably evolved to India-Asia collision. The timing of these

elements in the IYTSZ (particularly, 1, 2 and 3) is very much in line with the IMR (Liu et al., 2016; Aitchison et al., 2019; Morley et al., 2020): 1) with the Jurassic events in the Inner Belt (Jurassic-aged chert), and 2) the ages of Kalemio and Nagaland oceanic lithosphere fragments formed 130-115 Ma, and 3) the occurrence of high pressure metamorphic rocks (i.e. blueschist, glaucophane schist, jadeitite, eclogite) in Nagaland and the Jade Belt. In a review of the Nagaland ophiolite data Bhowmik et al. (2022) concluded there is evidence for a collage of a Late Triassic to Middle Jurassic-age (c. 205-172 Ma) intra-oceanic (Neo-Tethys) subduction system as well as a later subduction system that ended with Indian-Myanmar collision during the Eocene. In Nagaland peak high pressure-low temperature metamorphism is estimated to have occurred c. 95 Ma, while retrograde metamorphism during shear-related exhumation is dated at c. 90 Ma (Maibam et al., 2022). The divergences between intense magmatic activity in the WMT (36-42 Ma and 90-108 Ma) and the Gangdese Arc (160-190 Ma, 40-60 Ma, 10-20 Ma) and North Lhasa Plutonic Belt (105-120 Ma, 15-25 Ma) are significant (Licht et al., 2020) for the later history of the region. Nevertheless similarities in the timing of events between the Kalemio ophiolite and Neo-Tethyan ophiolites suggest that the Western Ophiolite Belt is the southern continuation of the IYTSZ in the Tibetan Plateau (Liu et al., 2016a).

Tectonic models for the IMR and WMT

The position of the suture between India and Asia in Myanmar remains uncertain and different tectonic scenarios have resulted in three proposals for suture locations as follows (Fig. 17): 1) concealed beneath overthrust Cretaceous-Cenozoic deepwater sediments in the outer Indo-Myanmar Ranges (Fig. 17A-C location 1). 2) Along the Western and Eastern Ophiolite belts

(Fig. 17A-C location 2). 3) Between the “West Myanmar Block” and Sundaland (Fig. 17B location 3).

Location 1 is related to the interpretation that there is active subduction of oceanic crust and/or the underthrusting of the leading edge of India below the Indo-Myanmar Ranges, based mostly on geophysical data (seismicity, mantle topography, gravity) (Steckler et al., 2008; Yang et al., 2022). Location 1 can simply be viewed as a continuation of the suture in location 2 following westwards slab rollback and the addition of sediment to the distal part of the accretionary prism (Fig. 17B, C). Alternatively, Soquet et al. (2002) proposed a scenario where locations 1 and 2 were two distinctly separate sites of Cenozoic suturing. In this scenario Late Cretaceous-Paleocene obduction occurred between an eastern continental block comprising the Shan Plateau sequence of Sundaland and the Central Myanmar Basin area, and a micro-continent they referred to as the “Bloc Ouest Birman” that lay west of an ophiolitic suture (location 2, Fig. 17A). In this scenario their “Bloc Ouest Birman” is a different entity from the West Myanmar Terrane in this study, which is typically envisioned as underlying the Central Myanmar Basin area and lying predominantly east of the ophiolites (Fig. 17B; see discussion in Morley et al., 2021).

Location 2 is related to the presence of numerous ophiolitic fragments along the core region of the Indo-Myanmar Ranges (Western Ophiolite Belt). The characteristics of these fragments are quite similar to those described for the Indus-Yarlung Tsangpo Suture zone (see section “Relationship to the Indus-Yarlung Tsangpo Suture Zone”). It can be further argued that the Pane Chaung Formation is of Indian affinity (see section “Provenance of Upper Triassic

sequence”) and consequently immediately west of the suture are units related to India, while east of the suture are units related to West Myanmar (which in turn may have been attached to Sundaland). However, the situation is not that simple since the Falam Formation is predominantly sourced from the WMT (see section “Upper Cretaceous – Paleogene provenance”). Nevertheless location 2 has a number of basic attributes that make it an obvious candidate for the suture zone between India and West Myanmar.

Location 3 (Fig. 17B) approximately separates Sundaland to the east from the West Myanmar Plate to the west, yet there is no clear geological evidence for a suture zone. Virtually no outcropping ophiolitic rocks, or Neo-Tethyan oceanic domain rocks have been described along the trend. It is difficult to define where the West Myanmar Plate ends and Sundaland begins. The only well-defined boundary, is the transform margin along the Sagaing Fault which is predominantly a Neogene age feature. There are ultrabasic rocks found along the Sagaing Fault, but it is also possible to interpret the paired magmatic belts of Central Myanmar, and the western Shan Plateau region in terms of an Andean subduction model (e.g. Mitchell, 1993; Gardiner et al. 2015), which implies close proximity of the two terranes throughout the Cenozoic. In spite of these issues, palaeomagnetic data provides a key piece of evidence that forces location 3 to be considered potentially as a major suture. Samples from Late Cretaceous, and Paleogene igneous and sedimentary localities provide consistent data that shows the West Myanmar Terrane migrated from south of the equator during the Late Cretaceous to a location about 5° N in the Late Eocene (Westerweel et al., 2019, 2020), implying significant loss by subduction of Tethyan oceanic crust between West Myanmar and Sundaland during the Cenozoic (see discussion in Morley et al., 2021). There is a suggestion that a slab can be identified below the Shan Plateau

from mantle tomography that supports the existence of this suture (Yang et al., 2022) (Fig. 17D, E).

Of the three locations, location 2 possesses many elements common to other suture zones and is, thus, arguably, a good candidate to mark the suture between India and West Myanmar. To assess this idea further, consideration of the timing events at location 2 is key. The western margin of the Central Myanmar Basin shows a stratigraphic sequence that comprises: mid-Cretaceous *Orbitolina* Limestone (Paung Chaung Formation), which is overlain by the Upper Cretaceous, shale-prone Kabaw Formation and the upper Paleocene Paunggyi Conglomerate. These sequences extend under the Central Myanmar Basin (i.e. they are part of the West Myanmar Terrane), and also overlie the eastern margin of the Indo-Myanmar Ranges. Only the Manaung Chaung area in the Southern Chin Hills is cited as a locality where pillow lavas associated with the core region of the Indo-Myanmar Ranges are seen unconformably underlying the Paung Chaung Formation (United Nations, 1979a; Mitchell et al., 2010; Mitchell, 2017). However, given the inconclusive evidence for a clear unconformable contact one possibility for location 2 is that the Paung Chaung Formation does not unconformably overly the ophiolites but is in a faulted contact. Rangin et al. (2013) cited the occurrence of ophiolite clasts in the Kabaw Formation as evidence for Maastrichian-age obduction. However, the 115 Ma age for the metamorphic sole of the Kalemmyo ophiolite (Liu et al., 2016) is more consistent with the Paung Chaung Formation marking the time shortly after obduction, than the Kabaw Formation. The mapped unconformable contacts between the Paung Chaung Formation and both the Paung Chaung Formation and the Kabaw Formation are widespread (United Nations, 1979a; see review in Morley et al., 2020). While the Paung Chaung Formation unconformity can be seen from

geological maps but has no clear contact in outcrop (United Nations, 1979a), the Pane Chaung and Kabaw Formation unconformity is observable and documented from outcrop (Socquet, 2002; Rangin et al., 2013; Zhang et al., 2017; Cai et al., 2020). Triassic detrital zircon peaks, and the predominantly schist and quartz composition of clasts in conglomerates of the lower Kabaw Formation, suggest the sediment source was the Pane Chaung Formation and Kanpetlet Schists (Cai et al., 2020). This unconformable relationship is crucial, because it indicates that whatever tectonic entity the Pane Chaung Formation was deposited on (whether the leading margin of India, the Mt Victoria microplate, or the West Myanmar Terrane; see discussion in Morley et al., 2020), it was overlain by sequences related to the Central Myanmar Basin during the Late Cretaceous.

Although it is within the same belt as the Chin Hills and Kalemmyo ophiolites, the age of the Naga Ophiolite is different and also needs to be considered in an assessment of location 2 as a potential suture. The Naga Ophiolite is interpreted to have formed in a suprasubduction zone setting around 116 Ma based on the U-Pb zircon age of plagiogranites and gabbros (Singh et al., 2017; Aitchison et al., 2019), i.e. very close to the age of the metamorphic sole of the Kalemmyo Ophiolite. The Naga ophiolite assemblage has subsequently been thrust over a *mélange* that contains Paleogene-Eocene radiolarians (Aitchison et al., 2019). This ophiolite emplacement is interpreted to be related to the collision of Greater India within an intra-oceanic island arc around the Paleocene-Eocene boundary (c.55 Ma) (Aitchison et al., 2019). While it is feasible for emplacement of accretionary-type ophiolites to occur at any time during the life of an accretionary prism, we also have dating of a metamorphic sole (115 ± 1 Ma to 119 ± 3 Ma; Liu et al., 2016; Zhang et al., 2017) indicated Early Cretaceous emplacement, and stratigraphic

evidence for some of the ophiolites in Myanmar to have been emplaced during the Late Cretaceous (e.g. Mitchell, 1993; Mitchell et al., 2010; Rangin et al., 2013). Consequently, does the thrusting of the Naga ophiolite onto Palaeogene sedimentary units represent a Palaeogene episode of ophiolite emplacement, or thrusting re-working an older ophiolite emplaced during the Cretaceous as a consequence of the onset of the collision of India with West Myanmar? This phase of ophiolite thrusting and exhumation is capped by the Late Eocene-Early Oligocene Phokphur Formation, which was deposited in shallow marine to fluvial environments and contains abundant ophiolite fragments and detrital zircons from a Permo-Triassic source, possibly the Pane Chaung Formation (Aitchison et al., 2019) (Fig. 13).

Based on this discussion of the timing of events in both the western CMB margin and the Naga Ophiolite, it would, thus, appear that Location 2 marks a succession of ophiolite deformation events beginning at 115 Ma with the emplacement of the Kalemmyo ophiolite (Liu et al., 2016), followed by thrusting, uplift and erosion prior to deposition of the Paung Chaung Formation (Mitchell, 1993). Peak metamorphism and exhumation of blueschists occurred between 95 and 90 Ma (Maibam et al., 2022), with uplift and erosion during the Maastrichtian deposition of the Kabaw Formation (Socquet et al., 2002). Finally, thrusting of the Naga Ophiolite over Paleogene mélangé took place around 55 Ma (Aitchison et al., 2019). These disparate histories of the two ophiolites are consistent with a complex history of accretion on the western margin of the WMT.

The change from deepwater sedimentation to molasse sedimentation in the Indo-Myanmar Ranges began, in places, in the Late Eocene (e.g. Aitchison et al., 2019; see review in Morley et

al., 2020), which strongly indicates India and West Myanmar had collided by this time. Low temperature thermochronology, from three transects, which shows the timing of onset of exhumation, varies between c. 24 Ma (Kalemyo-Kennedy Peak transect), to c.50- 49 Ma (Mindat section) (Najman et al., 2022). These results are not straightforward to interpret in terms of the onset of deformation because cooling will largely be related to erosion which requires subaerial exposure, or extension, which would post-date compressional or transpressional deformation. Deformation will initially cause burial, not exhumation of a unit in the footwall of a major thrust. In a submarine wedge even the hanging wall of a major thrust might not be subject to significant erosion (action by currents and gravitational instability can cause some degradation). Consequently, what the cooling ages may indicate is a transition from submarine to subaerial exposure of parts of the wedge. The c. 50 Ma age for the exhumation of the inner area of the Indo-Myanmar Ranges suggests: 1) The timing of onset of India-West Myanmar collision was Early Eocene (Searle & Morley 2011; Najman et al., 2022). 2) The inner area of the Indo-Myanmar Ranges was close to sea level even before collision. 3) The outer Indo-Myanmar Ranges remained as a submarine wedge for much longer, into the Miocene. There are other possible causes for exhumation besides collision with the leading edge of Greater India, such as subduction of an unusually thick or buoyant piece of crust (e.g. a seamount, or Mid Oceanic Ridge) or an increase in sediment supply to the accretionary prism, such as the Bengal Fan (Najman et al., 2020). Other strands of evidence that support India-West Myanmar collision are: 1) the rapid northwards motion of West Myanmar from the Eocene to the Miocene based on palaeomagnetic data is best explained by coupling with India at c. 60 Ma (Westerweel et al., 2019, 2020). 2) The Palaeocene – early Miocene timing of metamorphism along the Mogok belt (Searle et al., 2020; Lamont et al., 2021), and the 40-30 Ma rapid exhumation of the Katha

Ranges, which lie between the Jade Belt and the eastern ophiolite belt, also supports Eocene-age continent-continent collision (Myo Min et al., 2022). Consequently, it is considered that location 2 fits well with Eocene collision between India and the West Myanmar Terrane.

From the above review Location 2 marks a long-lived zone where a major segment of the Neo-Tethys was closed during the Mesozoic and Paleogene. But it does not appear to have accommodated convergence and loss of significant oceanic crust from the Oligocene to Recent. That leaves convergence to be accommodated at location 3. As noted above there is virtually no geological evidence for a suture, it is very difficult to locate what constitutes the eastern boundary of the West Myanmar Terrane, and there are multiple possible scenarios for how the West Myanmar Terrane interacted with the Andaman Sea region that have been discussed in Morley et al. (2021) and Bandopadhyay et al. (2022). These various scenarios have such poor correlation with known geological events and tectonic elements in the Andaman Sea that they were not features of tectonic models for the area until the palaeomagnetic data forced such considerations (Morley et al., 2021). The solution of Bandopadhyay et al. (2022) helps resolve the issue of the absence of a suture in Myanmar, by having a Paleocene-early Eocene collision of the WMT with the Andaman Islands. But there remains little direct geological evidence for such a collision, and for the scenario to be feasible, the palaeomagnetic data of Westerweel et al. (2019) was re-interpreted so that the positions of the WMT, most critically for the Oligocene, lie further north than the original interpretation. While the provenance data for the East Andaman Flysch is compatible the WMT being one of the sources (Bandopadhyay et al., 2022) (Fig. 15), it does not resolve whether this source lay to the west (Bandopadhyay et al., 2022) or to the north (Morley et al., 2021) of the Andaman Islands.

A possible tectonic scenario is shown in Figure 18. Since the Kabaw Formation unconformably overlies the Pane Chaung Formation on the western margin of the IMR, and the Falam Formation is sourced from the WMT, it is necessary for the Pane Chaung to be part of the West Myanmar Terrane prior to the Late Cretaceous. Hence the West Myanmar Terrane is shown as being close to India, perhaps in a rifted setting, and the Pane Chaung Formation was deposited across the rift on both the Indian and West Myanmar Terrane margin (Fig. 18A). Subsequently, subduction below West Myanmar incorporated the Pane Chaung Formation in an accretionary prism, where slivers of ophiolite were emplaced, and Jurassic oceanic sediments were incorporated into accretionary *mélange* (location 2, Fig. 17; Fig. 18B). During the mid-Cretaceous the West Myanmar Terrane underwent uplift, possibly as a consequence of magmatic underplating (collision with the Mount Victoria Terrane, subduction of a slab window, or seamount are other possibilities; Fig. 18C), and the Paung Chaung Formation carbonates were deposited over part of the accretionary prism. The accretionary prism built out oceanward as the Falam and Chunsang formations, predominantly sourced from the West Myanmar Terrane (this study, Allen et al., 2008; Tin Tin Naing et al., 2014; Najman et al., 2020), built out over oceanic crust (Fig. 18D). The Palaeogene part of the Disang Formation, in India, may be equivalent to the Chunsang Formation, and shows evidence for both a far-travelled sediment source from India, and a closer sediment source from the core region of the IMR to the east (Imchen et al., 2014). During the Early Eocene the highly extended leading edge of the Indian continent began to collide with the West Myanmar Terrane (Fig. 18E). The coupled India-West Myanmar Terrane also began its highly oblique convergence with the Shan Plateau region of the Sibumasu

terrane on the western Sundaland margin (location 3 Fig. 17B). Evolution into a transform margin marked by the Sagaing Fault began during the late Cenozoic (Fig. 18F).

Conclusions

Determining the age of deep water sandstone-shale sequences in the Inner IMR remains problematic. Detrital zircon age spectra for sandstones provide a useful check of lithostratigraphic and biostratigraphic correlations. The mapped extent of Palaeogene strata has been modified by recognition of the Triassic Pane Chaung Formation in the southern IMR (Gwa Road section area) and the discovery of Paleogene-age detrital zircons within rocks previously thought to be of Late Cretaceous in age (Padaung-Taungup Road section). Detrital zircons confirm an Eocene age for the Kennedy Sandstone with a maximum depositional age of 43 ± 2 Ma. Radiolarian cherts from the Yazagyo Dam area indicate Late Jurassic (U.A. Zone 9-11) biogenic deposition on oceanic crust and represent a rare record of sedimentation between that of the thicker clastic deepwater deposits of the Pane Chaung Formation (Upper Triassic-Lower Jurassic?) and the Upper Cretaceous Falam Formation.

Provenance analysis of the Pane Chaung Formation supports correlation with the Langjiexue Group in the northern Tethys Himalaya, considerably reducing the number of viable tectonic models for the origin of the IMR/West Myanmar Terrane. The Pane Chaung Formation was deposited on the northern margin of India, or on a continental block adjacent to India, and rifting of that continental fragment from Gondwana can only have occurred during the Jurassic or Early Cretaceous. Whether the Pane Chaung Formation was part of West Myanmar from inception, or a later accreted continental fragment (Mt. Victoria Land) remains uncertain. The Western

Ophiolite Belt represents the southern extension of the IYTSZ although its interpretation is complicated by the highly oblique convergence of the WMT with SE Asia.

Provenance of the Upper Cretaceous Falam Formation and Palaeogene section is inferred to be predominantly from the WPA and Inner Belt, with a secondary continental source that is probably the Naga Metamorphic-type basement. There is no indication of, or need for a source related to Eurasia or India for sediments deposited in the IMR during the Late Cretaceous-Eocene.

Declaration of competing interest

The authors declare that they have no known competing financial interests or personal relationships that could have appeared to influence the work reported in this paper.

Acknowledgements

This research is a part of the first author's PhD dissertation submitted to the Department of Earth Sciences, University of Oxford, UK in 2020. This work was primarily funded by Ophir Energy, London, the University of Oxford, and NERC Centre for Doctoral Training in Oil & Gas. The research was supported by a NERC Isotope Geosciences Facility grant in kind (IP-1778-1117). We thank Day Wa Aung and Tun Naing Zaw, University of Yangon and Saw Mu Tha Lay Paw for their help in planning and organizing the fieldwork. We thank Alexis Licht, Khin Zaw, and Jonathan Aitchison for very helpful and constructive reviews that helped improve the manuscript.

Figure Captions

Figure 1. Simplified geological map of Myanmar (Burma) from the eastern Himalayan syntaxis area south to Mergui, modified after Searle et al., 2007.

Figure 2. (a) Simplified geological map of Myanmar (Burma), dots show sample locations and squares show study areas. (b) Outline geological map of Rakhine area (modified from United Nations, 1979a), showing broadscale distribution of geological units and sample locations. For simplicity, the prefix 'IBR' is omitted from all sample labels on the map.

Figure 3. (a) Outline geological maps of Mt. Victoria area (modified from United Nations, 1979a; Mitchell et al., 2010), showing broadscale distribution of geological units and sample locations, and (b) Geological cross-section across the Mt Victoria belt (modified after Mitchell, 1993; Searle et al., 2017). See Fig. 2a for location.

Figure 4. (a) Outline geological maps of Kalemryo area (modified from United Nations, 1979a; Mitchell et al., 2010), showing broadscale distribution of geological units and sample locations, and (b) Geological cross-section along the Kalemryo-Falam road based on field observations. Z = hypothetical strike-slip faults driving uplift of Pane Chaung Formation. In the figure, around location X to help minimize the westwards thickening of the Palaeogene section (modified after Morley et al., 2020). See Fig. 2a for location.

Figure 5. Field photographs of outcrops sampled in the Indo-Myanmar Ranges. (a) Refolded recumbent fold in the Pane Chaung Formation, Mindat Road, (b) Kanpetlet Schists, Saw River, (c) Sub-vertical bedding in Falam Formation, Kalemryo-Falam Road, (d) Webula, serpentinised harzburgite, offset by strike-slip fault of probable Cenozoic age, (e) Palaeocene- Eocene Chunsang Formation, Falam-Kennedy Road, and (f) Eocene Kennedy Sandstone, Kennedy Peak. Red circle shows hammer place.

Figure 6. Photomicrographs of sandstones in the Indo-Myanmar Ranges: (a) Pane Chaung Formation, (b) Falam Formation, (c), (d) Eocene sandstones, and Central Myanmar Basin: (e) and (f) Kabaw Formation. Q = quartz, Pl = plagioclase, Ls = sedimentary lithic, Lm = metamorphic lithic, Lv = volcanic lithic, Z = zircon)

Figure 7. QFL and LmLvLs plots of the Indo-Myanmar Ranges and Central Myanmar Basin sandstones. (a) Sandstone classification following Garzanti (2016), (b) provenance and (c) LmLvLs fields following Dickinson (1985), and Garzanti (2019). QFL (quartz, feldspar, lithic fragments), LmLvLs (Lm-metamorphic; Lv-volcanic, Ls-sedimentary), Q = quartzose, F = feldspathic, L = lithic, IFQ = litho-feldspatho-quartzose, fLQ = feldspatho-litho-quartzose, lQF = litho-quartzo-feldspathic, fQL = feldspatho-quartzo-lithic, qLF = quartzo-litho-feldspathic, qFL = quartzo-feldspatho-lithic.

Figure 8. Histograms and kernel density plots, concordia diagrams and weighted average age diagrams showing detrital zircon U-Pb ages of the Pane Chaung Formation.

Figure 9. Histograms and kernel density plots, concordia diagrams and weighted average age diagrams showing detrital zircon U-Pb ages of the Falam Formation and Padaung – Taungup road section.

Figure 10. Histograms and kernel density plots, concordia diagrams and weighted average age diagrams showing detrital zircon U-Pb ages of the Kennedy Sandstone and Padaung – Taungup road section.

Figure 11. Detrital zircon U-Pb vs $\epsilon_{\text{Hf}}(t)$ data for Upper Cretaceous-Paleogene samples from the Indo-Myanmar Ranges. (a) is shown at 0–2200 Ma and (b) is shown at 0–250 Ma ages, see location on (a).

Figure 12. (a) Map of the Himalayan and Myanmar regions showing the location of Indus – Yarlung Tsangpo suture zone (IYTSZ) and Kalemryo – Nagaland suture zone (modified after Baxter et al., 2011), MBT, Main Boundary Thrust, IMR, Indo-Myanmar Ranges, TMB, Tagaung-Myitkyina Belt. The highlighted numbers are ten regions where radiolarians have been reported. (b) Chronostratigraphic chart summarizing the age constraints of deep-water sedimentation in the Neo-Tethys ocean.

Figure 13. Comparison of detrital zircon U-Pb data from the Pane Chaung Formation in the IMR (Sevastjanova et al., 2016; Yao et al., 2017; this study), with those from Langjiexue Group (Wang et al., 2016; Cai et al., 2016; Cao et al., 2018), Nagaland (Aitchison et al., 2019), Sibumasu (Cai et al., 2017), and Carnarvon Basin (Lewis and Sircombe, 2013). All ages are displayed in 20 Ma bins (0 to 3500 Ma). Ordinate axis indicates the number of detrital zircon ages in each bin on the abscissa. Bin size is 20 Ma.

Figure 14. Simplified Late Triassic palaeogeographic reconstruction illustrating our preferred scenario for provenance and depositional setting of the Pane Chaung Formation. Plotted on a stereographic projection that has been redrawn and modified from Sevestjanova et al., (2016), with additional information from Wang et al., (2016) and Aitchison et al., (2019).

Figure 15. Comparison of detrital zircon U-Pb data from the Indo-Myanmar Ranges (Allen et al., 2008; Tin Tin Naing et al., 2014; Najman et al., 2020; this study), with those from Central Myanmar Basin (Wang et al., 2014; Licht et al., 2019; Cai et al., 2019; Zhang et al., 2019; Arboit et al., 2021; Zhang et al., 2021; Najman et al., 2022; this study), Nagaland (Aitchison et al., 2019; Lin et al., 2022), and Andaman Flysch (Bandopadhyay et al., 2022). All ages are displayed in 20 Ma bins (0 to 3000 Ma, 400 to 3000 Ma) and 5 Ma bins (0 to 500 Ma). Ordinate axis indicates the number of detrital zircon ages in each bin on the abscissa. Bin size is 20 Ma.

Figure 16. Comparison of detrital zircon U-Pb ages and Hf isotopic data: (a) (b) Upper Cretaceous Falam Formation, IMR and Kabaw Formation, CMB, (c) (d) Paleogene units, IMR and CMB, and (e) (f) Upper Cretaceous – Middle Eocene Hf isotopic data from the IMR (Tin Tin Naing et al., 2014; this study) with those from the Central Myanmar Basin (Wang et al., 2014; Zhang et al., 2019). Ordinate axis indicates the number of detrital zircon ages in each bin on the abscissa. Bin size is 20 Ma.

Figure 17. Schematic cartoon cross-sections across the Indo-Myanmar Ranges from India to the Shan Plateau, illustrating the potential location of suture zones according to different tectonic models. A) West Myanmar Terrane model of Socquet et al. (2002), B) Independent West Myanmar Terrane model (e.g. Westerweel et al., 2019; Morley et al., 2020), C) West Myanmar Terrane as part of SE Asia since the Indosinian Orogeny (e.g. Sevastjanova et al., 2016; Morley, 2018). D and E results of mantle tomography study centered on Myanmar (redrawn from Yang et al., 2022). D) Time slice at 300 km. E) Depth section (see D for location). IMR = Indo-Myanmar Ranges, CMB = Central Myanmar Basin, SP = Shan Plateau, SF = Sagaing Fault. HV1 = high velocity zone 1, HV2 = high velocity zone 2 (interpreted as subducted slabs).

Figure 18. Tectonic model to explain the development of the Indo-Myanmar Ranges through time. CMB-FA = Central Myanmar Basin-Forearc, CMB-BA = Central Myanmar Basin-Backarc. Modified from Morley et al. (2020).

Plate captions

Plate 1. SEM images of microfossils and nannofossils from the Padaung-Taungup road section. Sample IBR108 consists species (a) and (c), IBR103 (b), IBR98 (d), (g) and (h), IBR06 (e), and IBR12 (f). (a) *Planohedbergella ultramicra* (Subbotina), (b) *Muricohedbergella planispira*

(Tappan), (c) and (d) *Planoheterohelix globulosa* (Ehrenberg), (e) *Chiloguembelina wilcoxensis* (Cushman & Ponton), (f) *Chiloguembelina ototara* (Finlay) (g) *Prediscosphaera columnata* (Stover), and (h) p for *Prediscosphaera columnata* (Stover) and w for *Watznaueria* sp..

Plate 2. SEM images of radiolarians yielded from a radiolarian chert sample KM37b associated to the Kalemio ophiolite. 1. *Zhamoidellum ovum* (Dumitrica), 2. *Fultacapsa sphaerica* (Ozoldova), 3,4. *Podobursa triacantha* (Fischli), 5. *Olanda* sp., 6. *Eoxitus dhimenaensis* (Baumgartner), 7,8. *Cinguloturris carpatica* (Dumitrica), 9. *Cinguloturris latiannulata* (Grill and Kozur), 10. *Higumastra* sp., 11. ? *Angulobracchia biordinalis* (Ozoldova).

Table Captions

Table 1. Detrital modes of samples analysed from Indo-Myanmar Ranges

Table 2. Summary of published data on ophiolite formation and emplacement

References

Acharyya, S. K., 1986. Tectono-stratigraphic history of Naga Hills Ophiolites, Geological Survey of India Memoirs 119, 94-103.

Acharyya, S. K., 2007. Collisional emplacement history of the Naga-Andaman ophiolites and the position of the eastern Indian suture. *Journal of Asian Earth Sciences*, 29, 229-242.

Acharyya, S. K., 2010. Tectonic evolution of Indo-Burma Range with special reference to Naga-Manipur Hills. *Geol Soc India Mem* 75:25-43.

Acharyya, S. K., 2015. Indo-Burma Range: a belt of accreted microcontinents, ophiolites and Mesozoic-Paleogene flyschoid sediments. *Int J Earth Sci (Geol Rundsch)* 104:1235-1251. DOI 10.1007/s00531-015-1154-6.

Advokaat, E.L., Bongers, M.L.M., Rudyawan, A., BouDagher-Fadel, M.K., Langerels, C.G., van Hinsbergen, D.J.J., 2018. Early Cretaceous origin of the woyla arc (Sumatra, Indonesia) on the Australian

plate. *Earth Planet. Sci. Lett.* 498, 348-361. Aitchison, J.C., Ali, J.R., Davis, A.M., 2007a. When and where did India and Asia collide? *Journal of Geophysical Research* 112, 1-19.

Aitchison, J.C., McDermid, I.R.C., Ali, J.R., Davis, A.M., Zyabrev, S.V. 2007b. Shoshonites in southern Tibet record Late Jurassic rifting of a Tethyan intraoceanic Island Arc. *Journal of Geology*, 115, 197-213.

Aitchison, J.C., Ao, A., Bhowmik, S., Clarke, G.L., Ireland, T.R., Kachovich, S., et al., 2019. Tectonic evolution of the western margin of the Burma microplate based on new fossil and radiometric age constraints. *Tectonics*, 38, 1718-1741. <https://doi.org/10.1029/2018TC005049>.

Ali, J.R., Aitchison, J.C., Chik, S.Y.S., Baxter, A.T., Bryan, S.E., 2012. Paleomagnetic data support Early Permian age for the Abor Volcanics in the lower Siang Valley, NE India: Significance for Gondwana-related break-up models. *Journal of Asian Earth Sciences*, 50, p. 105-115.

Doi:10.1016/j.jseas.2012.01.007.

Allen, R., Najman, Y., Carter, A., Barfod, D., Bickle, M.J., Chapman, H.J., Garzanti, E., Vezzoli, G., Ando, S., and Parrish, R.R., 2008. Provenance of the Tertiary sedimentary rocks of the Indo-Myanmar Ranges, Burma (Myanmar): Burman arc or Himalayan-derived? *Journal of the Geological Society*, London, 165, 1045-1057.

Arboit, F., Min, M., Chew, D., Mitchell, A., Drost, K., Badenszki, E., and Daly, J.S., 2021. Constraining the links between the Himalayan belt and the Central Myanmar Basins during the Cenozoic: An integrated multi-proxy detrital geochronology and trace-element geochemistry study. *Geoscience Frontiers*, 12, 657-676.

Audley-Charles, M.G., 1991. Tectonics of the New Guinea area. *Annual Reviews of Earth and Planetary Sciences* 19, 17-41.

Bandopadhyay, P., van Hinsbergen, D.J.J., Bandyopadhyay, D., Licht, A., Advokaat, E.L., Plunder, A., Dasgupta, A., Ghosh, B., and Trabucho-Alexandre, J., 2022, Paleogeography of the West Burma Block and the eastern Neotethys Ocean: constraints from Cenozoic sediments shed onto the Andaman-Nicobar ophiolites, *Gondwana Research* 103, 335-361

Bannert, D., Lyen, A.S., and Than Htay, 2011. The Geology of Indoburman Ranges in Myanmar. *Geologisches Jahrbuch Reihe B*, Heft, 101, Hannover.

Barber, A.J., and Crow, M.J., 2005. Chapter 4: Pre-Tertiary stratigraphy, In: Barber, A.J., Crow, M.J., Milsom, J.S. (Eds.), *Sumatra: Geology, Resources and Tectonic Evolution*. Geological Society, London, pp. 24-53.

Barber, A.J., and Crow, M.J., 2009. Structure of Sumatra and its implications for the tectonic assembly of Southeast Asia and the destruction of Paleothethys. *Island Arc*, 18, 3-20.

Barber, A.J., Khin Zaw, and Crow, M.J., 2017. Chapter 31. The pre-Cenozoic tectonic evolution of Myanmar. In: Barber, A.J., Khin Zaw, and Crow, M.J. (eds.), *Myanmar: Geology, Resources and Tectonics*, Geological Society of London, Memoirs, 48, 687-712.

Barley, M.E., Pickard, A.L., Khin Zaw, Rak, P., and Doyle, M.G., 2003. Jurassic to Miocene magmatism and metamorphism in the Mogok Metamorphic Belt and the India-Eurasia collision in Myanmar. *Tectonics*, 22. <https://doi.org/10.1029/2002TC001398>.

Baumgartner, P.O., O'Dogherty, L., Gorican, S., Urquhart, E., Pillecuit, A., De Wever, P., 1995. Middle Jurassic to lower Cretaceous radiolarian of Tethys: occurrences, systematics, biochronology. *Mémoires de Géologie (Lausanne)* 23, i-xxix, 1-1172.

Baxter, A.T., Aitchison, J.C., Zyabrev, S.V., and Ali, J.R., 2011. Upper Jurassic radiolarians from the Naga Ophiolite, Nagaland, northeast India. *Gondwana Research*, 20, 638-644.

Beccaro, P., 2004. Upper Jurassic radiolarians from Inici Mt. area (North-western Sicily, Italy): Biochronology and calibration by ammonites. *Rivista Italiana di Paleontologia e Stratigrafia*, vol 110 (1), pp. 289-301. doi:10.13130/2039-4942/6301

Bender, F., 1983. *Geology of Burma*, 1st edition, 239p. Gebruder Borntraeger, Berlin-Stuttgart.

Bertrand, G. and Rangin, C., 2003. Tectonics of the western margin of the Shan plateau (Central Myanmar): implication for the India-Indochina oblique convergence since the Oligocene. *Journal of Asian Earth Sciences*, 21, 1139-1157.

Bhowmik, S. K., Ao, A., Rajkakati, M., 2022. Tectonic framework of the high-pressure metamorphic rocks of the Nagaland Ophiolite Complex, North-east India, and its geodynamic significance: A review. *Geological Journal*, 57, 727-748

Bradshaw, J., Sayers, J., Bradshaw, M.T., Kneale, R., Ford, C., Spencer, I., Lisk, M., 1998. Palaeogeography and its impact on the petroleum systems of the North West Shelf, Australia. In: Purcell, P.G., Purcell, R.R. (Eds.), *The Sedimentary Basins of Western Australia*. Proceedings of the Petroleum Exploration Society of Australia Symposium, Perth, WA 2, pp. 95-121.

Brunnschweiler, R.O., 1966. On the geology of the Indoburman Ranges. *Journal of the Geological Society of Australia*, 13, 137-194.

Brunnschweiler, R.O., 1974. Indoburman Ranges. In: Spencer, A.M. (ed.), *Mesozoic-Cenozoic Orogenic Belts: Data for Orogenic Studies*. Geological Society of London Special Publication, 4, 279-299.

Cai, F., Ding, L., Yao, W., Laskowski, A.K., Xu, Q., Zhang, J., Kyaing Sein, 2016. Provenance and tectonic evolution of Lower Paleozoic-Upper Mesozoic strata from Sibumasu terrane, Myanmar. *Gondwana Research*, 41, 325-336.

Cai, F., Ding, L., Yao, W., Laskowski, A.K., Xu, Q., Zhang, J., Kyaing Sein, 2017. Provenance and tectonic evolution of Lower Paleozoic-Upper Mesozoic strata from Sibumasu terrane, Myanmar. *Gondwana Research*, 41, 325-336. <http://dx.doi.org/10.1016/j.gr.2015.03.005>.

Cai, F., Ding, L., Zhang, Q., Orme, D.A., Wei, H., Li, J., Zhang, J., Than Zaw, Kyaing Sein, 2020. Initiation and evolution of forearc basins in the Central Myanmar Depression. *GSA Bulletin*, 132, 1066-1082.

Cao, H., Huang, Y., Li, G., Zhang, L., Wu, J., Dong, L., Dai, Z., Lu, L., 2018. Late Triassic sedimentary records in the northern Tethyan Himalaya: Tectonic link with Greater India. *Geoscience Frontiers* 9: 273-291.

Chhibber, H. L., 1927. The serpentines and associated minerals of the Henzada and Bassein Districts, Burma. *Journal of the Burma Research Society*, 16, 195-196.

Chhibber, H.L., 1934. *Geology of Burma*. London, Macmillan, 538p.

Curray, J.R., Moore, D.G., Lawver, L.A., Emmel, F.J., Raitt, R.W., Henry, M. & Kieckhefer, R., 1979. Tectonics of the Andaman Sea and Burma. In: Watkins, J., Montadert, L. & Dickerson, P.W. (eds) *Geological and Geophysical Investigations of Continental Margins*. American Association of Petroleum Geologists, Memoirs, 29, 189-198.

Curray, J.R., 2005. Tectonics and history of the Andaman Sea region. *Journal of Asian Earth Sciences*, 25, 187-228.

De Wever, P., Dumitrica, P., Caulet, J.P., Nigrini, C., Caridroit, M., 2001. Radiolarians in the Sedimentary Record. Gordon and Breach Science Publishers. doi:10.1201/9781482283181

Dickinson, W.R., 1985. Interpreting provenance relations from detrital modes of sandstones. In: Zuffa, G.G. (Ed.), *Provenance of Arenites*. Reidel, Dordrecht, NATO ASI Series 148, pp. 333-361.

- Fang, D.-R., Wang, G.-H., Hisada, K.-I., Yuan, G.-L., Han, F.-L., and Li, D., 2018. Provenance of the Langjiexue Group to the south of the Yarlung-Tsangpo Suture Zone in southeastern Tibet: Insights on the evolution of the Neo-Tethys Ocean in the Late Triassic. *International Geology Review*, 61, 341-360.
- Fareeduddin and Dilek, Y., 2015. Structure and petrology of the Nagaland-Manipur Hill ophiolitic mélangé zone, NE India: A fossil Tethyan subduction channel at the India-Burma plate boundary. *Episodes*, December, 298-314.
- Gardiner, N. J., Robb, L., Searle, M., and Morley, C.K., 2015. Neotethyan magmatism and metallogeny in Myanmar - An Andean analogue? *Journal of Asian Earth Sciences* 106: 197 - 215.
- Gardiner, N. J., Robb, L.J., Morley, C.K., Searle, M.P., Cawook, P.A., Whitehouse, M.J., Kirkland, C.L., Roberts, N.M.W., Tin Aung Myint, 2016. The tectonic and metallogenic framework of Myanmar: A Tethyan mineral system. *Ore Geology Reviews* 79: 26-45.
- Gardiner, N. J., Searle, M.P., Robb, L.J., Morley, C.K., Kirkland, C.L., Spencer, C.J., 2018. The crustal architecture of Myanmar imaged through zircon U-Pb, Lu-Hf and O isotopes: tectonics and metallogenic implications. *Gondwana Res.* 62: 27-60.
- Garzanti, E., 2016. From static to dynamic provenance analysis-sedimentary petrology upgraded. *Sediment. Geol.* 336, 3-13.
- Garzanti, E., 2019. Petrographic classification of sand and sandstone. *Earth-Science Reviews*, 190, 545-563. <https://doi.org/10.1016/j.earscirev.2018.1012.1014>
- Ghose, N.C., Chatterjee, N., and Fareeduddin, 2014. A petrographic atlas of ophiolite: An example from the eastern India-Asia Collision Zone. Springer, 234 pp.
- Gramann, F., 1974. Some palaeontological data on the Triassic and Cretaceous of the western part of Burma (Arakan Islands, Arakan Yoma, western outcrops of Central Basin). *Newsletters in Stratigraphy*, 3, 277-290.
- Green, O.R., Searle, M.P., Corfield, R.I., and Corfield, R.M., 2008. Cretaceous-Tertiary Carbonate Platform Evolution and the Age of the India-Asia Collision along the Ladakh Himalaya (Northwest India). *Journal of Geology* 116: 331-353.
- Gunawan, I., 2012. Age, Character and Provenance of the Tipuma Formation, West Papua: New insights from Detrital Zircon Dating.

Hall, R., 2009. Hydrocarbon basins in SE Asia: understanding why they are there. *Petroleum Geoscience* 15, 131-146.

Hall, R., 2012. Late Jurassic-Cenozoic reconstructions of the Indonesian region and the Indian Ocean. *Tectonophysics* 570-571, 1-41.

Hall, R., 2014. The origin of Sundaland. In: Basuki, N.J., Dahilus, A.Z., (Eds.), MGEI Annual Convention. Proceedings of Sundaland Resources, Palembang, South Sumatra, Indonesia, pp. 1-25.

Harlow, G.E., Tsujimori, T., and Sorensen, S.S., 2014. Jadeitites and Plate Tectonics. *Annual Review of Earth and Planetary Sciences*, July, 105-138 Doi: 10.146/annurev-earth-060614-105215.

Hébert, R., Bezard, R., Guilmette, C., Dostal, J., Wang, C.S., Liu, Z.F., 2012. The Indus–Yarlung Zangbo ophiolites from Nanga Parbat to Namche Barwa syntaxes, southern Tibet: First synthesis of petrology, geochemistry, and geochronology with incidences on geodynamic reconstructions of Neo-Tethys. *Gondwana Research* 22: 377-397.

Hla Htay, Khin Zaw, Than Than Oo, 2017. Chapter 6. The mafic-ultramafic (ophiolitic) rocks of Myanmar. In: Barber, A.J., Khin Zaw, and Crow, M.J. (eds.), Myanmar: Geology, Resources and Tectonics, Geological Society of London, Memoirs, 48, 117-141.

Huber, B.T., Petrizzo, M.R., Young, J.R., Falzoni, F., Gilardoni, S.E., Bown, P.R., Wade, B.S., 2016. Pforams@microtax. *Micropaleontology* 62 (6), 429-438.

Huber, B.T., Petrizzo, M.R., Falzoni, F., 2022. Taxonomy and phylogeny of Albian-Maastrichtian planispiral planktonic foraminifera traditionally assigned to *Globigerinelloides*. *Micropaleontology* 68 (2), 117-183.

Hutchinson, C.S., 1989. *Geological Evolution of South East Asia*. Oxford University Press, New York.

Hutchinson, C.S., Tan, D.N.K., 2009. *Geology of Peninsular Malaysia*. The University of Malaya and the Geological Society of Malaysia, Kuala Lumpur, p.479.

Imchen, W., Thong, G.T., and Pongen, T., 2014. Provenance, tectonic setting and age of the sediments of the Upper Disang Formation in the Phek District, Nagaland. *Journal of Asian Earth Sciences*, 88, 11-27.

Jeon, H., Williams, I.S., Bennett, V.C., 2014. Uncoupled O and Hf isotopic systems in zircon from the contrasting granite suites of the New England Orogen, eastern Australia: implications for studies of Phanerozoic genesis. *Geochim. Cosmochim. Acta* 146, 132-149.

- Kapp, P. and DeCelles, P.G., 2019. Mesozoic-Cenozoic geological evolution of the Himalayan-Tibetan orogen and working tectonic hypothesis. *American Journal of Science*, 319, 159-254.
- Kemp, A.I.S., Hawkesworth, C.J., Collins, W.J., Gray, C.M., Blevin, P.L., EIMF, 2009. Isotopic evidence for rapid continental growth in an extensional accretionary orogen: the Tasmanides, eastern Australia. *Earth and Planetary Science Letters* 284, 455-466.
- Kyaw Linn Oo, Khin Zaw, Meffre, S., Myitta, Day Wa Aung, Lai, C.K., 2015. Provenance of the Eocene sandstones in the southern Chindwin Basin, Myanmar: implications for the unroofing history of the Cretaceous-Eocene magmatic arc. *J. Asian Earth Sci.* 107, 172-194.
- Kyi Khin, Sakai, T., Khin Zaw, 2017. Arakan Coastal Ranges in western Myanmar, geology and provenance of Neogene siliciclastic sequences: implication for the tectonic evolution of the Himalaya-Bengal System. In: Barber, A.J., Khin Zaw, and Crow, M.J. (eds.), *Myanmar: Geology, Resources and Tectonics*, Geological Society of London, Memoirs, 48, 81-116, <https://doi.org/10.1144/M48.5>
- Kyi Khin, Aung Moe, Kyi Pyar Aung, 2022. Tectono-structural framework of the Indo-Myanmar Ranges: Implications for the structural development on the geology of the Rakhine Coastal Region, Myanmar. *Geosystems and Geoenvironment* 1, 100079. <https://doi.org/10.1016/j.geogeo.2022.100079>
- Lamont, T.N., Searle, M.P., Hacker, B.R., Kyi, Htun, Kyaw Min Htun, Morley, C.K., Waters, D.J., White, R.W., 2021. Late Eocene-Oligocene granulite facies garnet-sillimanite migmatites from the Mogok Metamorphic belt, Myanmar, and implications for timing of slip along the Sagaing Fault. *Lithos* 386-387, 106027. <https://doi.org/10.1016/j.lithos.2021.106027>
- Lewis, C. J. and Sircombe, K., 2013. Use of U-Pb geochronology to delineate provenance of North West Shelf Sediments, Australia. *Geoscience Australia. In* Keep, M. & Moss, S.J. (Eds), *The Sedimentary Basins of Western Australia IV: Proceedings of the Petroleum Exploration Society of Australia Symposium*, Perth, WA, 2013, 27 pp.
- Li, G.W., Sandiford, M., Liu, X.H., Xu, Z.Q., We, L.J., Li, H.Q., 2014. Provenance of Late Triassic sediments in central Lhasa terrane, Tibet and its implication. *Gondwana Research* 25, 1680-1689.
- Li, J.X., Fan, W.M., Zhang, L.Y., Evans, N.J., Sun, Y.L., Ding, L., Kyaing Sein, 2019. Geochronology, geochemistry and Sr-Nd-Hf isotopic compositions of Late Cretaceous-Eocene granites in southern Myanmar: petrogenetic, tectonic and metallogenic implications. *Ore Geology Reviews* 112, 103031.

Li, X., Li, Y., Wang, C., Matsuoka, A., 2013. Late Jurassic Radiolarians from the Zhongba Melange in the Yarlung-Tsangpo Suture Zone, Southern Tibet. Pp.23-30. Science Reports of Niigata University (Geology) 28.

Licht, A., France-Lanord, C., Reisberg, L., Fontaine, C., Aung Naing Soe, Jaeger, J.J., 2013. A palaeo Tibet-Myanmar connection? Reconstructing the Late Eocene drainage system of central Myanmar using a multi-proxy approach: Journal of the Geological Society of London, v. 170, p. 929-939.

Licht, A., Reisberg, L., France-Lanord, C., Aung Naing Soe, Jaeger, J.J., 2014. Cenozoic evolution of the central Myanmar drainage system: insights from sediment provenance in the Minbu Sub-Basin. Basin Research, 28, 237-251, doi:10.1111/bre.12108.

Licht, A., Dupont-Nivet, G., Zaw Win, Hnin Hnin Swe, Myat Kaythi, Roperch, P., Ugrai, T., Littell, V., Park, D., Westerweel, J., Jones, D., Poblete, F., Day Wa Aung, Huang, H., Hoorn, C., Kyaing Sein, 2019. Paleogene evolution of the Burmese forearc basin and implications for the history of India-Asia convergence: GSA Bulletin, doi.org/10.1130/B35002.1

Licht, A., Zaw Win, Westerweel, J., Cogné, N., Morley, C.K., Chantraprasert, S., Poblete, F., Ugrai, T., Nelson, B., Day Wa Aung, Dupont-Nivet, G., 2020. Magmatic history of central Myanmar and implications for the evolution of the Burma Terrane. Gondwana Research 87, 303-319.

Lin, D., Goswami, T.K., Fulong, C., Barai, U., Sarmah, R.K., Bezbaruah, D., 2022. Detrital zircon U-Pb ages of Tertiary sequences (Palaeocene-Miocene): Inner Fold Belt and Belt of Schuppen, Indo-Myanmar Ranges, India. Geological Journal, doi:10.1002/gj.4446.

Liu, C.-Z., Chung, S.-L., Wu, F.-Y., Zhang, C., Xu, Y., Wang, J.-G., Chen, Y., and Guo, S., 2016. Tethyan suturing in Southeast Asia: Zircon U-Pb and Hf-O isotopic constraints from Myanmar ophiolites. Geology, 44, 311-314.

Liu, C.-Z., Zhang, C., Xu, Y., Wang, J.-G., Chen, Y., Guo, S., Wu, F.-Y., Kyaing Sein, 2016a. Petrology and geochemistry of mantle peridotites from the Kalembo and Myitkyina ophiolites (Myanmar): Implications for tectonic settings. Lithos, 264, 495-508.

Lokho, K., Aitchison, J.C., Whiso, K., Lhoupenyi, D., Zhou, R., and Raju, D.S.N. 2020. Eocene foraminifers of the Upper Disang Formation, Naga Hills of Manipur, Indo-Myanmar Range (IMR): Implications on age and basin evolution. Journal of Asian Earth Sciences, 191, 104259. doi.org/10.1016/j.jseaes.2020.104259

Longley, I.M., Buessenschuett, C., Clydsdale, L., Cubitt, C.J., Davis, R.C., Johnson, M.K., Marshall, N.M., Murray, A.P., Somerville, R., Spry, T.B., and Thompson, N.B., 2002. The North West Shelf of Australia – a Woodside perspective. *In: Keep, M. & Moss, S.J. (eds.). Sedimentary Basins of Western Australia. Proceedings of the Petroleum Exploration Society of Australia Symposium, Perth WA 3*, pp. 27-88.

Maibam, B., Palin, R.M., Gerdes, A., White, R.W., and Foley, S., 2022. Dating blueschist-facies metamorphism within the Naga ophiolite, Northeast India, using sheared carbonate veins. *International Geology Review*, doi: 10.1080/00206814.2022.2048271

Matsuoka, A., Yang, Q., Kobayashi, K., Takei, M., Nagahashi, T., Zeng, Q., Wang, Y., 2002. Jurassic-Cretaceous radiolarian biostratigraphy and sedimentary environments of the Cenozoic Tethys: records from the Xialu Chert in the Yarlung-Zangbo Suture Zone, southern Tibet. *Journal of Asian Earth Sciences* 20: 277-287.

Maurin, T. and Rangin, C., 2009. Structure and kinematics of the Indo-Burmese Wedge: recent and fast growth of the outer wedge. *Tectonics*, 28, TC20010.

McDermid, I.R.C., Aitchison, J.C., Davis, A.M., Harrison, M.T., and Grove, M., 2002. The Zedong terrane: a Late Jurassic intra-oceanic magmatic arc within the Yarlung-Tsangpo suture zone, southeastern Tibet. *Chemical Geology*, 187, 267-277.

Meng, Z., Wang, J., Ji, W., Zhang, H., Wu, F., and Garzanti, E., 2019. The Langjiexue Group is an *in situ* sedimentary sequence rather than an exotic block: Constraints from coeval Upper Triassic strata of the Tethys Himalaya (Qulonggongba Formation). *CrossMark* 62: 783-797.

Metcalf, I., 1990. Allochthonous terrane processes in Southeast Asia. *Philosophical Transactions. Royal Society of London A331*, 625-640.

Metcalf, I., 1996. Pre-Cretaceous evolution of SE Asian terranes. *In: Hall, R., Blundell, D.J. (Eds.), Tectonic Evolution of SE Asia. Geological Society, London, Special Publication 106*, pp. 97-122.

Metcalf, I., 2011. Tectonic framework and Phanerozoic evolution of Sundaland. *Gondwana Research* 19(1): 3-21.

Metcalf, I., 2013. Gondwana dispersion and Asian accretion: Tectonic and palaeogeographic evolution of eastern Tethys. *Journal of Asian Earth Sciences* 66, 1-33.

Mitchell, A.H.G., 1981. Phanerozoic plate boundaries in mainland SE Asia, the Himalayas and Tibet. *Journal of the Geological Society, London* 138, 109-122.

- Mitchell, A.H.G., 1986. Mesozoic and Cenozoic regional tectonics and metallogensis in mainland SE Asia. *GEOSEA V Proceedings, II, Geological Society of Malaysia Bulletin*, 20, 221-239.
- Mitchell, A.H.G., 1989. The Shan Plateau and western Burma: Mesozoic-Cenozoic plate boundaries and correlations with Tibet. In: Sengor, A.M.C. (ed.), *Tectonic Evolution of the Tethyan Region*, NATO Advanced Science Institute Series, Kluwer Academic Publishers, 259, 567-583.
- Mitchell, A.H.G., 1992. Late Permian-Mesozoic events and the Mergui group Nappe in Myanmar and Thailand. *Journal of SE Asian Earth Sciences* 7, 165-178.
- Mitchell, A. H. G., 1993. Cretaceous – Cenozoic tectonic events in the western Myanmar (Burma) – Assam region. *Journal of the Geological Society, London*, 150, 1089-1102.
- Mitchell, A.H.G., 2017. *Geological Belts, Plate Boundaries and Mineral Deposits in Myanmar*. Elsevier, Amsterdam 524 pp.
- Mitchell, A.H.G., Tin Hlaing, and Nyunt Htay, 2010. The Chin Hills Segment of the Indo-Myanmar Ranges: Not a simple accretionary wedge. *Memoir Geological Society of India*, No. 75, pp. 3-24.
- Mitchell, A.H.G., Chung, S.L., Oo, T., Lin, T.H., Hung, C.H., 2012. Zircon U-Pb ages in Myanmar: magmatic-metamorphic events and the closure of a neo-Tethys ocean? *Journal of Asian Earth Sciences* 56, 1-23.
- Mitchell, A.H.G., Myint Thein Htay, Kyaw Min Htun, 2015. The medial Myanmar suture zone and the western Myanmar-Mogok foreland. *Journal of the Myanmar Geosciences Society* 6, 73-88.
- Morley, C.K., 2009. Evolution from an Oblique Subduction Back-Arc mobile Belt to a Highly Oblique Collisional Margin: the Cenozoic Tectonic Development of Thailand and Eastern Myanmar 318. *Geological Society of London Special Publications*, pp. 373-403.
- Morley, C.K., 2012. Late Cretaceous-early Palaeogene tectonic development of SE Asia. *Earth Science Reviews* 115, 37-75.
- Morley, C.K., Searle, M.P., 2017. Regional tectonics, structure and evolution of the Andaman-Nicobar Islands from ophiolite formation and obduction to collision and back-arc spreading. In: Bandopadhyay, P.C. and Carter, A. (eds.) *The Andaman-Nicobar Accretionary ridge: Geology, Tectonics and Hazards*. *Geol. Soc. Lond. Mem.* 47, 51-74. <https://doi.org/10.1144/M47.5>
- Morley, C.K., 2018. Understanding Sibumasu in the context of ribbon continents. *Gondwana Res.* 64, 184-215.

Morley, C. K., and Arboit, F., 2019. Dating the onset of motion on the Sagaing fault: Evidence from detrital zircon and titanite U-Pb geochronology from the North Minwun Basin, Myanmar. *Geology*, v. 47, p. 581-585.

Morley, C. K., Tin Tin Naing, Searle, M.P., Robinson, S.A., 2020. Structural and tectonic development of the Indo-Burma ranges. *Earth-Science Reviews*, 200, 102992.
<https://doi.org/10.1016/j.earscirev.2019.102992>.

Morley, C. K., Chantraprasert, S., Kongchum, J., Chenoll, K., 2021. The West Myanmar Terrane, a review of recent paleo-latitude data, its geological implications and constraints. *Earth-Science Reviews*, 220, 103722. <https://doi.org/10.1016/j.earscirev.2021.103722>

Myo Min, Ratschbacher, L., Franz, L., Hacker, B.R., Enkelmann, Toreno, E.Y., Hartel, B., Schurr, B., Tichomirowa, M., and Pfander, J.A., 2022. India (Tethyan Himalayan Series) in Central Myanmar: Implications for the evolution of the Eastern Himalayan Syntaxis and the Sagaing transform-fault system. *Geophysical Research Letters*, 49, e2022GL099140.

Najman, Y., Sobel, E.R., Millar, I., Stockli, D.F., Govin, G., Lisker, F., Garzanti, E., Limonta, M., Vezzoli, G., Copley, A., Zhang, P., Szymanski, E., Kahn, A., 2019. The exhumation of the Indo-Myanmar Ranges, Myanmar. *Earth and Planetary Science Letters*, 1-14.
<https://doi.org/10.1016/j.epsl.2019.115948>.

Najman, Y., Sobel, E.R., Millar, I., Luan, X., Zapata, S., Garzanti, E., Parra, M., Vezzoli, G., Zhang, P., Day Wa Aung, Saw Mu Tha Lay Paw, Thae Naung Lwin, 2022. The timing of collision between Asia and the West Myanmar Terrane, and the development of the Indo-Burman Ranges. *Tectonics*, 41, e2021TC007057.

Niu, X., Liu, F., Yang, J., Dilek, Y., Xu, Z., Kyaing Sein, 2017. Mineralogy, geochemistry, and melt evolution of the Kalemio peridotite massif in the Indo-Myanmar Ranges (western Myanmar), and tectonic implications. *The Geological Society of America* <http://orcid.org/0000-0003-0862-6705>.

Pessagno, E.A., Newport, R.L., 1972. A technique for extracting Radiolaria from radiolarian cherts. *Micropaleontology* 18, 231-234.

Phillips, G., Landenberger, B., Belousova, E.A., 2011. Building the New England Batholith, eastern Australia-linking granite petrogenesis with geodynamic setting using Hf isotopes in zircon. *Lithos* 122, 1-12.

- Pivnik, D.A., Nahm, J., Tucker, R.S., Smith, G.O., Nyein, K., Nyunt, M. & Maung, P.H., 1998. Polyphase Deformation in a Fore-Arc/Back-Arc Basin, Salin Subbasin, Myanmar (Burma). *AAPG, Bulletin*, 82, 1837-1856.
- Poinar, G., 2019. Burmese amber: evidence of Gondwanan origin and Cretaceous dispersion. *Historical Biology*, 31, 1304-1309.
- Qi, M., Xian, H., Zhong, Z.Q., Qiu, H.N., Wang, H., Sun, X.L., Xu, B., 2013. $^{40}\text{Ar}/^{39}\text{Ar}$ geochronology constraints on the formation age of Myanmar jadeitite. *Lithos* 162-163, 107-114.
- Qi, M., Xian, H., Zhang, Z.M., Zhong, Z.Q., 2014. Zircon U-Pb ages of Myanmar jadeitite and constrain on the fluid in subduction zone of Neo-Tethys. *Acta Petrol. Sin.* 30 (8), 2279-2286 (in Chinese with English abstract).
- Rangin, C., 2017. Chapter 3. Active and recent tectonics of the Burma Platelet in Myanmar. In: Barber, A.J., Khin Zaw and Crow, M.J. (eds.), *Myanmar: Geology, Resources and Tectonics*, Geological Society of London, *Memoirs*, 48, 53-64.
- Rangin, C., 2018. *The Western Sunda Basins, and the India/Asia Collision: an Atlas*, Geotecto, Société Géologique de France 294 pp.
- Rangin, C., Maurin, T., and Masson, F., 2013. Combined effects of Eurasia/Sunda oblique convergence and East-Tibetan crustal flow on the active tectonics of Burma. *Journal of Asian Earth Sciences*, 76, 185-194.
- Rehman, H.U., Lee, H.Y., Chung, S.L., Khan, T., O'Brien, P.J., Yamamoto, H., 2016. Source and mode of the Permian Panjal Trap magmatism: evidence from zircon U-Pb and Hf isotopes and trace element data from the Himalayan ultrahigh-pressure rocks. *Lithos* 260, 286-299.
- Replumaz, A., and Tapponnier, P., 2003. Reconstruction of the deformed collision zone between India and Asia by backward motion of lithospheric blocks: *Journal of Geophysical Research*, v. 108. <https://doi.org/10.1029/2001JB000661>.
- Replumaz, A., Negredo, A.M., Guillot, S., Villasenor, A., 2010. Multiple episodes of continental subduction during India/Asia convergence: insight from seismic tomography and tectonic reconstruction. *Tectonophysics* 483, 125-134.
- Ridd, M.F. 2009. The Phuket Terrane: a Late Palaeozoic rift at the margin of Sibumasu. *Journal of Asian Earth Science*, 36, 238-251.

- Ridd, M.F., 2011. Lower Palaeozoic. In: Ridd, M.F., Barber, A.J. & Crow, M.J. (eds.) *The Geology of Thailand*. Geological Society, London, 33-51.
- Ridd, M. F., Watkinson, I., 2013. The Phuket-Slate Belt terrane: tectonic evolution and strike-slip emplacement of a major terrane on the Sundaland margin of Thailand and Myanmar. *Proceedings of the Geologists' Association* 124: 994-1010.
- Rowley, D.B., 1998. Minimum age of initiation of collision between Indian and Asia, north of Everest, based on subsidence history of the Zhepure mountain section. *Journal of Geology*, 106, 229-235.
- Searle, M.P., Noble, S.R., Cottle, J.M., Waters, D.J., Mitchell, A.H.G., Tin Hlaing, and Horstwood, M.S.A., 2007. Tectonic evolution of the Mogok metamorphic belt, Burma (Myanmar) constrained by U-Th-Pb dating of metamorphic and magmatic rocks. *Tectonics*, 26, TC3014, <https://doi.org/10.1029/2006TC002083>.
- Searle, M.P., Morley, C.K., Waters, D.J., Gardiner, N.J., U. Kyi Htun, Than Than Nu, and Robb, L.J., 2017. Chapter 12, Tectonic and metamorphic evolution of the Mogok Metamorphic and Jade Belts, and ophiolitic terranes of Burma (Myanmar). In: Barber, A.J., Khin Zaw and Crow, M.J. (eds.), *Myanmar: Geology, Resources and Tectonics*, Geological Society, London, Memoirs, 48, 263-295.
- Searle, M.P., Garber, J.M., Hacker, B.R., Kyi Htun, Gardiner, N.J., Waters, D.J., Robb, L.J., 2020. Timing of syenite-charnockite magmatism and ruby and sapphire metamorphism in the Mogok valley region, Myanmar. *Tectonics* 39. <https://doi.org/10.1029/2019TC005998> e2019TC005998.
- Sengör, A.M.C., 1987. Tectonics of the Tethysides: orogenic collage development in a collisional setting, *Annual Reviews of Earth and Planetary Sciences* 15, 213-244.
- Sevastjanova, I., Hall, R., Rittner, M., Saw Mu Tha Lay Paw, Tin Tin Naing, Alderton, D.H., Comfort, G., 2016. Myanmar and Asia united, Australia left behind long ago. *Gondwana Research*, 32, 24-40. <http://dx.doi.org/10.1016/j.gr.2015.02.001>.
- Shaw, S.E., Flood, R.H., 2009. Zircon Hf isotopic evidence for mixing of crustal and silicic mantle-derived magmas in a zoned granite pluton, Eastern Australia. *Journal of Petrology* 50, 147-168.
- Shaw, S.E., Flood, R.H., Pearson, N.J., 2011. The New England Batholith of eastern Australia: evidence of silicic magma mixing from zircon $^{176}\text{Hf}/^{177}\text{Hf}$ ratios. *Lithos* 126, 115-126.
- Shellnutt, J.G., Bhat, G.M., Wang, K.L., Brookfield, M.E., Jahn, B.M., Dostal, J., 2014. Petrogenesis of the flood basalts from the Early Permian Panjal Traps, Kashmir, India: Geochemical evidence for shallow melting of the mantle. *Lithos* 204, 159-171.

- Singh, A. K., 2013. Petrology and geochemistry of Abyssal Peridotites from the Manipur Ophiolite Complex, Indo-Myanmar Orogenic Belt, Northeast India. Implication for melt generation in mid-oceanic ridge environment. *Journal of Asian Earth Sciences* 66: 258-276.
- Singh, A.K., Chung, S.L., Bikramaditya, R.K. & Lee, H.Y., 2016. New U-Pb zircon ages of plagiogranites from the Nagaland-Manipur Ophiolites, Indo-Myanmar Orogenic Belt, NE India. *Journal of the Geological Society* doi:10.1144/jgs2016-048.
- Singh, A.K., Chung, S.-L., Bikramaditya, R.K., Lee, H.Y., 2017. New U-Pb zircon ages of plagiogranites from the Nagaland-Manipur ophiolites, Indo-Myanmar Orogenic Belt, NE India. *J. Geol. Soc.* 174, 170-179.
- Sloan, R.A., Elliott, J.R., Searle, M.P., and Morley, C.K., 2017. Chapter 2. Active tectonics of Myanmar and the Andaman Sea. In: Barber, A.J., Khin Zaw and Crow, M.J. (eds.), *Myanmar: Geology, Resources and Tectonics*, Geological Society of London, Memoirs, 48, 19-52.
- Socquet, A., Goffé, B., Pubellier, M., and Rangin, C., 2002. Le métamorphisme Tardi-Cretace à l'Eocène des zones internes de la chaîne Indo-Birmane (Burma occidentale): implication géodynamique. *Comptes Rendus, Geosciences*, 334, 573-580.
- Soe Thura Tun, Watkinson, I.M., 2017. Chapter 19. The Sagaing Fault, Myanmar. In: Barber, A.J., Khin Zaw, Crow, M.J. (eds.), *Myanmar: Geology, Resources and Tectonics*, Geological Society, London, Memoirs, 48, 415-443.
- Steckler, M.S., Akhter, S.H., and Seeber, L., 2008. Collision of the Ganges-Brahmaputra Delta with the Burma Arc: Implications for earthquake hazard. *Earth and Planetary Science Letters*, 273, 367-378.
- Steckler, M.S., Mondal, D.R., Akhter, S.H., Seeber, L., Feng, L., Gale, J., Hill, E.M., and Howe, M., 2016a. Locked and loading metathrust linked to active subduction beneath the Indo-Myanmar Ranges. *Nature Geoscience* 9, 615-618.
- Suzuki, H., Maung Maung, Aye Ko Aung, Takai, M., 2004. Jurassic radiolaria from chert pebbles of the Eocene Pondaung Formation, Central Myanmar. *Neues Jahrbuch für Geologie und Paläontologie-Abhandlungen*, 231, 369-393.
- Theobald, W., 1871. The axial group in Western Prome, British Burmah. *Geological Survey of India Records (Calcutta)*, 4, 33-44.
- Tin Tin Naing, Bussien, D.A., Winkler, W., Nold, M., von Quadt, A., 2014. Provenance study on Eocene-Miocene sandstones of the Rakhine Coastal Belt, Indo-Myanmar Ranges of Myanmar: Geodynamic

implications. *In*: Scott, R., Smyth, H., Morton, A. & Richardson, N. (eds.). *Sediment Provenance Studies in Hydrocarbon Exploration and Production*. Geological Society, London, Special Publication; doi 10.1144/SP386.10.

United Nations, 1979a. *Geology and Exploration Geochemistry of part of the Northern and Southern Chin Hills and Arakan Yoma, Western Burma*. Technical Report, 4, United Nations Development Programme, DP/UN/BUR-72-002/13, United Nations, New York, 59 p.

Veevers, J. J., 1988. Morphotectonics of Australia's northwestern margin – a review. *In*: Purcell, P.G., Purcell, R.R. (Eds.), *The North West Shelf Proceedings of Petroleum Exploration Society of Australia Symposium*. PESA, Perth, WA, pp. 19-27.

Wang, J.G., Wu, F.Y., Tan, X.-C., and Liu, C.-Z., 2014. Magmatic evolution of the Western Myanmar Arc documented by U-Pb and Hf isotopes in detrital zircon. *Tectonophysics*, 612-613, 97-105.

Wang, J.G., Wu, F.Y., Garzanti, E., Hu, X., Ji, W.Q., Liu, Z.C., Liu, X.C., 2016. Upper Triassic turbidites of the northern Tethyan Himalaya (Langjiexue Group): The terminal of a sediment-routing system sourced in the Gondwanide Orogen. *Gondwana Research* 34, 84-98.

Westerweel, J., Roperch, P., Licht, A., Dupont-Nivet, G., Zaw Win, Poblete, F., Day Wa Aung, 2019. Burma Terrane part of the Trans-Tethyan arc during collision with India according to palaeomagnetic data. *Nature Geoscience* 12 (10), 863-868. <https://doi.org/10.1038/s41561-019-0443-2>

Westerweel, J., Licht, A., Cogne, N., Roperch, P., Dupont-Nivet, G., Myat Kay Thi, Hnin Hnin Swe, Huang, H., Zaw Win, Day Wa Aung, 2020. Burma terrane collision and northward indentation in the Eastern Himalayas recorded in the Eocene-Miocene Chindwin Basin (Myanmar). *Tectonics*, 39, e2020TC006413.

Westerweel, J., 2020. *The India-Asia Collision from the Perspective of Myanmar: Insights from Paleomagnetism and Paleogeographic Reconstructions*. University of Rennes. PhD Thesis. 287 pp.

Yang, J.-S., Xu, Z.Q. et al., 2012. Discovery of a Jurassic SSZ ophiolite in the Myitkyina region of Myanmar. *Acta Petrological Sinica*, 28, 1710-1730.

Yang, S., Liang, X., Jiang, M., Chen, L., He, Y., Chit Thet Mon, Hou, G., Myo Thant, Kyaing Sein, Wan, B., 2022. Slab remnants beneath the Myanmar terrane evidencing double subduction of the Neo-Tethyan Ocean, *Scientific Advances*, 8, eabo1027.

Yao, W., Ding, L., Cai, F., Wang, H., Xu, Q., Than Zaw. 2017, Origin and tectonic evolution of upper Triassic turbidites in the Indo-Myanmar Ranges, West Myanmar. *Tectonophysics*, 721, 90-105.

- Zahirovic, S., Matthews, K.J., Flament, N., Muller, R.D., Hill, K.C., Seton, M., Gurnis, M., 2016. Tectonic evolution and deep mantle structure of the eastern Tethys since the latest Jurassic. *Earth-Sci. Rev.* 162, 293-337.
- Zhang, J.E, Xiao, W., Windley, B.F., Cai, F., Kyaing Sein, Soe Naing, 2017. Early Cretaceous wedge extrusion in the Indo-Burma Range accretionary complex: implications for the Mesozoic subduction of Neothethys in SE Asia. *International Journal of Earth Science*, Doi: 10.1007/s0053101714687.
- Zhang, J., Xiao, W., Windley, B.F., Wakabayashi, J., Cai, F., Kyaing Sein, Wu, H., Soe Naing, 2018. Multiple alternating forearc- and backarc-ward migration of magmatism in the Indo-Myanmar orogenic belt since the Jurassic: Documentation of the orogenic architecture of eastern Neotethys in SE Asia. *Earth Science Reviews*, 185, 704-731.
- Zhang, P., Mei, L., Hu, X., Li, R., Wu, L., Zhou, Z., Qiu, H., 2017. Structure, uplift, and magmatism of the Western Myanmar Arc: Constraints to mid-Cretaceous-Paleogene tectonic evolution of the western Myanmar continental margin. *Gondwana Res.* 52, 18-38.
- Zhang, P., Najman, Y., Mei, L., Millar, I., Sobel, E.R., Carter, A., Barfod, D., Dhuime, B., Garzanti, E., Govin, G., Vezzoli, G., Hu, X., 2019. Palaeodrainage evolution of the large rivers of East Asia, and Himalayan-Tibet tectonics. *Earth-Science Reviews* 192, 601-630.
- Zhang, X., Chung, S.-L., Tang, J.-T., Maulana, A., Mawaleda, M., Thura Oo, Tien, C.-Y., and Lee, H.-Y., 2021. Tracing Argoland in eastern Tethys and implications for India-Asia convergence. *GSA Bulletin*, 133, 1712-1722.
- Zhu, B., Kidd, W.S.F., Rowley, D.B., Currie, B.S., Shafique, N., 2005. Age of initiation of the India-Asia collision in the East-Central Himalaya. *J Geol* 113:265-285.

Figure 1

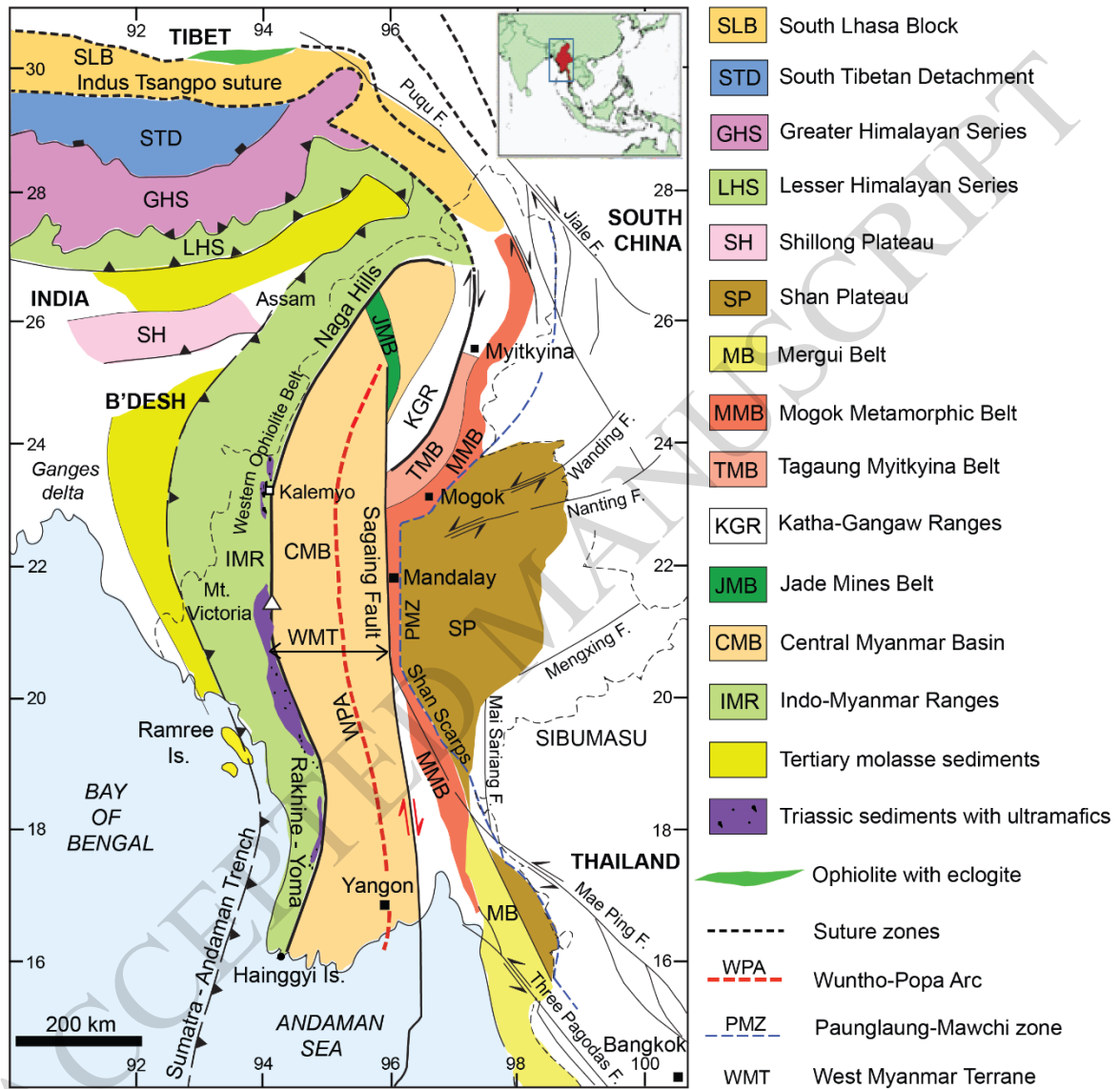


Figure 2

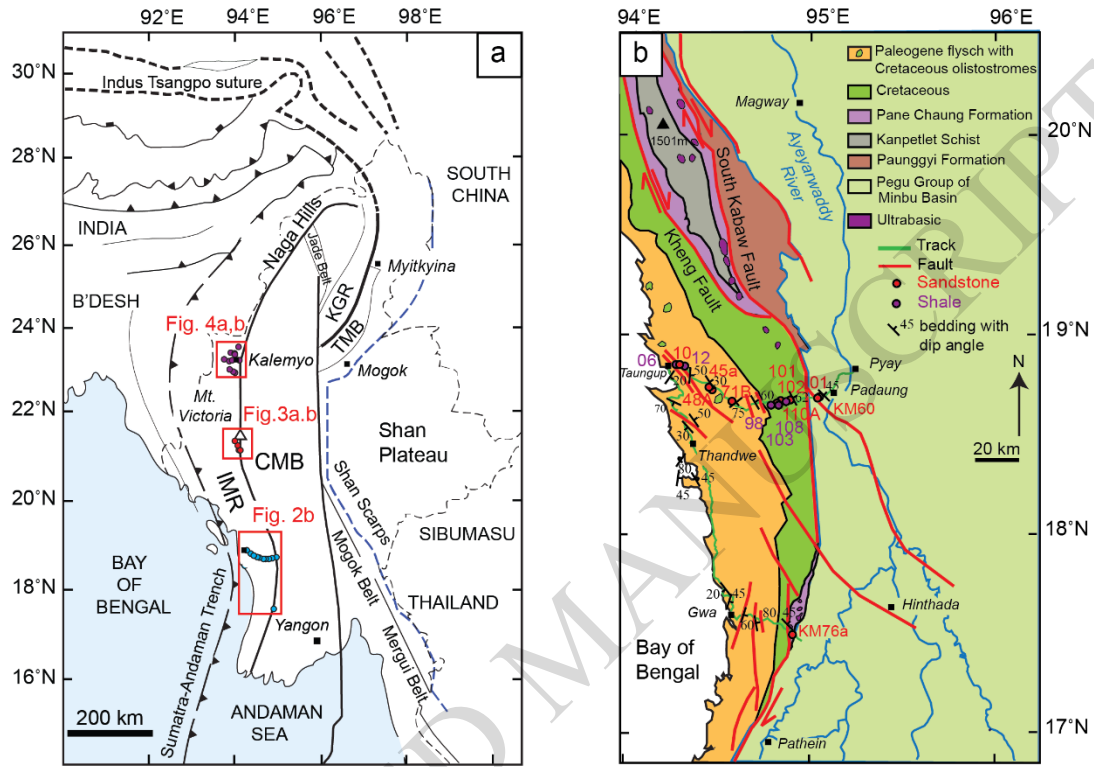


Figure 3

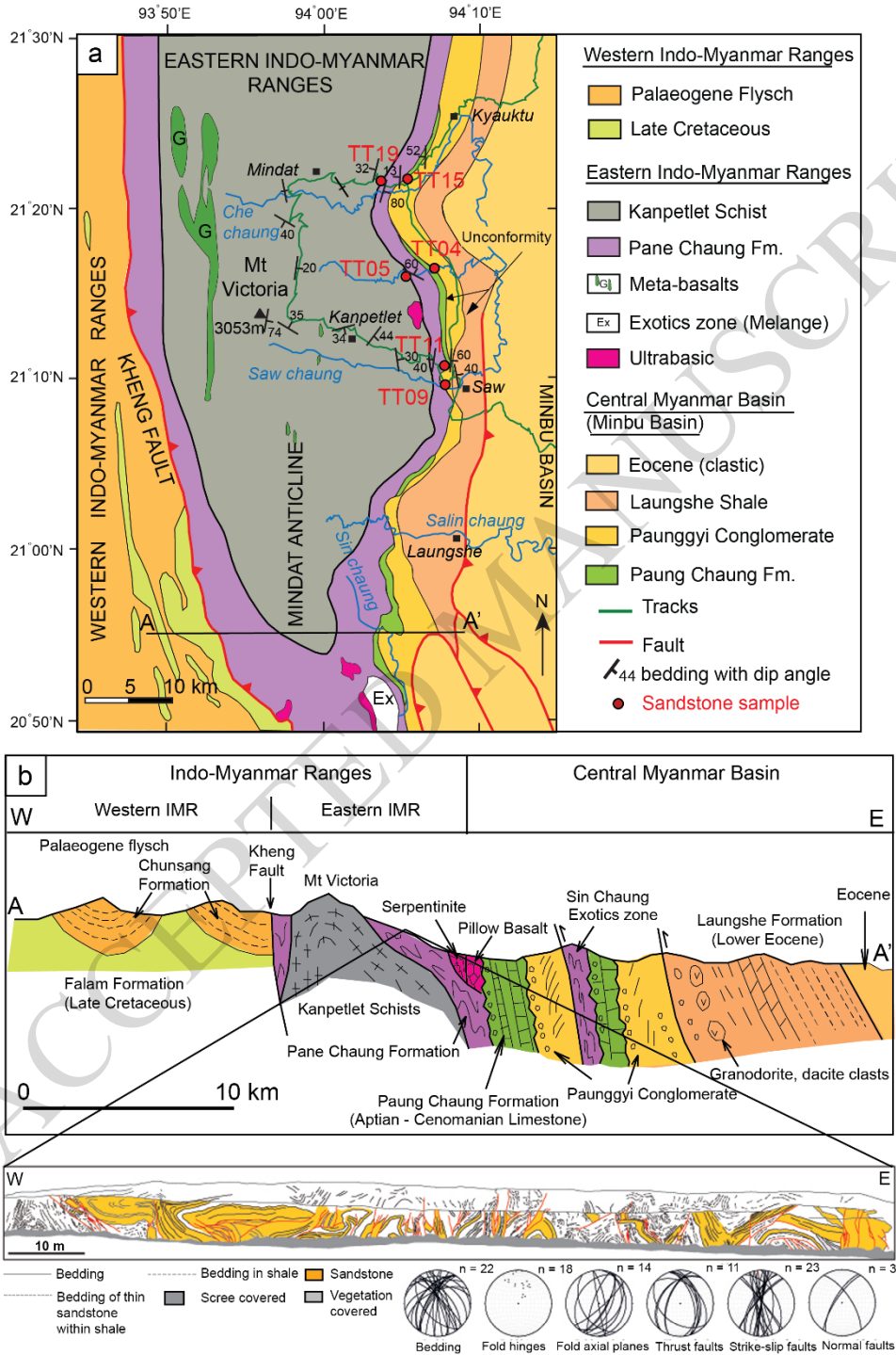


Figure 4

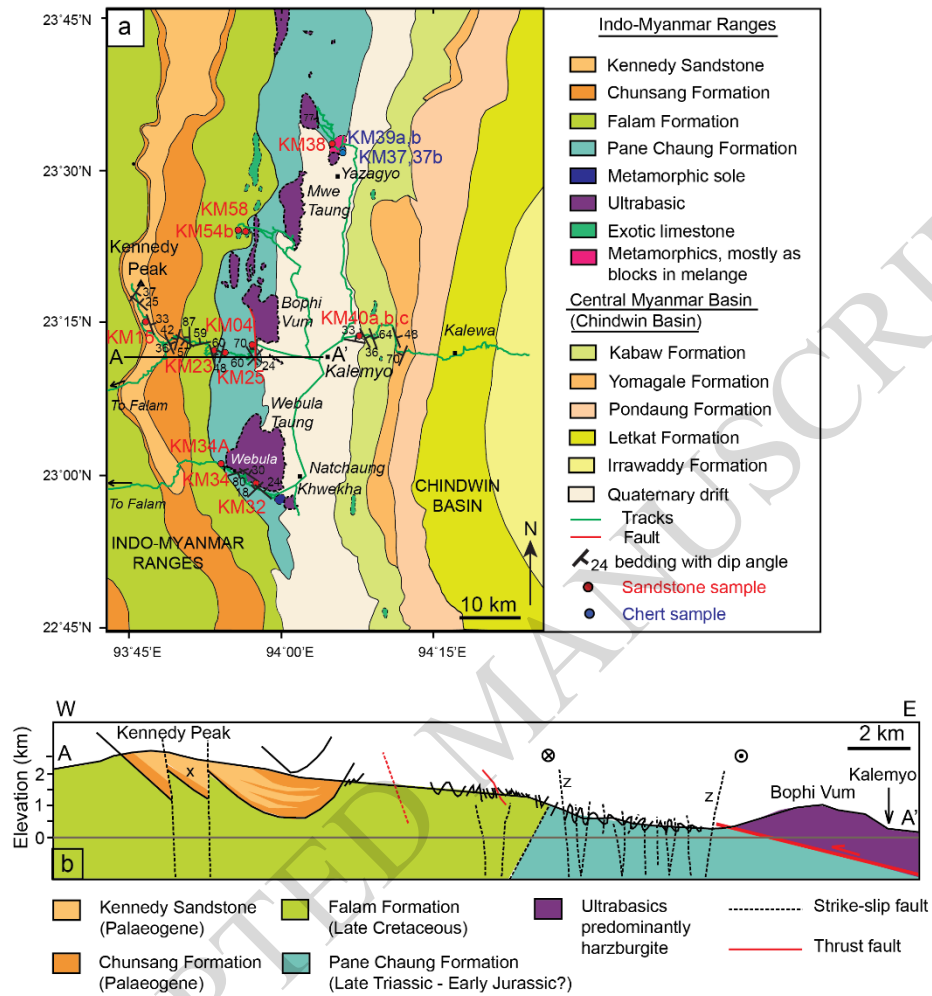


Figure 5

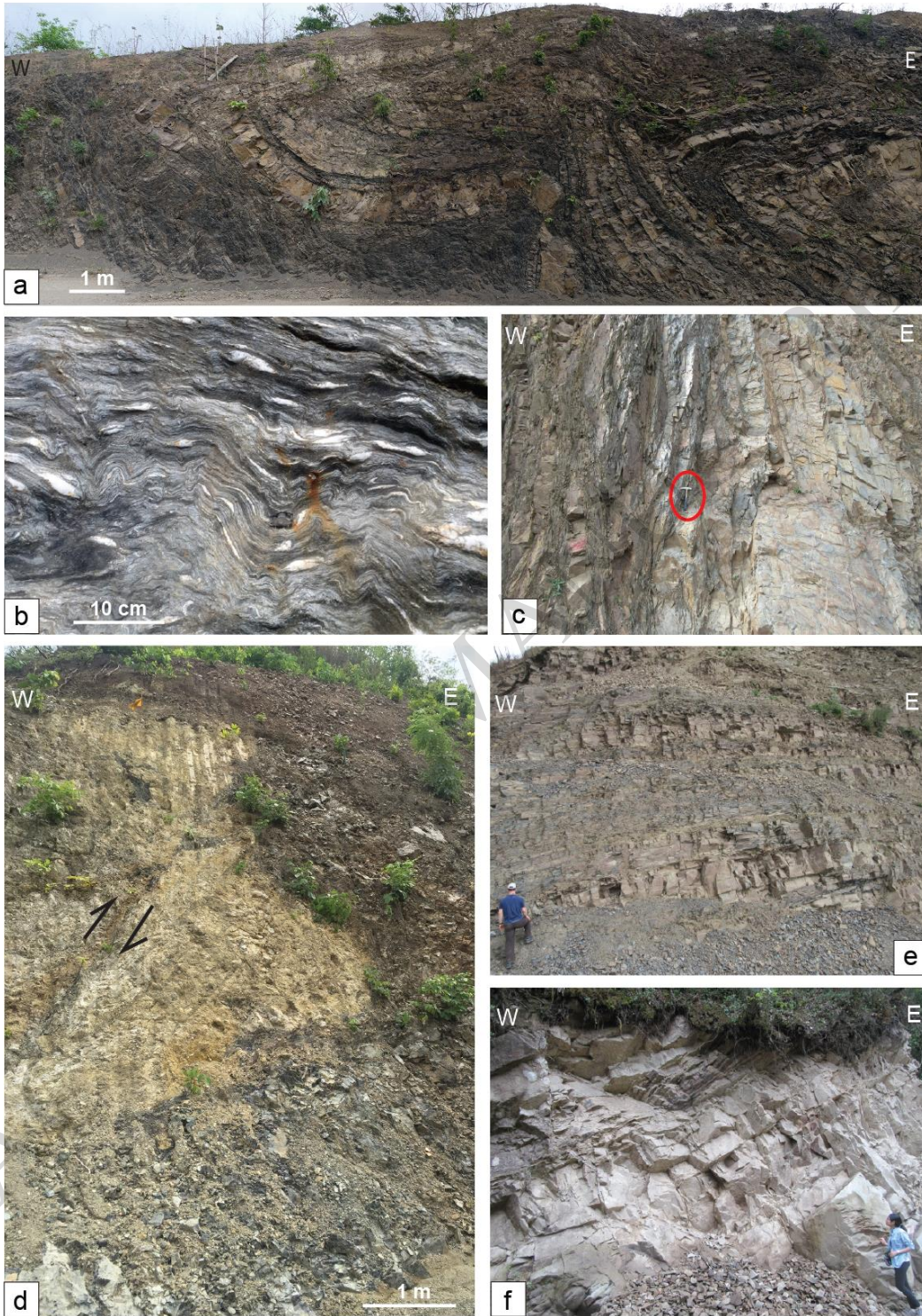


Figure 6

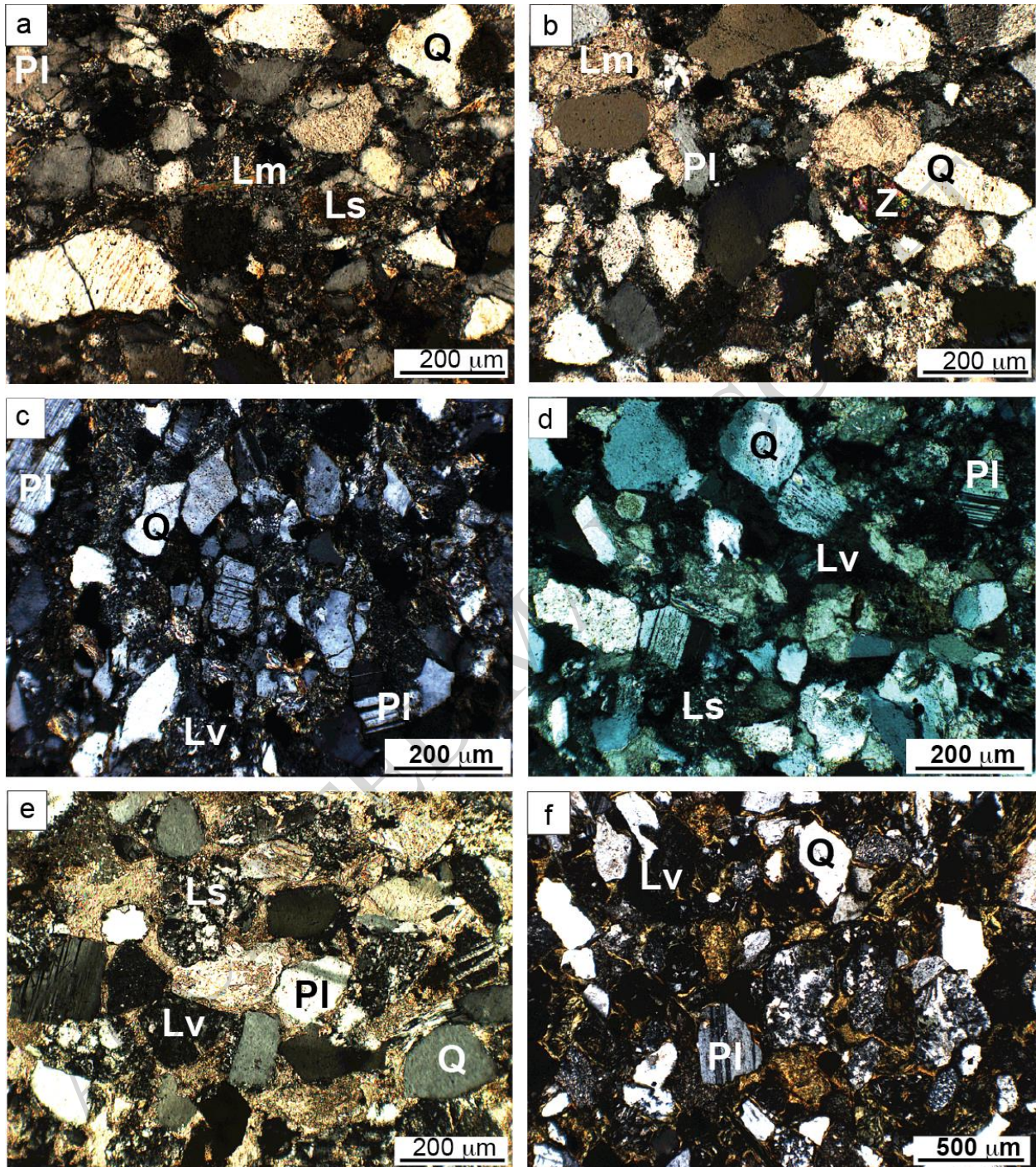


Figure 7

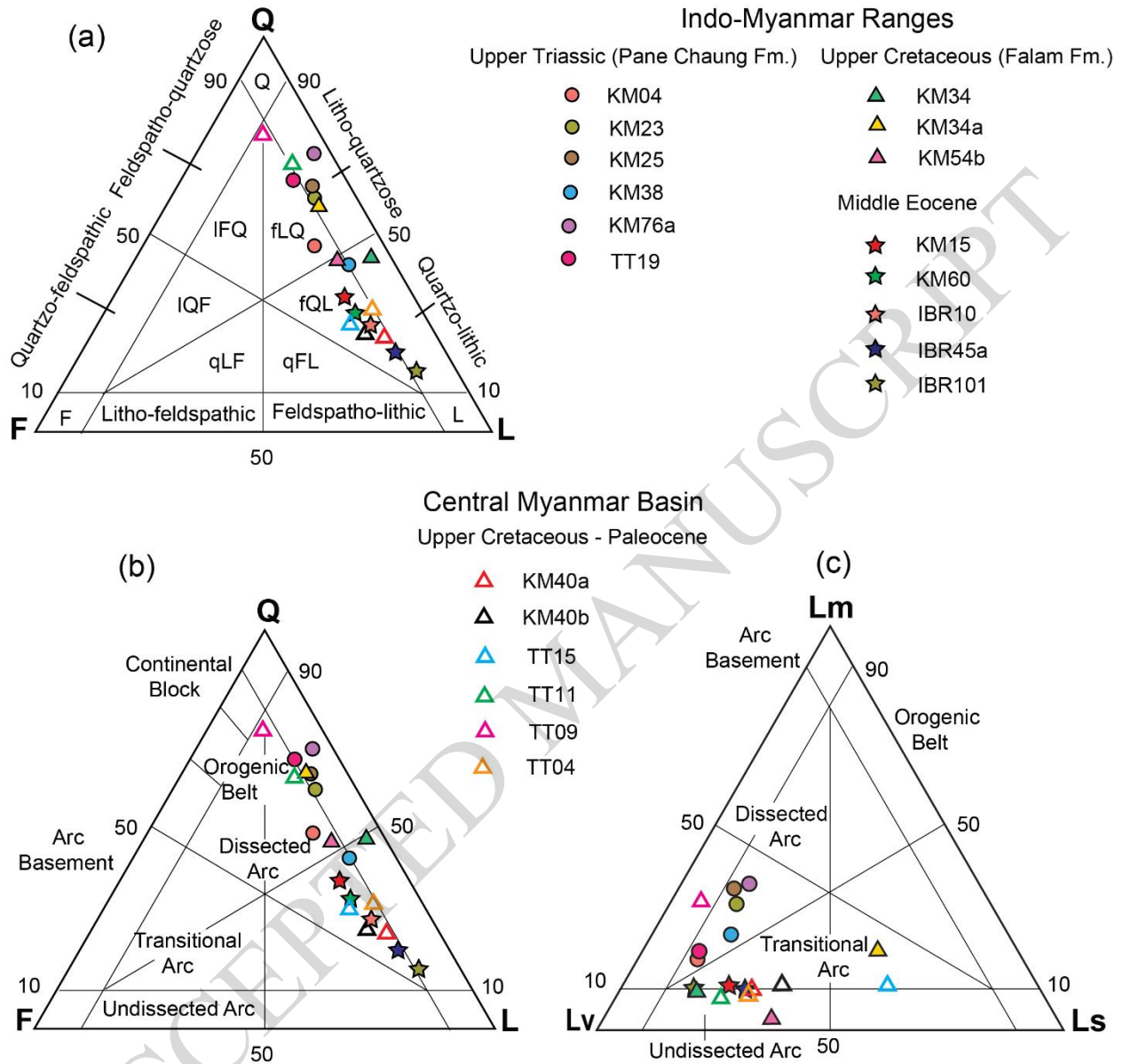


Figure 8

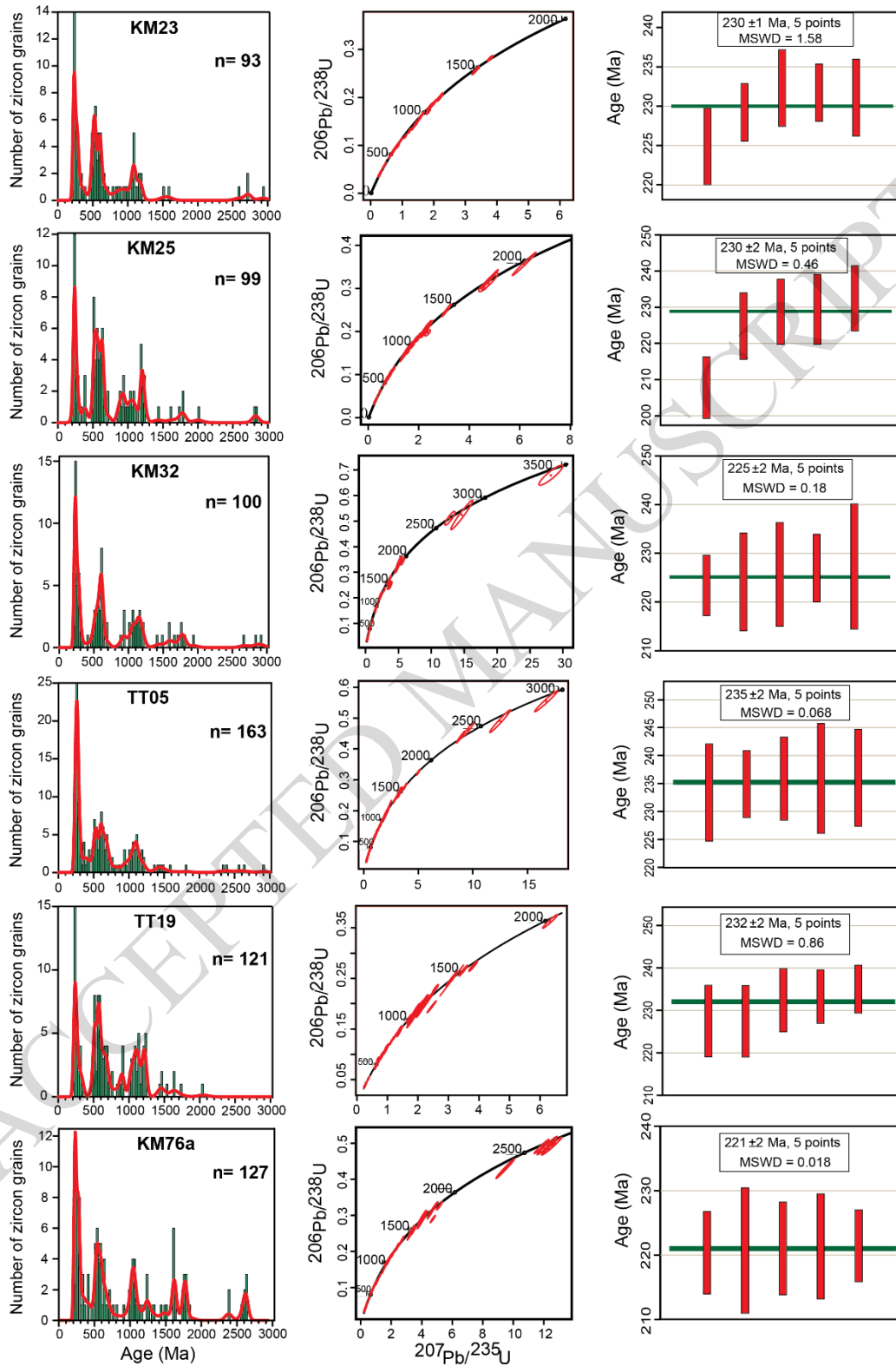


Figure 9

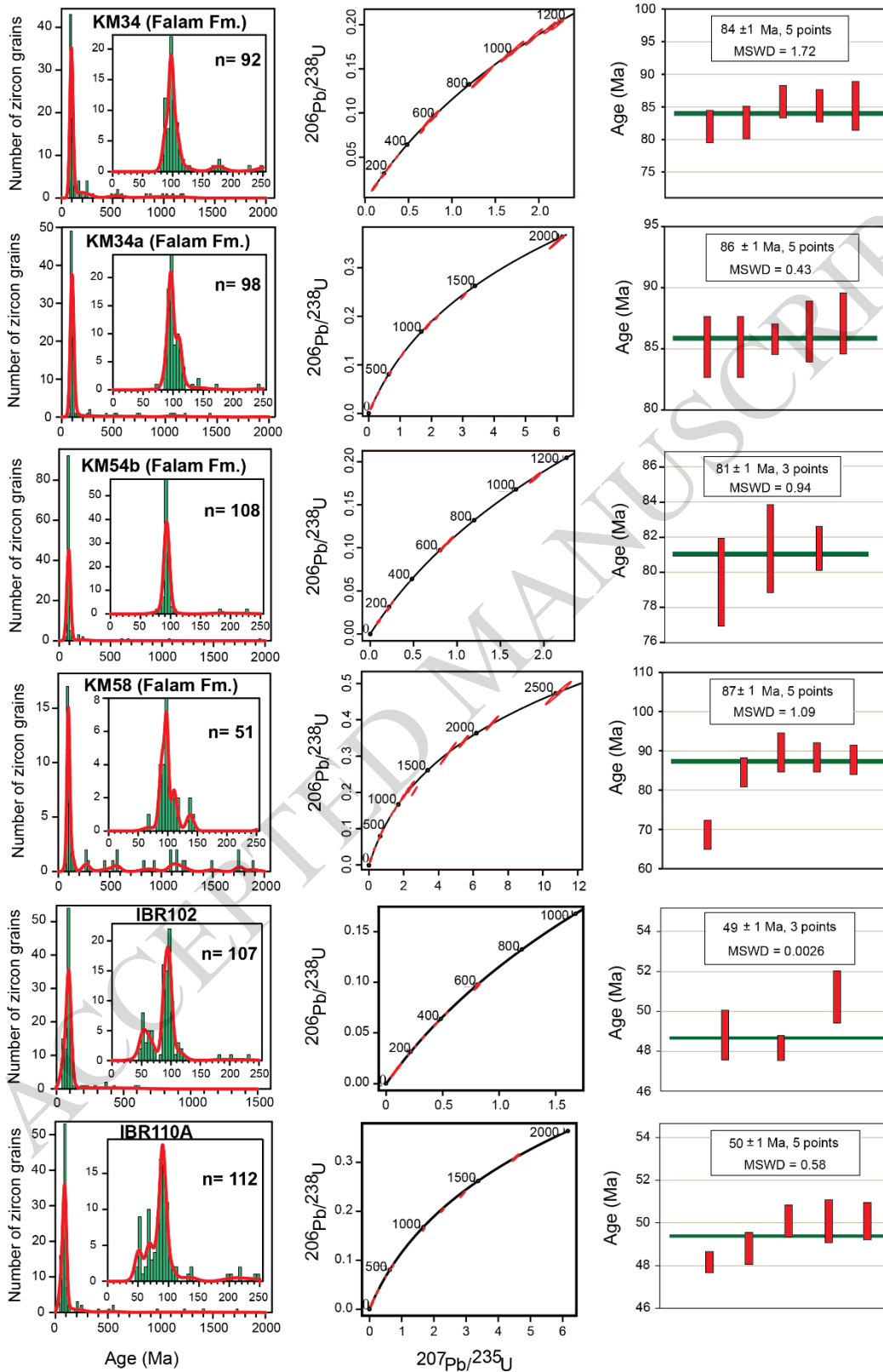


Figure 10

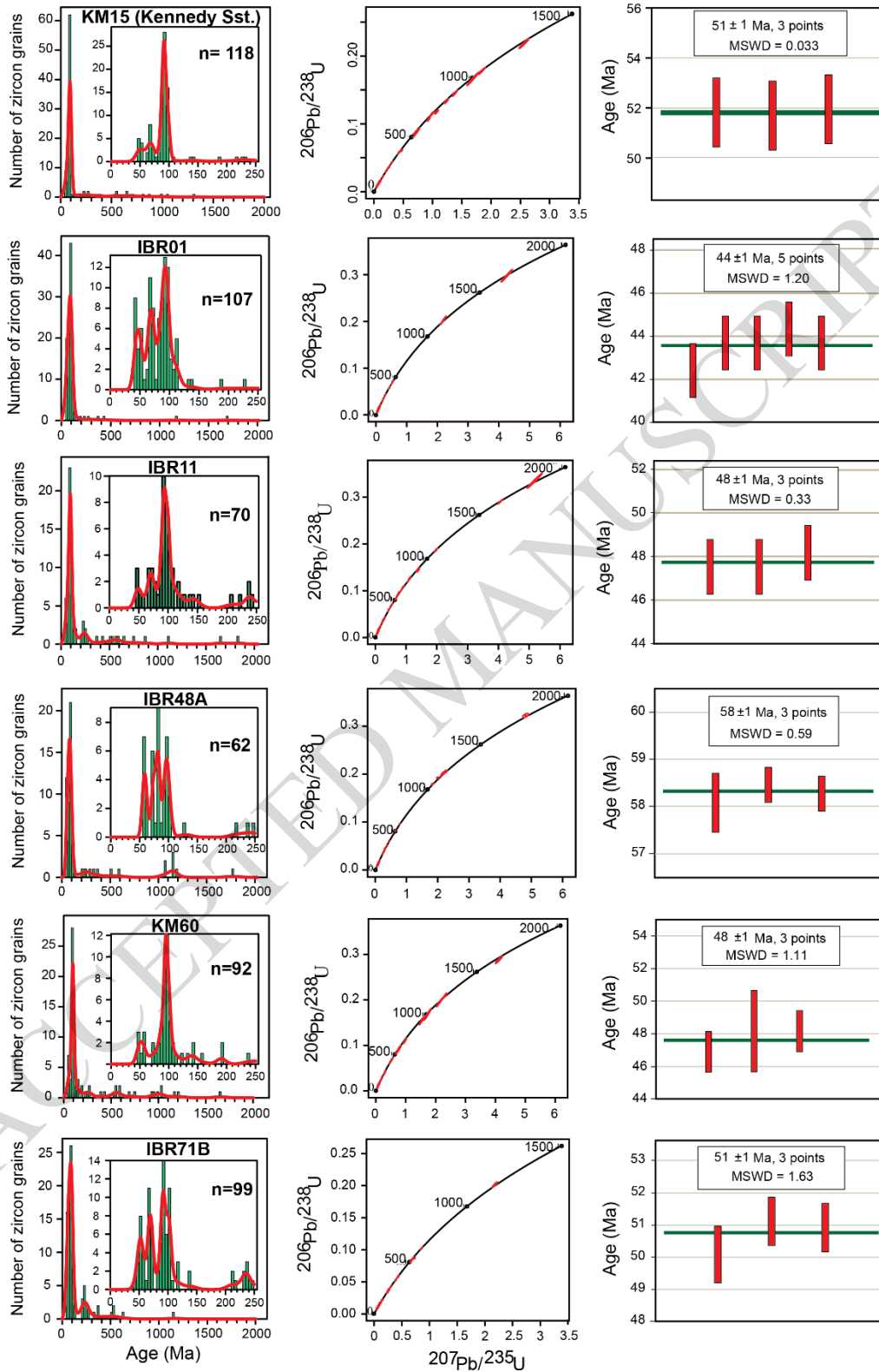


Figure 11

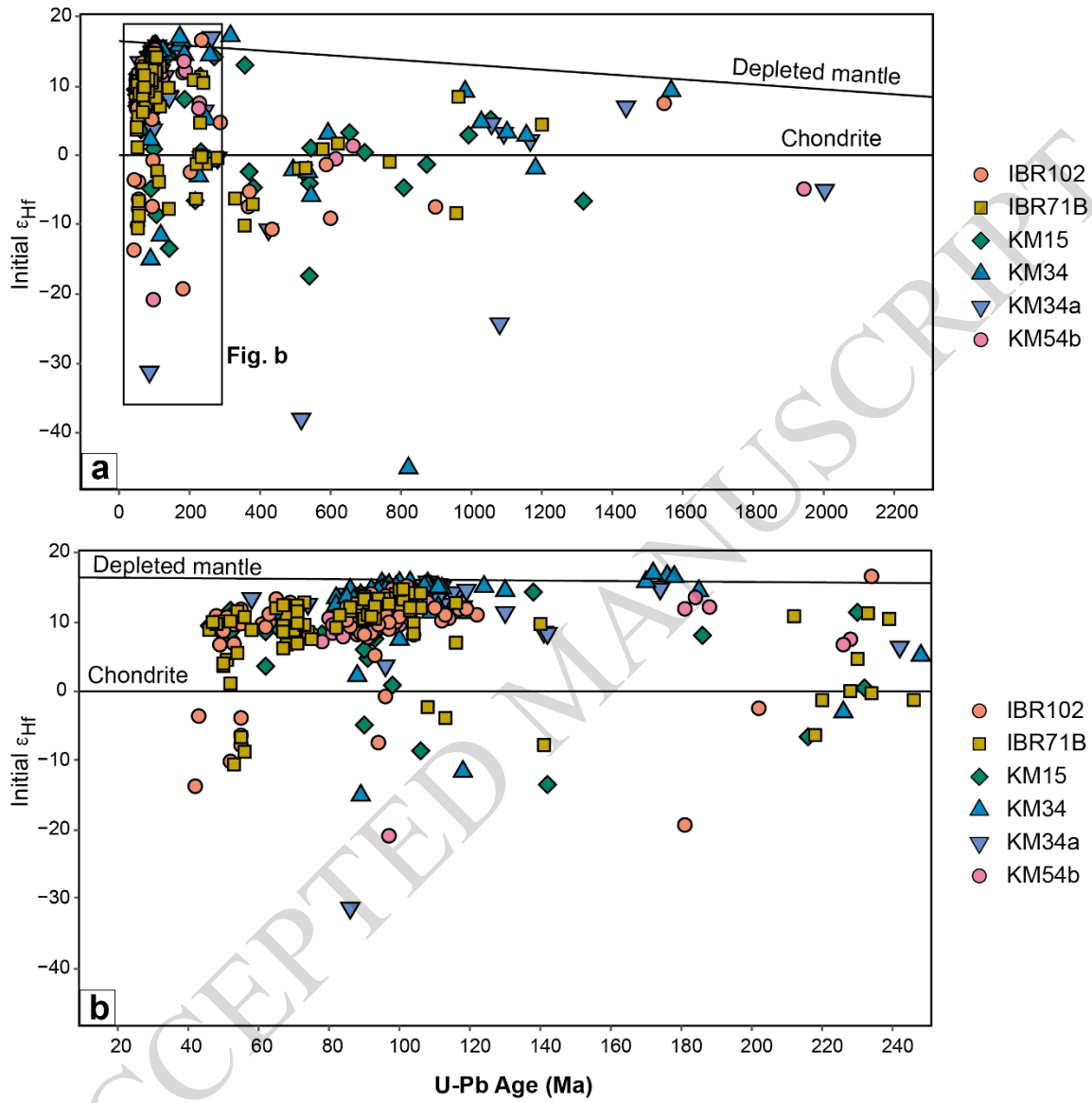
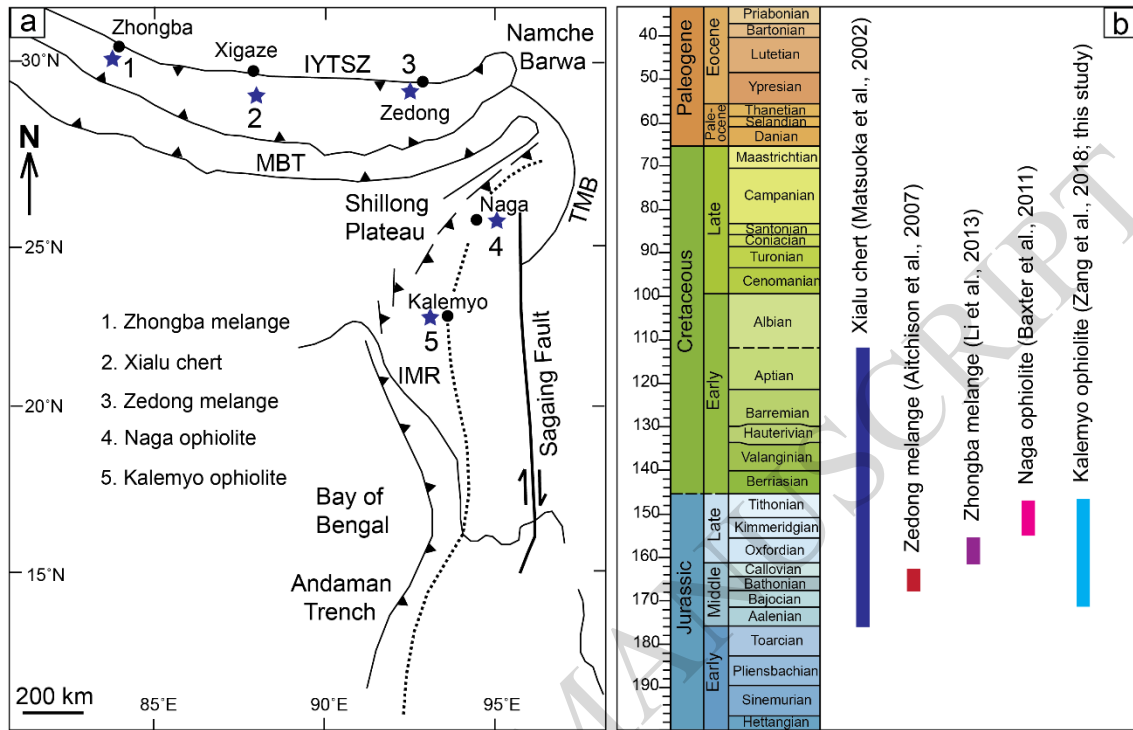


Figure 12



★ Middle Jurassic - Early Cretaceous radiolarian age

ACCEPTED MANUSCRIPT

Figure 13

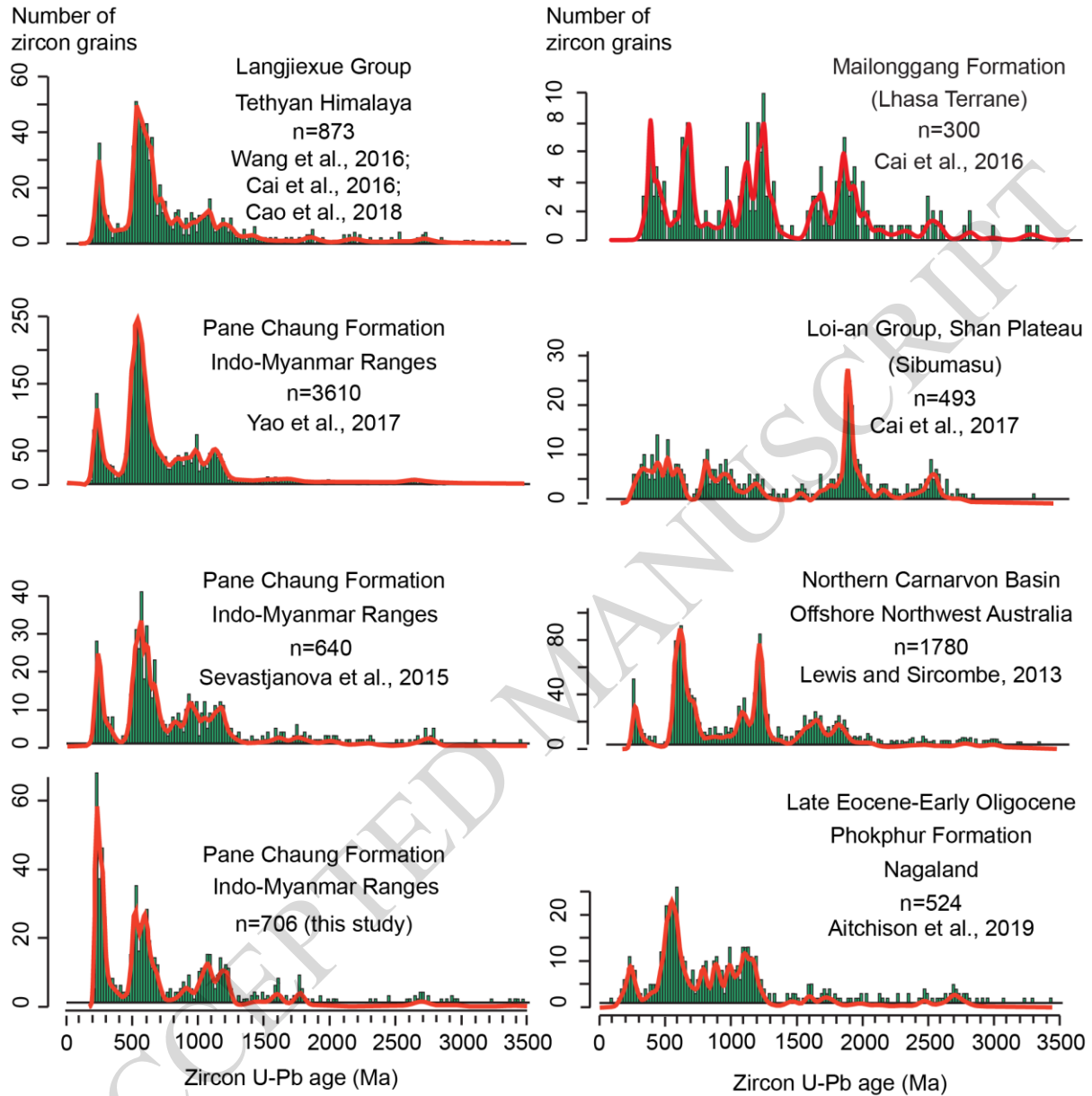


Figure 14

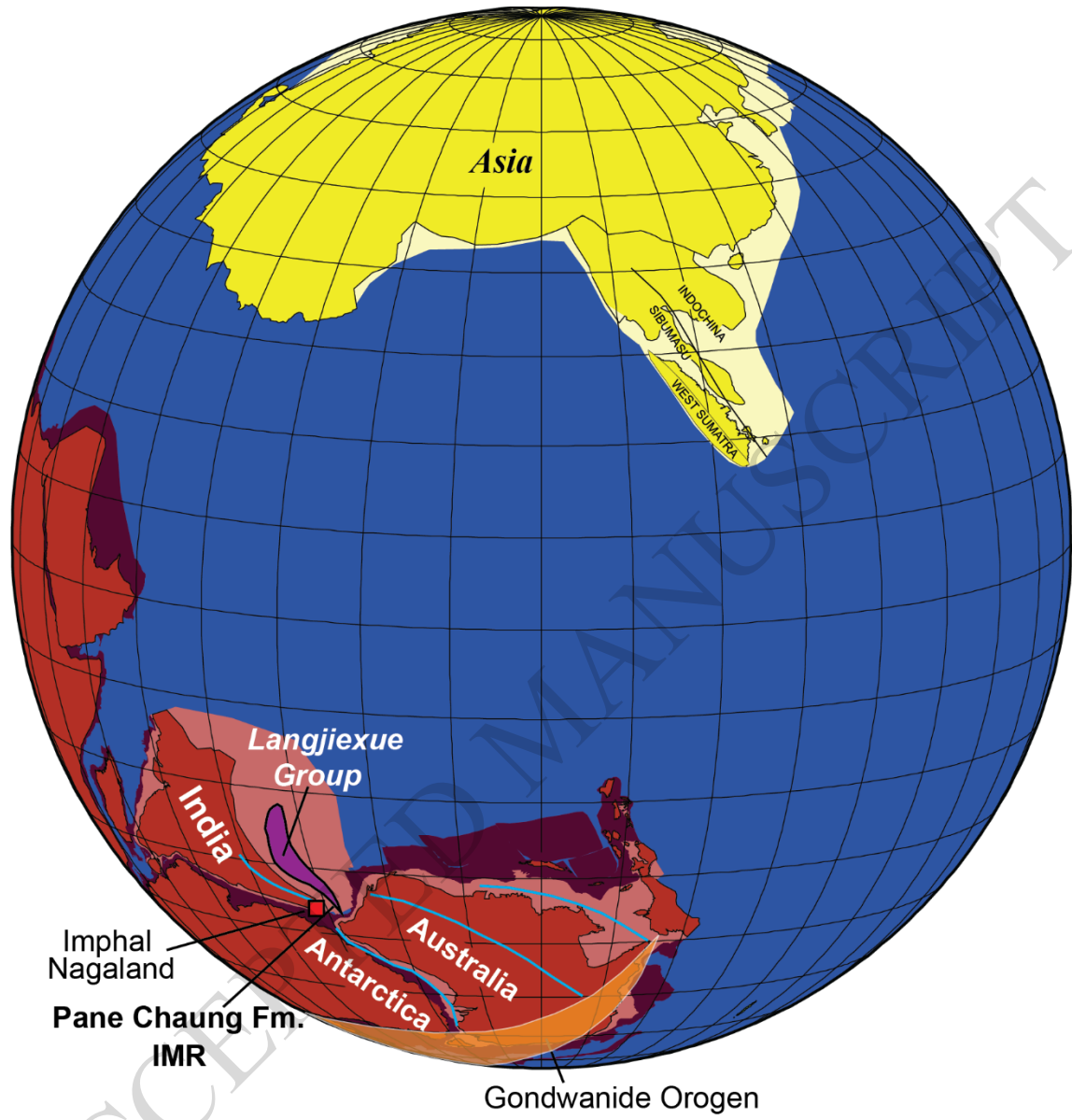


Figure 15

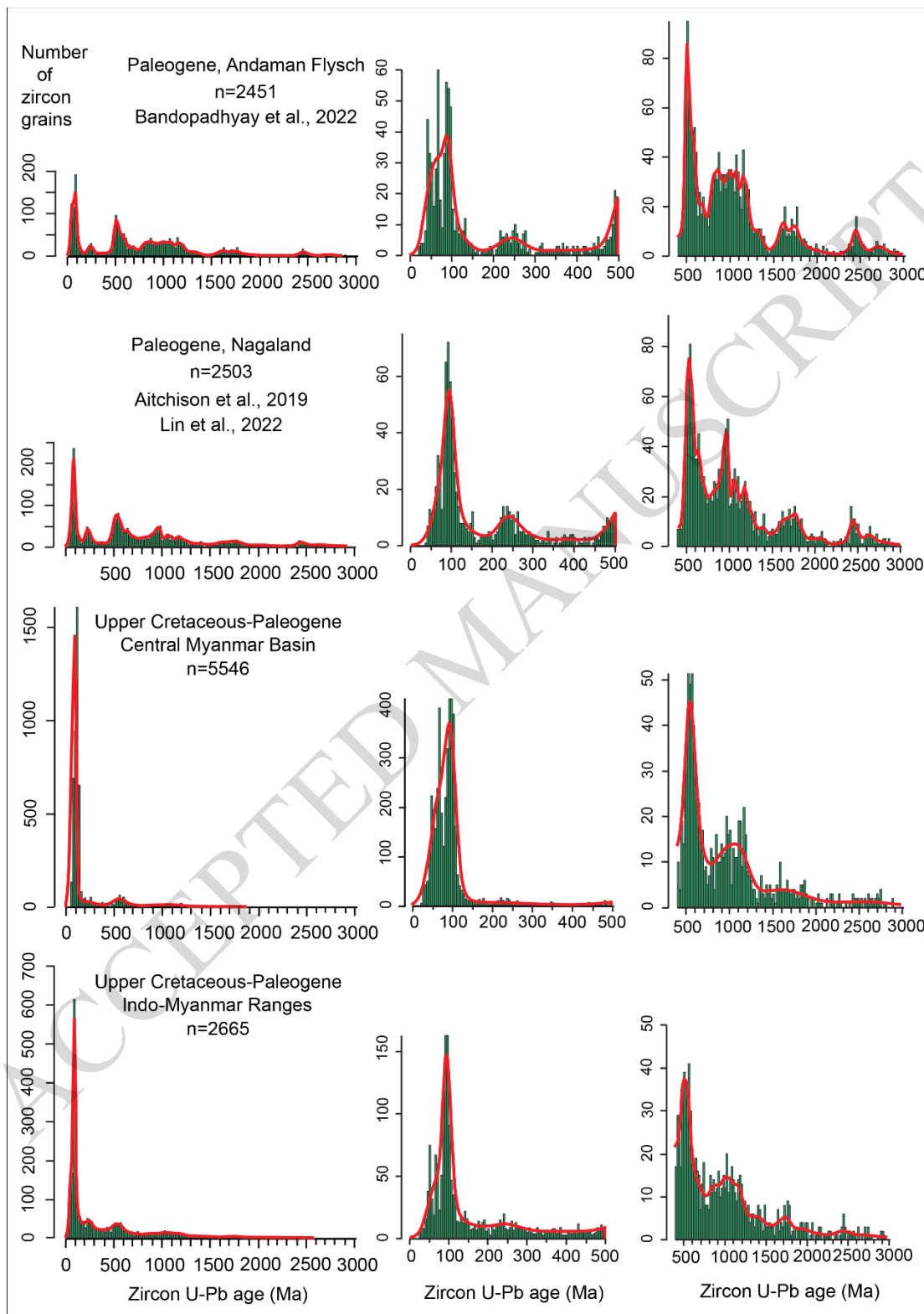


Figure 16

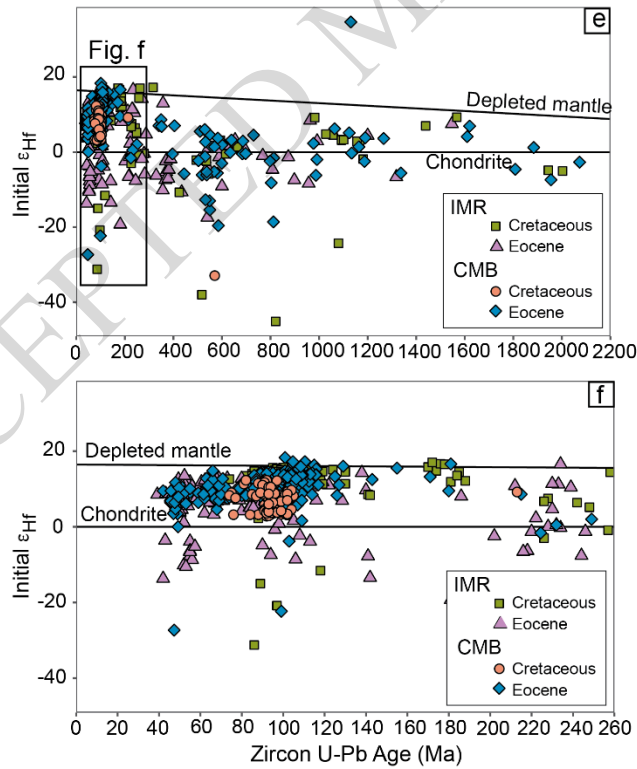
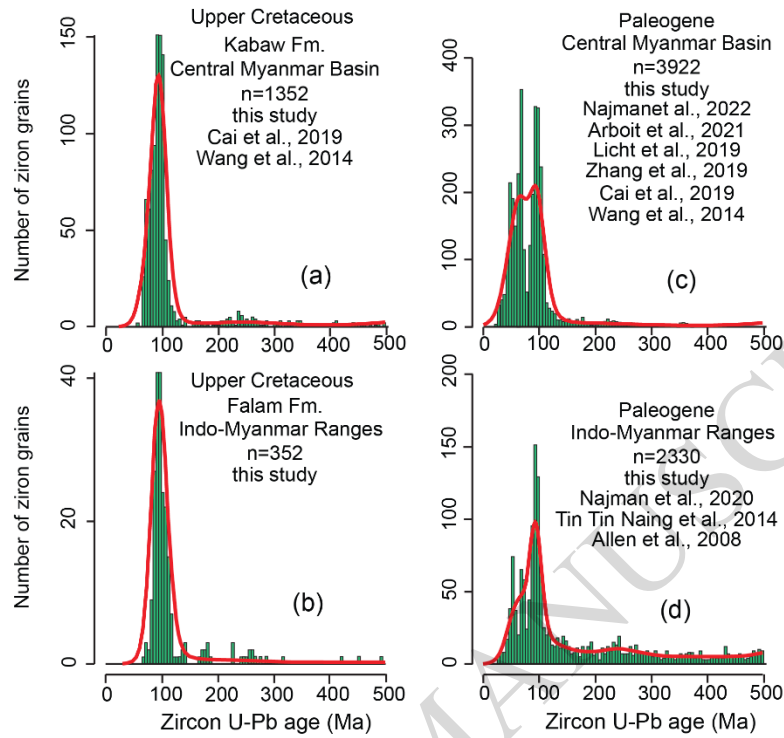


Figure 17

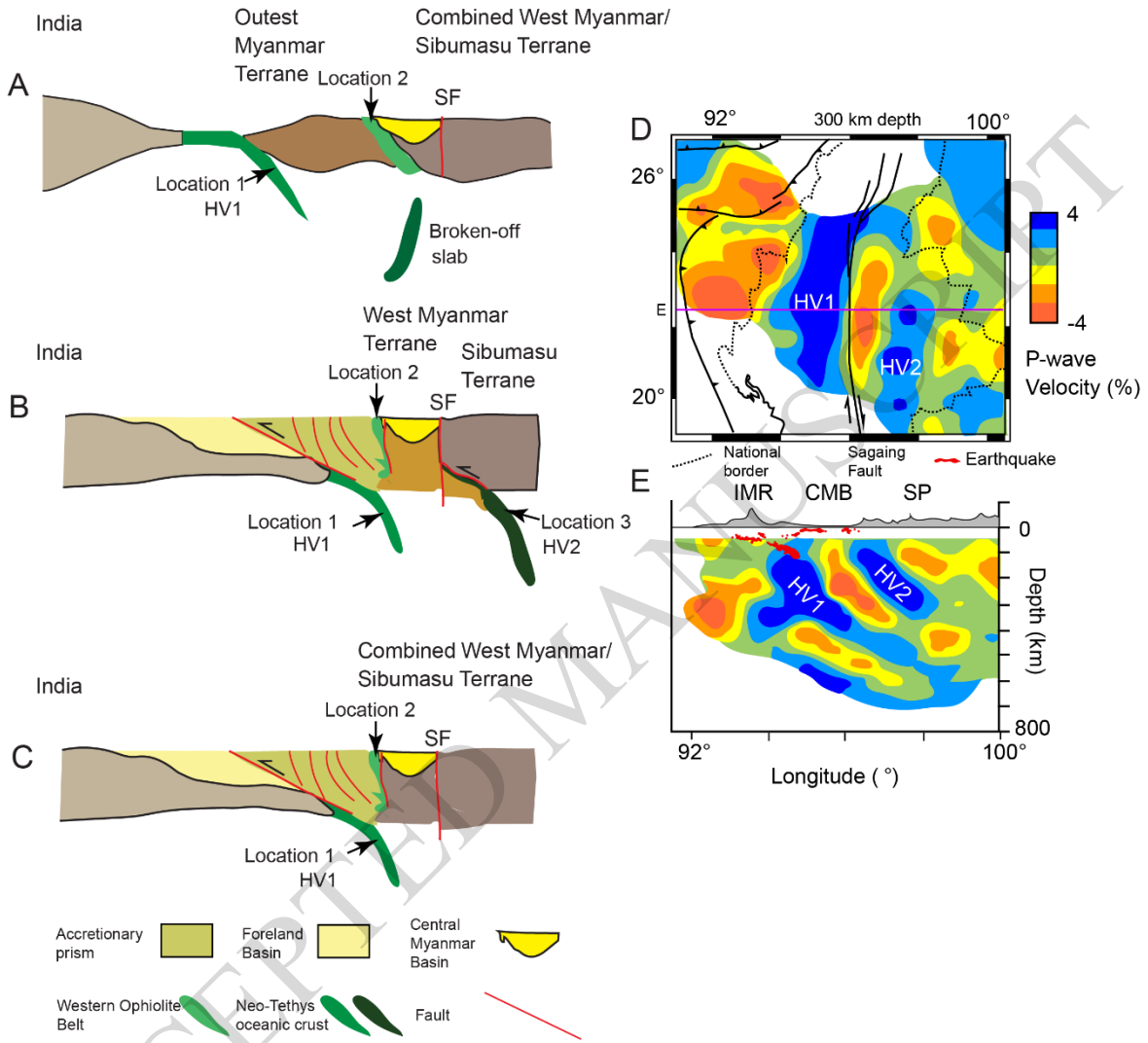


Figure 18

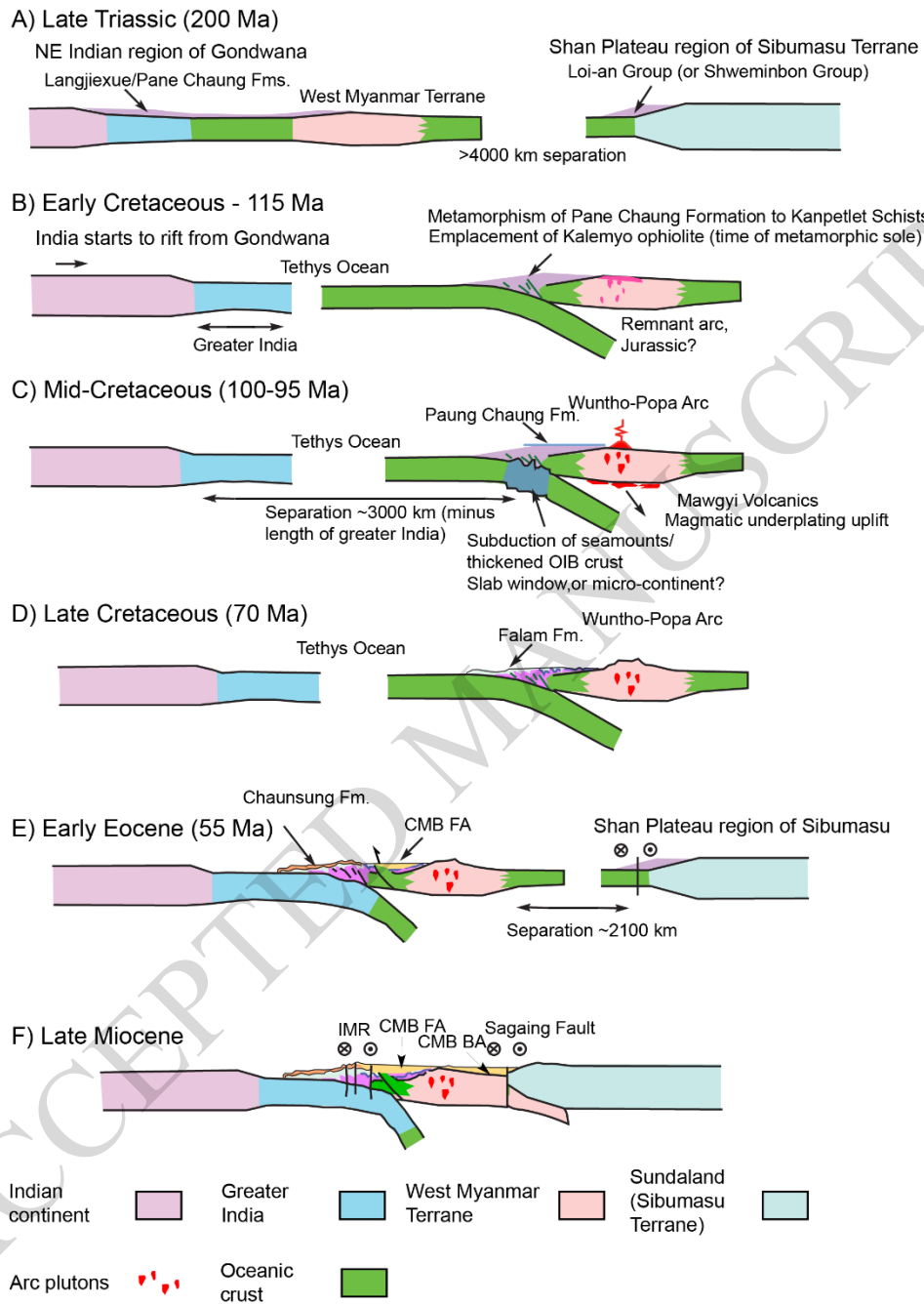


Plate 1

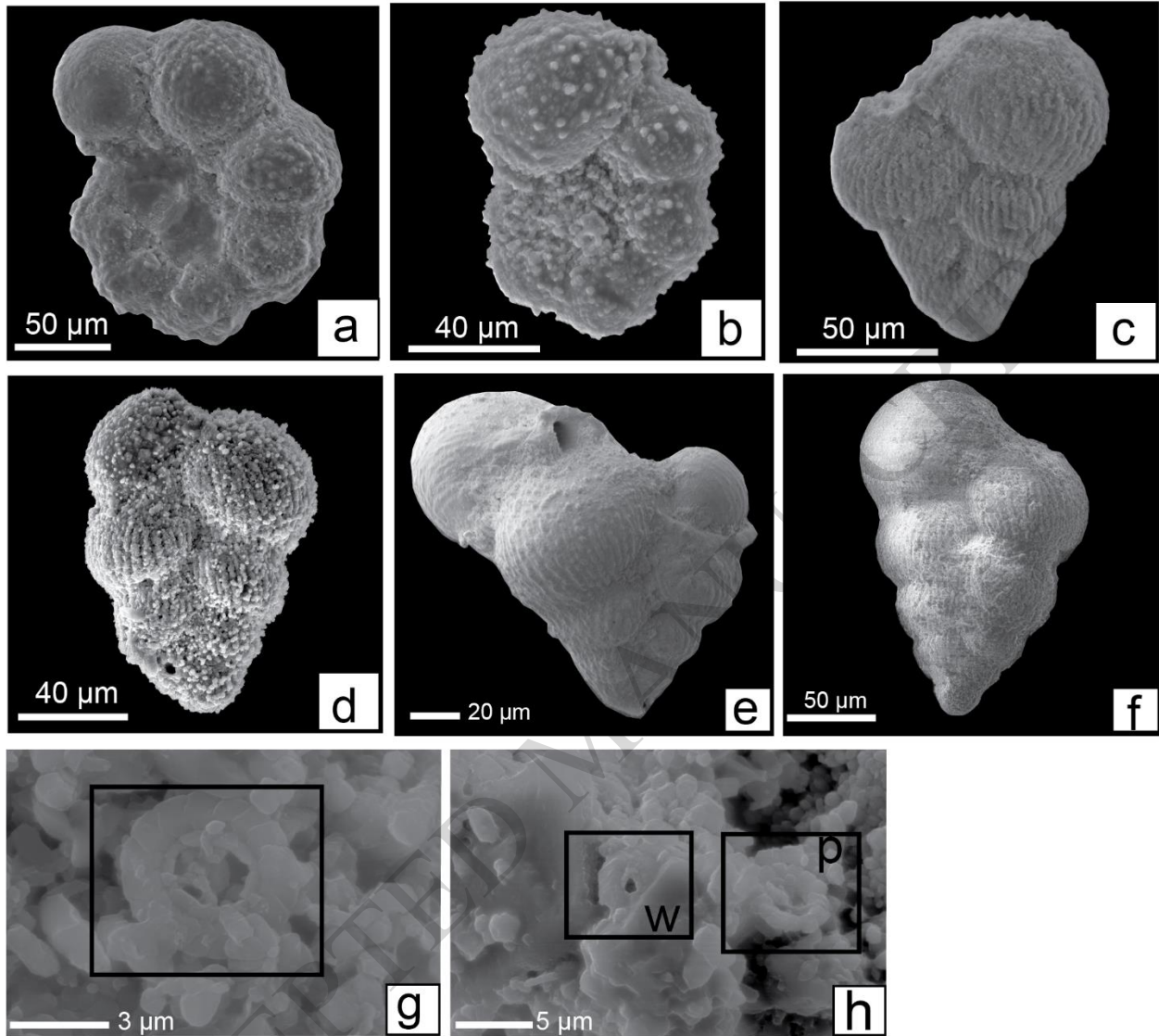


Plate 2

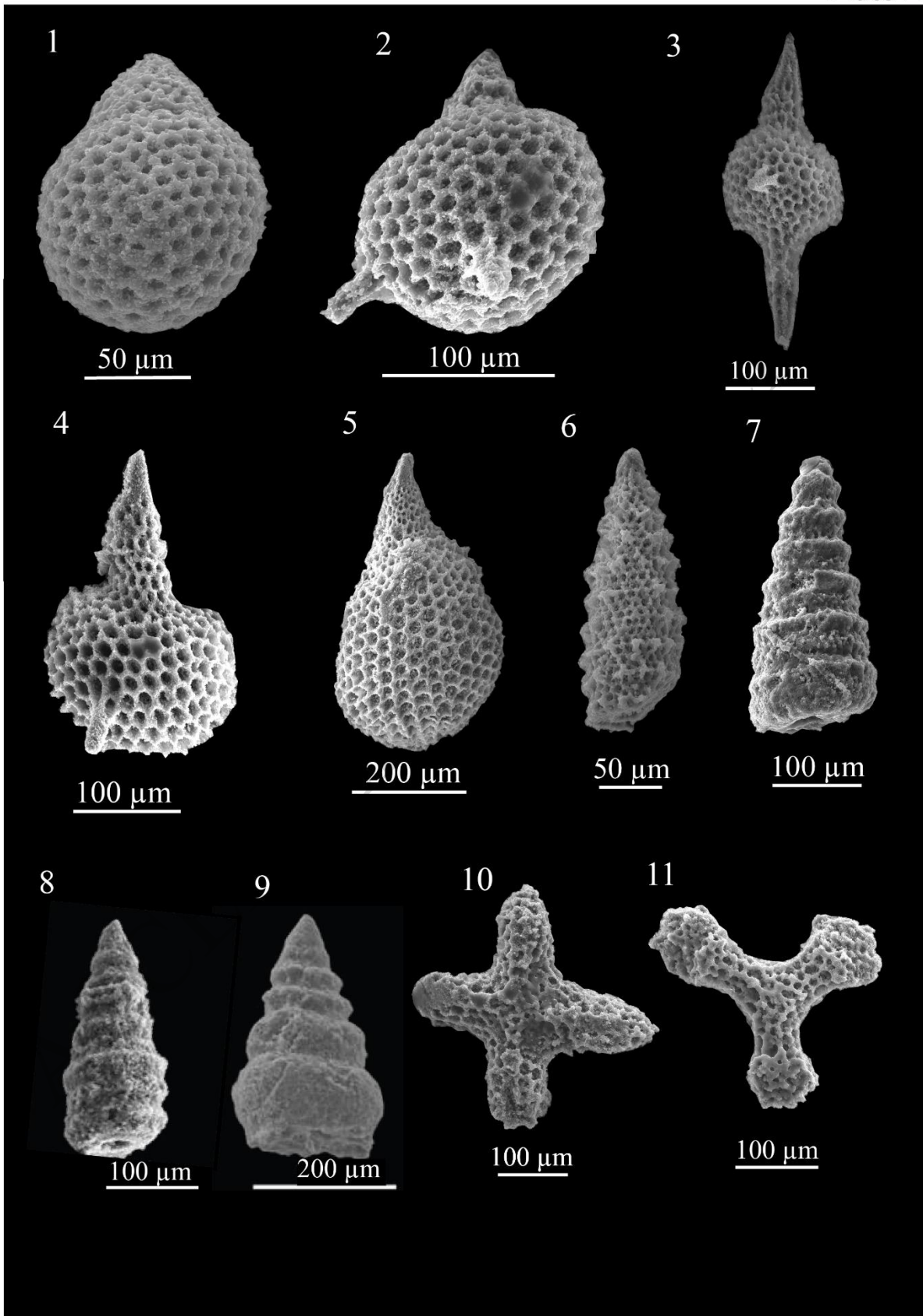


Table 1**Detrital modes of samples analysed from Indo-Burma Ranges**

Sample	Quartz			Feldspars			Lithics/Rock fragments							Authigenics & Matrix		Heavy mineral & Opaque
	Monocrystalline quartz	Polycrystalline quartz	Total quartz	Plagioclase Feldspars	K-feldspar	Total feldspar	Sedimentary lithic	Metamorphic lithic	Volcanic lithic	Chert	Muscovite	Biotite	Chlorite	Total lithics/Rock fragments	Quartz + Plagioclase + Calcite cement	
IBR10	14.5	8.0	22.5	10.5	0.0	10.5	14.2	4.2	31.0	0.0	1.4	0.0	0.0	50.8	13.8	2.4
IBR45a	12.0	5.4	17.4	9.8	0.0	9.8	15.4	5.8	35.8	0.0	0.0	0.6	1.6	59.2	13.2	0.4
IBR101	9.8	3.2	13.0	8.0	0.0	8.0	10.8	7.0	49.0	0.0	0.4	0.2	0.0	67.4	10.8	0.8
TT04	25.8	4.0	29.8	10.0	0.0	10.0	16.0	4.8	35.0	0.0	0.0	0.0	0.0	55.8	4.0	0.4
TT09	42.0	10.0	52.0	9.0	0.0	9.0	0.6	2.5	5.0	0.3	0.3	0.2	0.0	8.9	30.0	0.1
TT11	33.7	9.0	42.7	8.0	0.0	8.0	3.0	1.0	9.0	0.0	1.0	1.5	1.0	16.5	32.5	0.3
TT15	20.0	5.0	25.0	15.0	0.0	15.0	25.0	5.0	15.0	1.0	0.0	1.0	1.0	48.0	12.0	0.0
TT19	41.5	8.0	49.5	7.0	0.0	7.0	2.0	3.0	11.0	0.0	0.2	0.3	0.0	16.5	27.0	0.0
KM04	25.8	14.0	39.8	12.6		12.6	3.8	5.0	20.0	2.2	1.2		0.2	32.4	15.0	0.2
KM15	17.0	11.0	28.0	12.0		12.0	8.4	4.0	24.0	3.0	1.2	1.0	0.6	42.2	15.8	2.0
KM23	41.0	9.0	50.0	7.4		7.4	2.8	5.6	10.0	1.2	4.2	2.6	0.6	27.0	13.6	2.0
KM25	40.5	10.2	50.7	6.8		6.8	2.2	6.0	9.3	1.2	3.2	1.2	0.8	23.9	17.1	1.5
KM34	15.0	8.0	23.0	2.0		2.0	4.2	2.4	18.0	2.0		0.2	0.2	27.0	46.6	1.4
KM34a	34.0	12.4	46.4	6.6	0.2	6.8	9.8	3.8	6.0	5.2			2.0	26.8	19.6	0.4
KM38	27.6	9.2	36.8	8.4		8.4	5.6	7.2	19.0	0.8	1.0	7.2	0.6	41.4	12.6	0.8
KM40a	13.5	7.0	20.5	9.5	0.2	9.7	15.0	5.0	32.0	2.4			0.8	55.2	13.2	1.4
KM40b	14.5	7.0	21.5	12.6	0.4	13.0	16.0	5.0	25.5	4.8				51.3	13.4	0.8
KM54b	25.8	4.8	30.6	8.5		8.5	10.4	1.0	17.5	3.0				31.9	27.8	1.2
KM60	20.4	5.6	26.0	13.0	0.0	13.0	12.5	5.8	23.4	2.0	1.6	0.2	1.2	46.7	14.1	0.2
KM76a	29.8	26.2	56.0	3.2	0.0	3.2	3.2	7.6	11.0	0.4	0.2	0.0	0.6	23.0	17.4	0.4

ACCEPTED MANUSCRIPT

Table 2**Summary of published data on ophiolite formation and emplacement in the IBR and Tibet.**

Locality of suture zone	Ophiolite formed in a nascent arc (Ma)	Ophiolite generation in the subduction zone (Ma)	Environment of formation	Presence of HP-LT metamorphism	Dating of ophiolite emplacement	References
Tibet Indus-Yarlung Tsangpo suture zone	177 - 150	130 - 88	MOR & SSZ	Yes	Late Cretaceous	Hébert et al. (2012)
Indo-Burma Ranges Kalemyo Naga-Manipur Andaman Islands		127 118 - 116 95 ± 2	MOR MOR & SSZ SSZ	No Yes Age? No	Pre-Middle Cretaceous Late Eocene-Early Oligocene Palaeogene	Liu et al. (2016), Zhang et al. (2017, 2018) Baxter et al. (2011), Ningthoujam et al. (2012), Ghose et al. (2014), Singh et al. (2019), Aitchison et al. (2019) Pedersen et al. (2010), Ghost et al. (2009), Pal (2011)

ACCEPTED MANUSCRIPT